DEVELOPMENT AND CHARACTERISATION OF PHOTOCROSSLINKABLE POLY(ETHYLENE CARBONATE) ELASTOMERS FOR LOCAL PROTEIN DELIVERY

by

Laura Anne Cornacchione

A thesis submitted to the Department of Chemical Engineering

In conformity with the requirements for

the degree of Master of Applied Science

Queen's University

Kingston, Ontario, Canada

January, 2011

Abstract

Therapeutic angiogenesis is a promising application of local protein delivery. Poly(ethylene carbonate) (PEC) is an interesting polymer due to its special degradation mechanism and good immunocompatibility and cytocompatibility. Its biggest advantage over commonly used aliphatic polyesters is that it does not degrade to acidic products implicated in protein denaturation and tissue inflammation. The degradation mechanism of linear PEC is thought to be oxidative, however the *in vivo* degradation rate is inappropriately rapid for angiogenic growth factor delivery. To reduce the PEC degradation rate, low molecular weight PEC diacrylates were formed and then UV photocrosslinked to form elastomers. The aims of this thesis were to evaluate the degradation and biocompatibility of these elastomers, and to determine formulation parameters that control the release of a model protein, bovine serum albumin, from porous elastomer matrices.

Diacrylated prepolymers were successfully prepared with molecular weights from 2,000 Da to 12,000 Da. Elastomers were prepared from these prepolymers and characterised using NMR, DSC, ATR-FTIR, sol content and tensile testing. As hypothesized, crosslinking PEC slowed its degradation rate signifficantly compared to 60 kDa linear PEC (37 ± 4% mass loss in 12 weeks as compared to 78 ± 11% in 3 weeks). This result suggested that PEC degradation properties can be tuned for a range of tissue engineering or drug delivery applications. For both linear and elastomeric PEC, a typical foreign body reaction was observed. The degradation mechanism observed for the elastomer was the same as that for linear PEC and was consistent with the literature: cell-mediated surface erosion, which is demonstrated by linear mass loss, SEM observations, and pitted surface features.

The *in vitro* release of BSA-loaded porous formulations was rapid and/or incomplete. The most promising formulation (12% BSA) produced a more prolonged release of two weeks than the other formulations tested, however the total fraction of BSA released was only 23%. The formulation parameter that most significantly affected the release of BSA was the amount of DMSO used to vortex BSA particles. These findings provide insight into the potential and limitations of PEC elastomers in protein delivery applications.

Acknowledgements

I could write several chapters of gratitude to the following wonderful people for helping make these past two years a supportive and educational experience. Luckily for the printer, I have only included the abbreviated version and will save the extended thank-you's for in person.

Firstly, I thank my supervisor, Dr. Brian Amsden, for all the guidance, for being a great teacher, translating his vast knowledge of the field of biomaterials, for financial support, and especially for caring about my life outside of, and after, graduate school. I wish to extend great thanks to our lab manager, Dr. Dale Marecak, for keeping the lab running smoothly, equipment assistance, and sampling when I was unable to be in Kingston. I wish to thank Chris Ryan who conducted the animal care surgeries; Charles Cooney for SEM training and tips; and John Da Costa for the paraffin sections and H&E stains (and for teaching me how to get to the Azores, which I will one day visit).

I owe thanks to my friends in my lab group, especially Moira Vyner who translated her knowledge and enthusiasm of histology staining through the bologna slicer analogy, resulting in the successful completion of my first Masson's Trichrome stain. I thank her also for sampling when I was out of town, for proof-reading help (for resisting the temptation to add the term "double-dog-dare" to my thesis), and for naming all lab equipment, which ensured that they "behaved" for the most part. Thanks to Julian Chesterman for providing help for NMR problems and computer issues.

I owe a big thanks to many other friends within the department, especially Dr. Ian Parrag, who has been a wonderful mentor and advisor. I owe thanks to Eric Potter … even if I only ever needed a bandaid, it was great to gain such a great friend through the Emergency Buddy System. His presence made Biosci seem *less* haunted. Thanks goes out to Adam Hepburn for his friendship, in the form of "props".

I extend a special thank-you to Tanya Khan, for fusion dinners, roadtrips, girl talks, and especially for the overwhelming encouragement (and cup of cement) given to me when at crossroads in this last semester, helping me realize one of my dreams.

I will always be grateful to Katie McAlindon for the many wonderful memories we've shared at Queen's, for her friendship and inspiration. I am honoured to have known her, and she will be deeply missed.

Most of all, I would like to send an enormous THANK YOU to Michael Fitzpatrick and my family, the people who have been there for me for years, no matter what else is going on. Mike, I couldn't have done it without all your love and support. I am so thankful to have shared this graduate experience with you. For my family, thank you for your unconditional love and support (emotional and financial) and especially for your patience! I love you so much.

The financial support provided by National Sciences and Engineering Research Council (NSERC) was very much appreciated.

Table of Contents

List of Figures

List of Tables

List of Abbreviations

AC	Acryloyl Chloride
Ang	Angiopoietin
ATR-FTIR	Attenuated Total Reflection Fourier-Transform Infrared Spectroscopy
bFGF	Basic Fibroblast Growth Factor
BMP	Bone Morphogenetic Protein
BSA	Bovine Serum Albumin
CABG	Coronary Artery Bypass Graft
$CDCl_3$	Deuterated Chloroform
DCM	Dichloromethane
DMAP	4-(Dimethylamino)pyridine
DMPA	2,2-Dimethoxy-2-Phenyl-Acetophenone
DMSO	Dimethyl Sulfoxide
DSC	Differential Scanning Calorimetry
EC	Ethylene Carbonate
ECM	Extracellular Matrix
EC's	Endothelial Cells
ECU	Ethylene Carbonate Units
EF	Ether Function
EG	Ethylene Glycol
EGF	Epidermal Growth Factor
EVA	Ethylene Vinyl Acetate
FDA	Food and Drug Administration
FITC-BSA	Fluorescein Isothiocyanate Conjugated Bovine Serum Albumin
GPC	Gel Permeation Chromatography
HGF	Hepatocyte Growth Factor
hIL-3	Human Interleukin-3
HPLC	High-Performance Liquid Chromatography
IEF	Incorporated Ether Function
IFN-γ	Interferon-gamma
IGF-1	Insulin-Like Growth Factor
IL-2	Interleukin-2
MW	Molecular Weight
NADH	Nicotinamide Adenine Dinucleotide
NADPH	Nicotinamide Adenine Dinucleotide Phosphate
NGF	Nerve Growth Factor
NMR	Nuclear Magnetic Resonance

PBS	Phosphate Buffered Saline
PDGF	Platelet-Derived Growth Factor
PEC	Poly(ethylene carbonate)
PEG	Poly(ethylene glycol)
PEO	Poly(ethylene oxide)
PGA	Poly(glycolide)
PLG	Poly(lactide-co-glycolide)
PlGF	Placental Growth Factor
PLLA	Poly(L-lactide)
PTMC	Poly(trimethylene carbonate)
PVA	Poly(vinyl alcohol)
RGD	Arg-Gly-Asp
SCID	Severe Combined Immunodeficient
SEM	Scanning Electron Microscopy
TEA	Triethylamine
TFA	Trifluoroacetic Acid
T_g	Glass Transition Temperature
TGF-α	Transforming Growth Factor-α
TGF-β	Transforming Growth Factor-β
THF	Tetrahydrofuran
TMC	Trimethylene Carbonate
UV	Ultraviolet
VEGF	Vascular Endothelial Growth Factor

Chapter 1

Introduction and Literature Review

1.1 Proteins as Therapeutic Agents

1.1.1 The Promise of Protein Therapy

Proteins have a wide range of dynamic roles in the body, such as catalyzing biochemical reactions, forming receptors and channels in membranes, providing intracellular and extracellular scaffold support, and transporting molecules within a cell or from one organ to another[1]. With the number of functionally distinct proteins predicted to be higher than the estimated 30,000 genes in the human genome[2], there is a large opportunity to take advantage of proteins for therapeutic treatments of many conditions. In 2008, more than 130 different protein-based therapies were approved by the U.S. Food and Drug Administration (FDA)[1].

Compared to small-molecule drugs, proteins have several advantages as therapeutic agents[1]. One such advantage is that proteins serve highly specific and complex functions that cannot be achieved with simple synthetic compounds. Due to this high specificity, there is less potential for interference with normal biological processes and thus less adverse effects, especially if delivered locally[1]. Another advantage is that proteins used as therapeutics are often naturally produced in the body and therefore may be better tolerated[1]. A final major advantage of using proteins as therapeutics is that, clinical time and FDA approval can be faster for proteins than for small drugs[1]. In 2003, a study showed that the average development and approval time was 1 year

shorter for 33 protein therapeutics approved in 2002, than for 294 small-molecule drugs approved during the same time[3].

Growth factors are proteins responsible for the control of normal cellular activities such as proliferation, differentiation, migration, and adhesion[4]. They initiate these actions by binding to cell surface receptors. The term "growth factors" is often used synonymously with morphogens, cytokines, or chemokines. The growth factor type, concentration, duration and environment (e.g. presence and sequence of multiple growth factors) dictate cell fate, and therefore determine the ultimate therapeutic effect[5]. For example, some growth factors induce angiogenesis, maturation, or maintain the integrity of established vasculature[5]. See Table 1-1 for a list of representative growth factors and their activities.

There has been an abundance of promising studies describing the use of growth factors for therapeutic applications. For example, local drug delivery of insulin-like growth factor (IGF-1) and transforming growth factor- β1 (TGF-β1) have been evaluated for biological stimulation of the healing process to improve the clinical outcome in the treatment of long bone fractures[6]. Vascular endothelial growth factor (VEGF) has been successfully used at the intimal surface of a balloon-injured artery (after balloon angioplasty) resulting in enhanced reendothelialization and reduced neointimal thickening in a rat model[7]. Recent studies have shown that basic fibroblast growth factor (bFGF) was effective in enhancing periodontal tissue regeneration [8]. This growth factor has also been delivered to microencapsulated islets for the treatment of type I diabetes[9]. Epidermal growth factor (EGF) has been locally delivered via Pluronic/chitosan hydrogels for enhanced would healing of diabetic foot ulcers[10]. These examples represent only a small fraction of the potential applications of growth factor delivery.

Table 1-1: Representative list of commonly used growth factors for therapeutic applications[4].

Growth Factor Name	Abbrev.	Representative Activities
Epidermal growth factor	EGF	Proliferation of epithelial, mesenchymal, glial, and fibroblast cells
Basic fibroblast growth factor	bFGF	Proliferation of fibroblasts and initiation of angiogenesis
Insulin-like growth factor	IGF-1	Proliferation and differentiation of satellite cells; activation of muscle stem cells
Vascular endothelial growth factor	VEGF	Migration, proliferation, and survival of endothelial cells
Transforming growth factor - α	TGF-α	Migration and proliferation of keratinocytes
Transforming growth factor - β	TGF-β	Proliferation and differentiation of bone forming cells; chemoattractant for fibroblasts
Platelet-derived growth factor (two polypeptide chains A and B that form homodimers, AA or BB, or a heterodimer, AB)	PDGF-AA, PDGF-AB, PDGF-BB	Proliferation and chemoattractant for smooth muscle cells
Hepatocyte growth factor	HGF	Proliferation, migration, and differentiation of mesenchymal stem cells
Nerve growth factor	NGF	Promotes neurite outgrowth and neural cell survival
Bone morphogenetic protein (family of protein, of which six, BMP-2 through BMP-7 belong to TGF-b family of proteins)	BMP-2/ BMP-7	Differentiation and migration of bone forming cells

1.1.2 Role of the Extracellular Matrix

Growth factors are released by cells close to the site of action. After being released, many growth factors, such as VEGF, IGF, bFGF, TGF- β, and hepatocyte growth factor (HGF) bind with glycosaminoglycans (heparin or heparin sulphate) within the extracellular matrix (ECM)[11]. This binding acts to stabilize the active protein conformation, to protect it from immediate clearance and proteolytic inactivation and to promote its release in proximity to the cells involved in proteolytic remodelling of the ECM[11]. Since ECM-degrading enzymes are regulated to exert

their activity directly at the cell surface, the release of growth factors is localised[11]. Therefore, it is clear that the ECM plays a highly functionalized role in modulating the stability, activity, release and spatial localization of endogenous growth factors.

1.1.3 Protein Therapy vs. Gene Therapy

Gene therapy is an alternative to protein delivery, but there are many problems associated with this approach. To date, serious and unresolved problems related to gene therapy include: a) low transfection efficiency, b) risks of an undesired immune response, c) the potential for toxicity, inflammatory responses and oncogenesis related to the viral vectors, and d) the injection of a single gene will not be beneficial for disorders which are likely caused by the combined effects of variations in many genes (e.g. heart disease, high blood pressure, and diabetes)[12, 13]. The U.S. FDA has not yet approved any gene therapy products for sale[14].

In contrast to gene therapy, localized protein delivery has a number of advantages: the biological effects of proteins are better characterised than genes, it is possible to deliver a therapeutic protein with minimal immunogenic response, there is no need for a viral or synthetic vector, there is a localized effect at the target site, and more predictability of dosing. For protein delivery, the biggest challenges are associated with selecting a delivery device that is appropriate for the protein dose and duration required, and maintaining the bioactivity of the therapeutic agent until it reaches the target cell. Considering the challenges of both approaches, protein therapy may be the dominant treatment choice for many disorders for at least the next decade (at least until more research further evaluates whether the risks and challenges of gene therapy can be resolved).

1.1.4 Clinical Motivation of Angiogenic Growth Factor Therapeutics

The administration of angiogenic growth factors has been investigated clinically for the treatment of tissue ischemia (e.g. for peripheral vascular disease or coronary artery disease), which results from arterial blockage due to plaque deposition[11]. Given that cardiovascular disease currently accounts for 30% of deaths in Canada, and that 54% of these are due to ischemic heart disease[15], the promise of angiogenic growth factor therapy provides a significant opportunity to develop life-saving technologies. Promising clinical results from angiogenic growth factor therapy are also meaningful for other applications, such as for vascularisation in tissue engineering, which is currently an unmet challenge that has limited the success of tissue engineering approaches so far to simple avascular tissues such as skin (epidermis), cornea and cartilage[16].

It has been shown that administration of a number of angiogenic growth factors improves regional blood flow. Growth factors shown to be involved in angiogenesis include: vascular endothelial growth factor (VEGF) and basic fibroblast growth factor (bFGF), which initiate endothelial capillary formation by promoting endothelial cell migration, proliferation and survival; platelet-derived growth factor (PDGF), which stabilizes the newly formed vessels by the recruitment of mural cells; and transforming growth factor-β (TGF-β) which is involved in the maturation by promoting ECM deposition[17-20]. A list of commonly used angiogenic growth factors are listed in Table 1-2.

1.2 The Need for Local Protein Delivery

The delivery of protein drugs is often more challenging than small-molecule drugs for many reasons. One major challenge is maintaining the bioactivity of the therapeutic agent since soluble

Table 1-2: Most commonly used growth factors in therapeutic angiogenesis[21].

Growth Factor	Abbreviation	Relevant Known Activities
Vascular endothelial growth factor	VEGF	Migration, proliferation, and survival of endothelial cells
Basic fibroblast growth factor	bFGF	Migration, proliferation, and survival of endothelial cells and many other types of cells
Platelet derived growth factor	PDGF	Promotes the maturation of blood vessels by recruiting smooth muscle cells
Angiopoietin-1	Ang-1	Strengthens endothelial cell-smooth muscle cell interaction
Angiopoietin-2	Ang-2	Weakens endothelial cell-smooth muscle cell interaction
Placental growth factor	PlGF	Stimulates angiogenesis
Transforming growth factor	TGF	Stabilizes new blood vessels by promoting matrix deposition
Hepatocyte growth factor	HGF	Mitogen, motogen, morphogen of epithelial and endothelial cells

proteins are prone to degradation, deactivation by enzymes, and chemical and physical reactions at body temperature. Therefore, most proteins possess short plasma half-lives. For example, the half life of bFGF is only 3 minutes[22], that of VEGF is 30-90 minutes[18, 23, 24] and that of interleukin-2, (IL-2) is 30 minutes[25]. Protein denaturation can also result in the protein becoming immunogenic when released *in vivo*[26, 27]. This inherent instability of protein drugs must be taken into account when designing delivery systems to ensure that the protein is protected during fabrication, storage, and during release.

In addition to short half-lives, proteins are relatively large in size, penetrate tissue slowly and are potentially toxic at high systemic levels[4, 27]. Therefore, conventional systemic routes of administration are not effective and may even be dangerous. Administration of growth factor alone via bolus injection has been shown to result in systemic problems caused by distribution, fast clearance, and overdose side effects[27]. Oral administration is not effective due to proteolytic degradation in the acidic environment of the gastro-intestinal tract and low permeability across

biological membranes due to the large size and polar surface characteristics of proteins[28]. Therefore to be effective, due to these special challenges, the delivery of protein therapeutics must be local, as is done in nature.

1.3 Advantages of Polymeric Controlled Delivery Systems

There are significant advantages to using polymers for controlled protein delivery. Most importantly, polymer delivery devices are capable of improving the efficacy of drug therapy by delivering the protein therapeutic locally, to avoid dangerous systemic effects, and delivering the protein in a sustained fashion within the therapeutic window, to prevent overdose effects. They also allow for stabilization of the protein drug to maintain its bioactivity until release by providing protection against physiological conditions, which is important for reasons described in the previous section. If they are efficient, controlled release devices allow for lower dosage administration to accomplish the same therapeutic effect in patients as compared to systemic routes of administration such as injections. Additionally, the convenience of fewer, more efficient dosages increases patient compliance[29].

Polymers also offer the advantage of device design flexibility. The chemical and physical properties of polymers can be tailored, especially through copolymerization, to produce a range of different release profiles which can be used for different therapeutic applications[18, 30]. Polymers can also be fabricated by various techniques to have different geometries, surface morphology, and porosity[31]. Altering these characteristics can alter the release profile and/or mode of administration (e.g. minimally invasive injectables using hydrogels, microspheres or low viscosity material)[32]. Several different release mechanisms are available (diffusion alone, matrix erosion, a combination of diffusion and matrix erosion, or osmotic release mechanism)[33]

depending on the polymer system selected. In some protein release applications, the polymer also serves to provide structural support, as a tissue engineering scaffold, or to provide a barrier to prevent the formation of post surgical adhesions[34].

1.4 Challenges of Current Polymeric Protein Delivery Systems

There are many challenges in designing an effective protein delivery system, as summarized in Table 1-3. Some of these problems are attributed to the polymer degradation mechanism and hydrophilicity. Others are associated with the fabrication process of the protein-loaded device, such as protein denaturation due to exposure to heat, shear, or moisture. These problems must be simultaneously resolved in order to produce an efficient and safe protein delivery device.

Table 1-3: Technical challenges for developing sustained release protein delivery devices. Adapted from Wu *et al*. [27].

Challenges	**Possible Causes**
Protein denaturing during polymer degradation	Acidic degradation products of hydrolysis
Protein denaturing during formulation process	High temperature, shear, cavitations, cross-linking reagent
Protein denaturing, aggregation, adsorption to polymer	Environmental factors like temperature, moisture
Immunogenicity of denatured proteins	Denaturation, aggregation
Burst Release	*In vivo* conditions like body temperature, pH, buffer, hydrophilic polymers
Incomplete Release	Denaturation, aggregation, low loading or limited interconnectivity of pores
Poor loading capacity, loading efficiency, and reproducibility	Formulation, complicated procedures, high cost, polymer type/properties
Formulation complexity	Denaturation, aggregation

1.4.1 Degradation Mechanism

The specific degradation mechanism of the selected polymer must be understood, since it will determine the microenvironment into which the drug is released. Biodegradable polymers can be degraded by bulk erosion and/or surface erosion.

Bulk degradation often takes place by hydrolysis, which is the result of water absorption into the polymer matrix; ester hydrolysis; byproduct diffusion to the surface of the implant; and local internal decrease in pH since the acidic degradation products are temporarily retained catalyzing further hydrolysis [35]. The degradation is characterised by an initial decrease in mechanical properties with little mass loss, followed by a period of mass loss, water uptake, further mechanical strength decrease, and finally the release of low molecular weight degradation products [36-40]. Bulk degradation may also be accompanied by cracks and crevices throughout the device that may rapidly crumble into pieces [41]. This is especially dangerous for drug delivery applications since cracks and/or failure may cause a bolus/large release of the drug. These fragments may even cause tissue irritation depending on the mechanical properties of the material and tissue location of the implant. Bulk eroding materials also possess limited predictability of erosion and the lack of protection of drug molecules from water [42]. Commonly used bulk degrading biomaterials include poly(glycolide)[43], poly(L,lactide)[44, 45], poly(D,L-lactide)[46], and poly(ε-caprolactone)[46] and their copolymers. Therefore, there are several reasons to conclude that bulk eroding polymers are not ideal for protein delivery applications.

Surface eroding biomaterials, on the other hand, are advantageous for protein delivery applications because they do not experience these problems. They degrade by oxidation and/or enzymatic degradation at the surface of the implant where adherent phagocytes produce reactive

oxidative species or enzymes [47-50]. Since this degradation occurs primarily in the intimate environment between the adherent phagocytes and the implant surface, the bulk remains inaccessible to the degrading species during most of the degradation period, and mechanical properties and other bulk properties do not change. Mass loss begins immediately and is linear with time. For some elastomers (especially thermosetting elastomers), hydrolysis also occurs on the surface[50]. Surface eroding biomaterials include poly(ethylene carbonate)[47, 51], poly(trimethylene carbonate)[48], poly(urethane carbonate)[52], poly(glycerol sebacate)[50], poly(polyol sebacate)[50], poly(ortho esters)[53], and poly(anhydrides)[54, 55].

1.4.2 Burst Release

One of the most common problems with the release of drugs via delivery devices is the "burst release", which refers to the initial large bolus release occurring immediately after the device has been placed in release medium (between 24 hours to several days). This burst release must be minimized because overdose is a concern for the entire release period, and is economically inefficient, especially considering the high cost of growth factor therapeutics. Among the strategies that have been successfully applied in decreasing the burst release, some have used plasticizers such as poly(ethylene glycol)[56, 57] and poly(ethylene oxide monooleate)-block-poly(D,L-lactide) [58] which work by producing a smoother surface, thereby reducing the surface area available for the initial burst release. Other strategies have coated a drug loaded device with another polymer or embedded microspheres in thermal gelling systems, poly(vinyl alcohol) (PVA), or fibrin[59-61].

1.4.3 Incomplete Release

Incomplete release is also a common problem in delivery systems[62]. It has been attributed, in many cases, to the protein aggregation during formulation, as well as the protein adsorption onto porous (hydrophobic) surfaces as the surface area increases during polymer degradation. To solve this problem for a salicylic delivery system, one study applied low intensity ultrasound, which created cracks and crevices in a poly(ethylene-co-vinyl acetate) elastomer with 40% EVA and allowed more trapped drug to be released [63,27]. However, this technique has not been applied to growth factor delivery systems where localized heat and pressure during ultrasound exposure could degrade incorporated growth factor [27].

1.4.4 Polymer Hydrophobicity

Proteins can denature during sustained release by protein aggregation and protein adsorption onto a hydrophobic polymer matrix. The energy barrier for protein unfolding was reported to be 5-20 kcal/mol which is close to that of protein-hydrophobic surface interaction [64, 65]. On the other hand, the use of completely hydrophilic systems has not proven to be completely successful. Disadvantages of some hydrogels have included low growth factor encapsulation yields, a rapid and significant initial burst followed by short release durations (4-7 days), low total fraction released, or the exposure of proteins to reactive cross-linkers [27, 66, 67].

1.5 Delivery Challenges of Vascular Endothelial Growth Factor

The most commonly used growth factor for initiating angiogenesis is vascular endothelial growth factor (VEGF) because it is more potent than basic fibroblast growth factor (bFGF) for endothelial cells (EC's)[68]. VEGF-A_{165} is the most common and biologically active isoform[68] and for the remainder of this thesis, it will be referred to as VEGF.

Early studies involving administration of VEGF by bolus injection at high doses demonstrated the need for a delivery system that prevents local and systemic overdose effects. Observed complications of bolus VEGF delivery have included severe vascular leakage leading to edema, nitric-oxide dependent hypotension[69, 70], and the unregulated formation of a dense bed of abnormal non-functional and short-lived vessels[71].

There have also been problems with distribution and clearance of VEGF unless a delivery device is utilized. A study conducted in a rat model by Kim *et al*. compared the pharmacokinetics following subcutaneous injection of VEGF alone to subcutaneous injection of VEGF-containing microspheres made from one of the most common drug delivery polymers, poly(lactide-co-glycolide) (PLG). When VEGF was injected on its own, the result was a very high plasma concentration (low concentration in the subcutaneous area), clearance of only four hours, and 70% of the VEGF was located in the blood, liver, spleen, lung and kidneys[72]. Therefore, it is clear that a controlled delivery device is necessary for effective VEGF therapy.

It should be noted that for the Kim *et al*. study while the administration of VEGF in PLG microspheres produced low VEGF plasma concentrations but high subcutaneous concentrations over 7 weeks, significant reduction in protein activity was reported and the study concluded that this reduction was due to the degradation byproducts[73]. This significant limitation is a concern for the application of many of the most commonly used drug delivery polymers, and will be further discussed.

As when designing delivery devices for almost any growth factor, the potential for stability issues must be taken into account. The acidic byproducts produced by many commonly used drug delivery polymers are detrimental for VEGF delivery, since VEGF degradation is accelerated at

low pH values. The N-terminal residues of recombinant human VEGF, which participate in receptor binding, are prone to deamidation, oxidation, and diketopiperazine reactions. These reactions occur at 7.4, 2.5 and 5.2 times faster, respectively, when environmental pH is 5 as compared to pH 8[74]. Therefore hydrolysable polymers are not recommended for the release of VEGF.

1.5.1 Therapeutic Regimen for Angiogenesis

One of the requirements of an effective and safe drug delivery system is that the release rate is within the therapeutic window, and that the duration of drug release is appropriate for this application. In therapeutic angiogenesis, newly formed blood vessels must be functional (i.e. perfused), and stablilized by surrounding smooth muscle cells in order to remain stable and therapeutically helpful. Preliminary experiments and preclinical trials have shown that the delivery of the growth factor must be continuous and local to induce effective vascularisation[75-78]. Many studies have shown that VEGF should be presented at the target site for 3-4 weeks[75, 79-81]. For example, Dor *et al*. administered VEGF for two weeks followed by cessation, which resulted in the production of new blood vessels that disappeared two weeks after cessation of delivery. When the delivery was extended to 4 weeks followed by cessation, however, the newly formed blood vessels persisted[80]. This prolonged multi-week exposure is necessary because many growth factors are also survival factors for endothelial cells, and exposure must be sustained to prevent early apoptosis of the migrating endothelial cells.

While it is generally accepted that this prolonged exposure to angiogenic growth factors is required, there is not widespread agreement regarding what concentration and combination of growth factors should be the goal of a delivery devices for therapeutic angiogenesis. It is

expected that when the VEGF concentration is too low, there is insufficient growth factor for activation of microvascular endothelial cells. On the other hand, if VEGF concentrations are too high, cell receptors can be potentially saturated and this may disrupt cell guidance[4]. There is support from several studies that indicate that single factor (VEGF) delivery at the correct concentration and duration is enough to produce functional long-lasting blood vessels. For example, in a study conducted by von Degenfeld *et al*., the local delivery of a high concentration of VEGF (440ng/day) for two weeks into ischemic tissue in SCID mice resulted in improved blood flow and the development of persistent new blood vessels, even at 15 months. On the other hand, doses of 48 ng/day and 804 ng/day did not produce long-lasting blood vessels[81]. This dosage dependence was confirmed by another study by Davies *et al*. through continuous infusion of 15, 150 or 1500 ng/day into a porous polyurethane scaffold implanted subcutaneously into the back of rats. Only the 150 ng/day dosage resulted in increased blood vessel density and persistent blood vessels[82].

On the other hand, there have also been many studies concluding that for new blood vessels to remain stable, the co-administration of a pro-angiogenic growth factor and pro-maturation factor is required. For example, PDGF-BB is a potential pro-maturation factor because it recruits pericytes, which may help stabilize the nascent blood vessel. Richardson *et al*. reported that the co-administration of VEGF and PDGF-BB at rates of 79 ng/day and 3 ng/day in a subcutaneous pocket in Lewis rats produced larger and more mature blood vessels than the delivery of either factor alone [83]. Another study demonstrated that the sequential delivery of these two growth factors induced the formation of mature, stable vessels by recruitment of smooth muscle cells [84]. As another approach, Xin *et al*. reported that the combined delivery of VEGF and HGF achieved a more effective therapeutic results than that achieved with either single factor administered alone and this combined therapy had an amplified, synergistic effect [85].

Unlike with conventional routes of drug administration, controlled delivery devices can be designed to deliver multiple growth factors sequentially, in combination, at different rates. This approach is seen as more biomimetic since in nature cell fate processes are most likely controlled by coordinating cell exposure to multiple growth factors. This design would be accomplished through fabrication using several different approaches where each growth factor is incorporated at different stages of the device fabrication. Recent approaches include encapsulating one growth factor within beads before incorporation into another polymer containing matrix [83], coating one growth factor containing device with another polymer-containing coating material [86, 87], or taking advantage of different growth factors affinity to heparine sulphate (heparinization) [88].

Since the best drug regimen for therapeutic angiogenesis is not known for certain, there is a need for growth factor delivery systems with tunable release rates, as well as adjustable mechanical and degradation properties. The latter is especially true if there is interest in using the delivery device for therapeutic angiogenesis in tissue engineering of a range of tissues since it is assumed that the degradation rate of the scaffold should match the rate of regeneration of tissue. The purpose of this work is to develop a new biodegradable elastomer and investigate its potential as a protein delivery device, with the ultimate interest in therapeutic angiogenesis. Therefore, the present literature review will focus especially on biomaterials that have been applied to angiogenic growth factor delivery.

1.6 Angiogenic Growth Factor Delivery Approaches and Their Limitations

1.6.1 Protein Loading Methods

There are a number of strategies for obtaining growth factor release from various porous scaffolds. However, the potential for denaturation of the growth factor as well as the need for the release kinetics to meet the design criteria for this application must be considered for each option. These strategies include adsorbing growth factors to the scaffold, coating the interior surface of the scaffold with a protein/polymer emulsion, blending growth factor-containing microspheres into the scaffold, or directly mixing growth factor containing lyophilized protein into the scaffold during preparation [89]. Adsorbing growth factors to the scaffold has shown low loading efficiencies, rapid release, and an initial burst in the first few hours of 25% [90]. For loading growth factors into microspheres [91], or into the emulsion coating [92], water/organic solvent emulsions are involved and therefore there is a decrease in protein bioactivity observed. Proteins are prone to denaturation during exposure to water-organic solvent interfaces, [27]. As mentioned, the energy barrier for protein unfolding was reported to be 5-20 kcal/mol, which is also close to that of water-oil and water-air interfacial tension [64, 65]. To minimizing the chance of denaturation during protein particle fabrication, one approach uses stabilizers, however often this results in burst release [93], protein aggregation [94, 95], reduced efficacy [96] and formulation complexity [97]. Incorporating solid protein particles is an attractive option because it is simple, and achieves nearly 100% protein incorporation efficiency and does not involve the use of an organic solvent so it is recommended for use if possible, which depends on the processing properties of the polymer selected.

1.6.2 Biomaterials for Growth Factor Delivery

A number of natural and synthetic polymers have been studied as controlled drug delivery devices. Naturally-derived materials available include proteins (collagen, gelatin, fibrin), and polysaccharides (alginate, chitosan, hyaluronic acid) [98]. While natural materials are often similar

to ECM, and may have the innate ability to interact with cells and/or undergo cell-mediated degradation, there can be issues including batch-to-batch variation, mechanical properties, immunocompatibility, and source/availability [4, 99].

Alternatively, synthetic materials have also been applied to drug delivery applications because they do not possess issues with source and are more controllable and reproducible from compositional and materials processing viewpoints [98, 100]. Use of synthetics also eliminates the concerns associated with the infectious pathogens from using animal or plant derived substances[18]. Although they may not be recognised by cells due to the absence of biological signals, architecture parameters and surface modification techniques have been employed to successfully improve cell adhesion and migration for synthetic options [31, 99]. Classes that are widely used include poly(α-hydroxyesters)s, polyanhydrides, and polyorthoesters [31]. So far, the poly(α-hydroxyesters)s such as poly(lactide) (PLA) and poly(glycolide) (PGA) and its copolymers have been most widely used.

Depending on the mechanical properties required and the delivery route for a certain application, synthetic polymers can be processed into porous scaffolds, particles or hydrogels. Hydrogels are physically or chemically crosslinked water-soluble polymers that swell in the presence of water. Poly(vinyl alcohol) (PVA) and poly(ethylene glycol) (PEG) are commonly applied examples. Porous scaffolds can be fabricated using solvent casting [101], gas foaming [102], particulate leaching [103], electrospinning [104], or rapid prototyping [31]. The most commonly used polymers that are processed into porous scaffolds for drug delivery are poly(α-hydroxyester)s such as PLG or PLLA, polyanhydrides, polyorthoesters, poly(ethylene glycolide) and PVA.

A number of biodegradable polymers have been investigated for protein delivery. Among biodegradable polymers, polyesters[105], polyamides[106], poly(anhydrides)[107], poly(orthoesters)[53], poly(phosphazene)s[108], and many other synthetic polymers have been studied. These polymers degrade by hydrolysis, which releases acid byproducts into the local environment. These acidic degradation products have been shown to reduce the bioactivity of released protein drugs [17, 109-116] and have been even implicated in causing tissue inflammation surrounding the implant[117]. A number of synthetic polymers do not significantly degrade in hydrolytic conditions at physiological pH, and are known to degrade by oxidation *in vivo*. These are, poly(carbonates), poly(urethane)s, poly(carbamate)s, and poly(ether urethane urea)[118, 119].

1.6.2.1 Poly(lactide-co-glycolide), PLG

PLG is one of the most commonly used synthetic biodegradable materials and it has a history of use as degradable synthetic sutures and bone fixatives [120]. The advantages of this material include good mechanical and degradation properties that can be tuned by the lactide to glycolide monomer ratio and the degree of polymerization [17]. PLG also possesses good cell adhesive properties for application as a drug-delivering tissue engineering scaffold.

The high temperatures or organic solvents used in conventional PLG scaffold processing techniques are inappropriate for maintaining the activity of loaded growth factors. However, new variations of the processing techniques have been developed to avoid denaturation [121]. A gas foaming process was developed using high pressure CO_2 gas and NaCl leaching which resulted in completely amorphous, highly porous matrices of PLG with interconnectivity that degrade over a period of 2-6 months [121]. Since these conditions are relatively mild for VEGF, it was shown that the bioactivity of the loaded protein was maintained using this process[121]. However, the loading

capacity using this method was only 20-30% since the growth factor was released during the aqueous salt removal. This is too low considering the high cost of growth factors. This was improved by pre-encapsulating the VEGF into alginate microspheres before incorporation into PLG which resulted in a 55% loading capacity of growth factor. This approach resulted in a more sustained release over the course of several weeks as compared to releasing from alginate microspheres alone [121]. Histological examination of mouse subcutaneous implants revealed locally induced formation of a new vascular network around the implant [121].

The first dual delivery release system was applied in this area using porous PLG as a scaffold. Dual release hypothesizes that the administration of a pro-angiogenic growth factor, VEGF, with pro-maturation factor, PDGF, will result in mural cell recruitment to stabilize newly formed blood vessels. This hypothesis was supported by the study results [83]. PLG scaffolds were prepared to allow the release of VEGF and PDGF by loading at different times. While VEGF was mixed with the polymer particles before processing, the PDGF was encapsulated into the polymer particles before processing (a gas foaming technique). This resulted in somewhat distinct release kinetics of the two growth factors since VEGF was largely associated with the surface and therefore released initially, and the PDGF was located in the bulk, released later by bulk erosion [83]. Although the data were not shown by the authors, the paper indicated that both growth factors were measured to be bioactive over the first three weeks of an *in vitro* release study.

More importantly, it was shown that this dual delivery led to both a high density of vessels and the formation of thicker and larger vessels [83]. This was further confirmed in a mouse model of hind limb ischemia where an increased number of mural cells were identified by histochemical

staining. This staining was for α-smooth muscle actin (a marker of mural cells), which was present when both factors were delivered as compared to just VEGF or PDGF alone [83].

There are serious limitations to PLG materials, as they degrade by hydrolysis. The degradation byproducts are lactic acid and glycolic acid which can significantly decrease the local pH as the scaffold degrades, and this is likely to denature the releasing growth factor [109-111, 113-116] and may cause tissue inflammation [117]. Studies have been conducted attempting to resolve this limitation of PLG by incorporating basic excipient (e.g. $Mg(OH)_2$ and $MgCO_3$) along with the growth factor before loading [122]. Other studies have blended PLG with PEG [123]. For addition of basic excipients, some control over the microenvironmental pH was accomplished for a short term, but the internal pH did eventually drop [122]. Blending with PEG resulted in an improved control over microenvironmental pH (5 to 5.8 for 4 weeks), however this was accompanied by a significant burst release (60% of loaded VEGF was released within the first 4 days) [123]. As mentioned, burst release should be avoided because it may cause serious overdose effects.

1.6.2.2 Poly(ethylene oxide), PEO

The most commonly used synthetic hydrogel in drug delivery is poly(ethylene oxide) (PEO), which is a component in several FDA-approved medical devices [124]. Since it is very hydrophilic, it can absorb water from its surroundings and form a hydrogel. A significant advantage of hydrogels is that they can be injected which is minimally invasive. PEO can also be UV crosslinked by modifying each end with acrylate or methacrylate and adding a photoinitiator [125].

Disadvantages of unmodified PEO gels include that it is not biodegradable and it does not allow protein adsorption (therefore giving PEO poor cell adhesion properties, rendering it unsuitable as

an angiogenic growth factor delivering scaffold for tissue engineering on its own). Modifications to overcome these limitations include conjugation to a number of natural and synthetic molecules. For example, the copolymer PEO-co-PLLA is biodegradable and can form thermally reversible hydrogels [126]. It should still be noted that experiments where PEO is copolymerized to achieve degradable scaffolds have involved the addition of hydrolysable segments, which release acid degradation products. Another modification includes the incorporation of affinity sites to provide association/dissociation sites for growth factor release, as well as cleavage sites for biodegradability. For example, PEG derivatives with proteolytically degradable peptides in their backbone have been used to form hydrogels that are degraded by enzymes involved in cell migration, such as collagenase and elastase [127]. RGD has been incorporated into the scaffold to achieve biospecific cell adhesion to enhance cellular ingrowth of neighbouring tissue. A heparin-binding peptide-conjugated star PEG was used to form bFGF loaded gels and the release was closely related to the erosion rate [128].

1.6.2.3 Alginate

Alginate is a commonly used natural biomaterial and is an anionic polysaccharide composed of beta-D-mannuronic acid and alpha-L-glucuronic acid which is derived from marine brown algae. When exposed to divalent cations (e.g. calcium), it complexes and forms a gel that will solubilise if the calcium is chelated and gets exchanged with sodium ions [17]. This hydrogel is used widely in food additives and wound dressings. Since this material will gel in an aqueous environment, alginate microspheres provide mild conditions for the entrapment of angiogenic growth factors. However, when simply loaded in this way, *in vitro* release under static conditions showed an uncontrolled burst release within the first 4 days followed by a zero-order release for 3 weeks [129]. To minimize the initial burst, heparinization has shown to be a more effective growth factor-

loading strategy, which involves covalently binding heparin to the scaffold surface, and then incubating in a growth factor solution. Since alginate is a hydrogel, the growth factors easily diffuse to binding sites, and bind reversibly. After rinsing, the release of the growth factor is then a function of its affinity to heparin or heparin sulfate. Sustained release of bFGF from heparinized alginate beads has been applied to the treatment of myocardial ischemia in human and animal models. Implantation of these beads loaded with 10-100 μg of bFGF resulted in significant improvement of coronary blood flow in a pig model with coronary occlusion [130]. Since there was no rise in bFGF plasma levels, and no hemodynamic effects or toxicity detected as a result of the treatment, it was suggested that bFGF delivery was safe. Positive results were also observed when 100 μg bFGF was delivered by heparin-alginate beads in human patients undergoing coronary bypass surgery (CABG). Nuclear perfusion imaging revealed significant improvement in myocardial perfusion for these patients as compared to controls [131].

Freeman *et al.* [88] used alginate-sulfate for the sequential delivery of VEGF, PDGF and TGF-β. Distinct release kinetics were achieved because each growth factor had a different binding affinity for alginate-sulfate, which was shown to have an affinity similar to that of heparin [88]. The results from this study showed that incorporating alginate-sulfate into alginate scaffolds significantly sustained factor release as compared to alginate scaffolds. A small, 20% burst release was observed for VEGF, followed by a much lower rate of factor release. For PDGF and TGF-β, no burst is seen and the release is relatively constant. By day 6, VEGF and PDGF releases plateau while TGF-β continues to be released. Considering the roles of VEGF as an initiator of angiogenesis, and of PDGF and TGF- β as stabilizers of the newly formed blood vessels, the results from histology and immunohistochemistry are not surprising: that the multi-release system produces more mature blood vessels than either factor released alone, or the

controls [88]. However, disadvantages of alginate include slow and uncontrollable degradation properties [132] and reports of the stimulation of inflammatory cells [17].

1.6.2.4 Poly(carbonates)

Polycarbonates are attractive options for protein delivery devices because they are one of the only degradable synthetic polymers available that degrade to yield non-acidic degradation products [133-135]. As mentioned, acid degradation products have been implicated in the denaturation of the protein to be delivered, including VEGF [75]. They may also cause tissue inflammation surrounding the implant [117]. Therefore, polycarbonates have an important advantage. See Figure 1-1 for structures of poly(ethylene carbonate) (PEC) and poly(trimethylene carbonate) (PTMC).

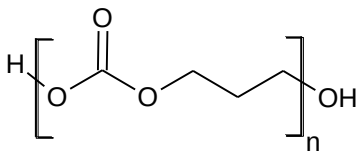

poly(trimethylene carbonate)

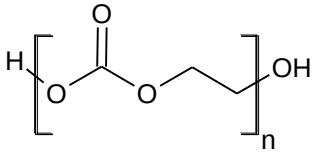

poly(ethylene carbonate)

Figure 1-1: Structures of PEC and PTMC.

PTMC, has been shown to have good biocompatibility and degradation properties [48, 49, 136] for several applications in protein delivery and tissue engineering, and has a history of use in the body as a component of Biosyn, Maxon and Caprosyn sutures. High molecular weight PTMC (>200 kDa) undergoes surface erosion at a rapid degradation rate [48, 136]. For example, 457 kDa PTMC was implanted into the femurs of rabbits, and 8 weeks later had lost 60% of its mass, and

mass loss over time was nearly linear [48]. In investigating PTMC as a drug delivery scaffold material which would not be prone to creep, Chapanian *et al*. produced PTMC elastomers by UV initiated photocrosslinking a triacrylated star-PTMC which was produced by ring opening polymerization with glycerol as an initiator [49]. After subcutaneous implantation in rats, it was demonstrated that crosslinking drastically reduced the degradation rate. Surface erosion, and a nearly linear mass loss with time was observed, reaching a total mass loss of 33 ± 8% in 44 weeks [35]. Despite its desirable degradation mechanism, acceptable host response and release potential, this degradation rate is too slow for many drug delivery and tissue engineering applications.

To formulate these PTMC elastomers for osmotic release, the star triacrylate was formed by copolymerization of TMC and D,L-lactide since the elastomers formed from TMC alone had large tear properties and therefore were not able to provide efficient osmotic release [137]. While D,L-lactide was used also to increase the *in vivo* degradation, poly(D,L-lactide) segments are susceptible to acid-catalyzed hydrolysis. Therefore, only a small fraction of D,L-lactide was incorporated and this is not expected to increase the degradation rate significantly to an appropriate level for certain drug delivery applications. Since the study by Chapanian *et al*. showed that the fluorescein isothiocyanate conjugated bovine serum albumin (FITC-BSA) particles (which become less fluorescent below pH of 5) remained fluorescent after 17 days, they concluded that the small fraction of D,L-lactide did not significantly reduce the microenvironmental pH [137].

1.6.2.4.1 Poly(ethylene carbonate)

Poly(ethylene carbonate) (PEC) has attracted attention in the literature as an interesting synthetic polymer due to its special degradation mechanism, good cytocompatibility and

immunocompatibility, and potentially beneficial drug carrier properties, although it has been evaluated for only a few therapeutic applications.

1.6.2.4.1.1 Degradation and Biocompatibility

The first published *in vivo* study of linear PEC was in 1983 by Kawaguchi *et al*., where the biodegradation of PEC pellets in the peritoneal cavity of rats was studied. The molecular weight of this PEC was not reported. It was found that the implants were nearly completely degraded in 2 weeks [138]. Cha *et al.* also concluded that the *in vivo* degradation of PEC (Mw = 105,000 Da) in rats was very fast, being completely degraded in 2 weeks for subcutaneously implanted films, 90% degraded in 3 weeks for intraperitoneal films, and 80% degraded in 3 weeks for intramuscular polymer rods [139]. These degradation rates are far too fast for almost all applications in tissue engineering and drug delivery.

In 1997, a study was published that evaluated the effects of different factors on the *in vivo* degradation rate of PECs in rats. PECs were synthesized by copolymerization of ethylene oxide and carbon dioxide with different organometallic catalysts, resulting in a range of molecular weights from 13 kDa to over 1,000 kDa. As a consequence of this copolymerization process, the PECs comprised oxyethylene units in the polymer chain in addition to ethylene carbonate units [140]. This study concluded that the biodegradation of these PECs depended on molecular weight, ethylene carbonate fraction, and catalyst choice. As expected, polymers with a higher ethylene carbonate content degraded more quickly [140] considering that poly(ethylene oxide) resists biodegradation. Contrary to what is expected, when the molecular weight was lower than approximately 70-100 kDa, degradation is strongly suppressed, degrading about 30-40% in 27 days, as compared to implants greater than 100kDa which were completely degraded in this

time[140]. The results from this study were rationalized by means of a non-hydrolytic degradation mechanism.

A follow-up study published by the same Novartis group [47] further investigated the degradation mechanism of PEC (MW 300-450 kDa). PEC was found to specifically degrade *in vivo* and *in vitro* by superoxide radical anions ($\bullet O_2^-$) which are mostly produced by inflammatory cells [47]. It was also demonstrated that the degradation is cell-mediated [47]. *In vivo*, degradation took place by surface erosion without significant change in molecular weight, producing ethylene glycol as the main degradation product of PEC, formed presumably by the hydrolysis of ethylene carbonate. A chain reaction mechanism which starts at polymer chain ends is implied by the splitting of a ring structure from the PEC [47]. No degradation was observed when incubated with hydrolases, serum or blood [47]. No *in vitro* degradation in aqueous media was seen in a wide range of pH values (pH 1 to 15.5). The two studies by Cha *et al*. and Acemoglu *et al.* also tested *in vitro* hydrolysis of PEC and found that there was negligible mass loss after up to 40 days in phosphate buffered saline (pH 7.0-7.4) [139, 140].

In another study conducted by Dadsetan *et al*., PEC degradation and immunocompatibility was evaluated using the *in vivo* cage implant system. Exudate analysis showed that PEC and PEC degradation products were biocompatible and induced minimal inflammatory and wound healing responses [141]. Once again, the surface erosion mechanism was seen, and pitting on the implant surface was present caused by adherent foreign body giant cells, and degradation was dependent on contact with cells. Using attenuated total reflectance Fourier transform infrared (ATR-FTIR) spectroscopy to characterise the degradation, it was concluded that superoxide anions released from adherent inflammatory cells appeared to initiate an "unzipping" mechanism of degradation, beginning with deprotonation of the polymer hydroxyl end groups. Acemoglu *et al.* proposed a

chain reaction mechanism as shown in Figure 1-2, which superoxide anion radicals can initiate, according to either an anionic- or radical-based mechanism. Ethylene carbonate is the product of degradation in both cases, which may further break down into ethylene glycol and carbon dioxide via hydrolysis.

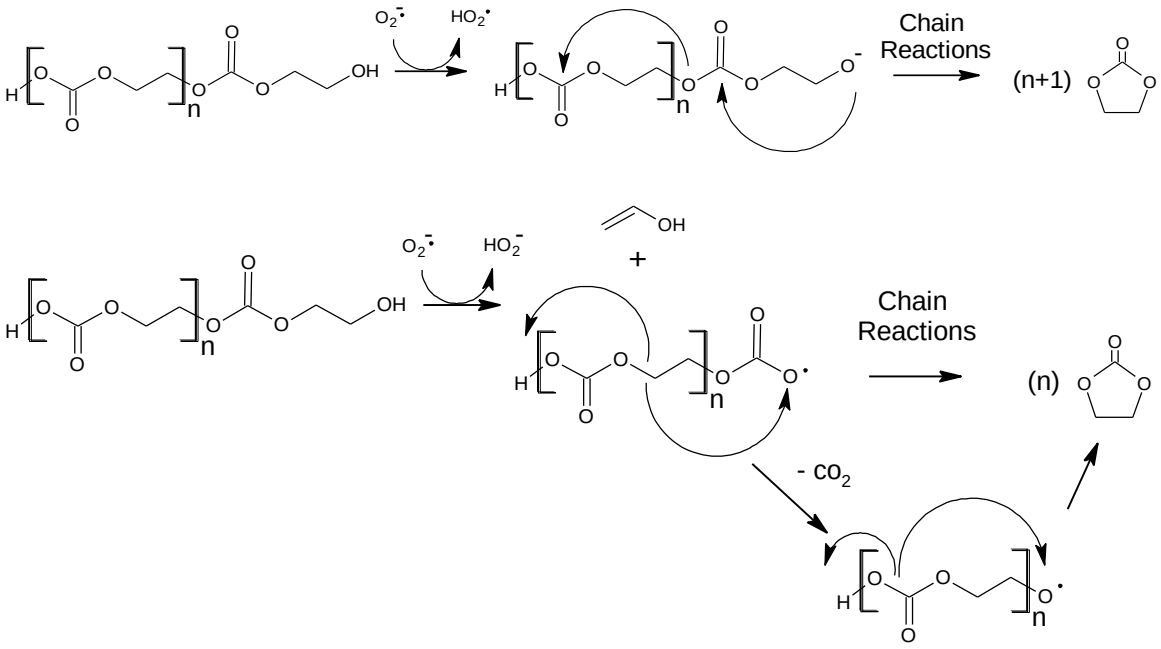

Figure 1-2: Proposed anionic- and radical-based mechanisms for the biodegradation of PEC *in vivo*. Adapted from Acemoglu *et al.* [51]

From these studies it can be concluded that PEC does not degrade hydrolytically by hydrolases or aqueous conditions, and the main mechanism of degradation is oxidation caused by reactive oxygen species (superoxide anion) released by inflammatory cells. Degradation is a cell-mediated surface erosion process. Since PEC does not degrade to produce acidic by-products, it has an advantage over many other polymers as a drug delivery device. The exact differences in degradation rates may be associated with the composition and molecular weight of PEC, however, in all cases PEC degrades too quickly for almost all applications in tissue engineering

and many in drug delivery. It has also been demonstrated the PEC elicits minimal inflammatory and wound healing responses.

1.6.2.4.1.2 Drug Delivery

Stoll *et al*. evaluated PEC as a drug carrier for human interleukin-3 (hIL-3, 15 kDa) and octreotide (1kDa) using a tablet press and the result was a 1:1 correlation between drug release and polymer mass loss [47]. Furthermore, the release rate of hIL-3 after subcutaneous implantation in rats was roughly linear. However, a tablet press using heat (50-85°C) and pressure (100-160 bar) was used for formulating the protein-containing polymer tablets, which may not be suitable for preserving the bioactivity of all protein drugs. However, in this case, Stoll *et al.* reported that for subcutaneous rat implants, the bioactivity of hIL-3 was maintained at about 50% (compared to the standard) based on a cell proliferation assay. Although this value was held constant for the 7-day duration, it is quite low. Another reason to be concerned about reduced bioactivity of released proteins loaded into a delivery device in this way is that using the surface erosion mechanism to control the release may imply that proteins are directly exposed to the same reactive species released by inflammatory cells, which degrade the polymer.

High molecular weight PEC (Mw 242 kDa) was evaluated as a secondary coating for a drug eluting stent for "on demand" delivery of paclitaxel, a small antiproliferative drug [142]. In this study, cytotoxicity tests showed excellent cytocompatibility of PEC. PEC was also found to be an amorphous polymer with elastic properties, and a high stress to strain failure of more than 600% when heated to 37°C. Dynamic Mechanical Thermal Analysis was utilized to obtain a T_g of 31.1°C. The use of PEC's special inflammatory cell-dependent degradation being applied as an "on demand" delivery stent coating is interesting, since the drug will be released at an inflamed implantation site upon direct contact with macrophages. This is based on the

assumption that an inflammatory response will precede reendothelialization. The use of high molecular weight linear PEC is appropriate in this application because to prevent restenosis the desired drug delivery period is relatively short.

1.6.2.5 Biodegradable Elastomers

Biodegradable elastomers have been applied to many different areas in controlled released, since they possess several advantages over linear uncrosslinked polymers. Thermosetting elastomers are not prone to creep, and therefore a porous architecture can be formed and maintained. This also means that device geometry may not change during degradation, potentially providing more predictable release when the release of the drug is controlled by diffusion. Also, different release kinetics are available with elastomers, including osmotic release. Examples of growth factors delivered from elastomers using osmotic release include VEGF, interferon-gamma (IFN-γ) and IL-2 [143]. While the release of these growth factors from the elastomers was constant until 60-80 % mass loss, there were issues with the bioactivity of released growth factors after 7 days when the polymer backbones were composed of hydrolysable linkages which degraded to produce acid byproducts[143].

Elastomers are most advantageous in applications where flexibility as well as drug delivering properties are desired, for example a biodegradable drug eluting stent, or as a tissue engineering scaffold for the regeneration of elastic soft tissue [26]. By adjustment of the crosslink density, the mechanical properties can be adjusted to the desired properties, matching the surrounding tissue of the drug delivery device and/or the elastic soft tissue that is to be regenerated, in the case of tissue engineering scaffolds [26]. The role of mechanical stimulation on the regeneration of elastic soft tissues has recently been well-established [144-148].

Examples of biodegradable elastomers applied to drug delivery include thermosetting star-poly(caprolactone-co-D,L, lactide) and star-poly(trimethylene carbonate-co-caprolactone) which were produced by photoinitiated free radical polymerization of acrylated star-shaped prepolymers [26]. Thermoplastic elastomer examples include copolymers of ε-caprolactone and 1,4-butanediamine, butyldiisocyanate, D,L, lactide, L-lactide, and 2,6-diisocyanato methyl caproate.

1.6.2.6 Fabrication of Porous Scaffolds

Depending on the biomaterial selected for the delivery device, a number of fabrication options are available to produce a porous matrix. It is a requirement of the proposed delivery device because porosity is expected to reduce the formation of the fibrous capsule since there is greater surface area for host cell infiltration meaning better integration into the tissue [149]. The fibrous capsule can also be a barrier to the diffusion of the drug.

While natural polymeric scaffolds are usually fabricated by freeze drying or crosslinking in aqueous environments, synthetic polymer scaffolds have been prepared by various methods including solvent casting, particulate leaching, phase separation, and electrospinning [31, 150]. One method of creating a porous scaffold involves freeze drying an emulsion solution of an organic polymer-containing phase dispersed in water, and this can give rise to porous scaffolds with various pore sizes and interconnectivities as demonstrated for the preparation of poly(lactide-co-glycolide) (PLG) scaffolds which have porosities up to 95% and pore sizes up to 200 μm [151].

The most convenient way to prepare a porous scaffold is to use solvent casting and particulate leaching. Using this method, the polymer is cast in an organic solvent mixture with a salt, and

then the solvent is evaporated. The salt is then dissolved in aqueous solution. Results show up to 93% porosity with open-cell morphology [31]. However, the limitations include that it may still contain residual salt particles, and that it is capable of making only thin scaffolds. PLG sheets produced in this way have been laminated into multi-layer structures [31]. Gas foaming in combination with particulate leaching has been evaluated as a porous fabrication technique [31, 152]. This method involves a binary mixture of polymer solvent gel containing salt particles, and is cast in a mold. Then it is immersed in hot water, whereby CO_2 gas is evolved and particulates leach out. Using this method, a highly porous network with high interconnectivity can been accomplished [31]. Particulate leaching is said to be the most convenient method for preparing porous material [150].

1.7 Summary

Therapeutic angiogenesis is a promising application of local protein delivery. However, there are many protein delivery problems that are commonly faced that must simultaneously be resolved in order to produce an efficient and safe delivery device to promote the production of new, functional and stable blood vessels. These issues include protein denaturation during fabrication or during polymer degradation, burst release and incomplete release.

PEC is an interesting polymer due to its special degradation mechanism, good biocompatibility and potentially beneficial drug carrier properties. The biggest advantage of using PEC is that, unlike the most commonly used synthetic polymers in drug delivery (polyesters, poly(ortho ester), polyanhydrides), it does not degrade to form acidic byproducts implicated in growth factor denaturation and tissue inflammation. However the degradation of linear PEC is inappropriately fast for angiogenic growth factor delivery since the release of bioactive angiogenic growth factor

must last for 3-4 weeks. Therefore the aim of this thesis was to develop photocrosslinkable PEC elastomers, test *in vitro* and *in vivo* degradation and *in vivo* biocompatibility, and to evaluate formulation parameters that may control the release of an example protein, bovine serum albumin, from porous PEC elastomer matrices. These experiments comprise the first steps in determining the potential of these porous PEC elastomers as biomaterials for angiogenic growth factor delivery and other applications.

Chapter 2

Scope of Research and Objectives

In overcoming the challenges of therapeutic protein delivery, there is a need to develop new biodegradable polymer systems for the delivery of protein therapeutics that maintain protein bioactivity, and delivers them locally to the site of interest within the therapeutic window to avoid systemic and overdose effects. There has been increasing interest in using biodegradable elastomers for this purpose [26] (for example, as an angiogenic growth factor delivery device for treating myocardial ischemia, or as a soft tissue engineering scaffold which promotes vascularisation). Poly(ethylene carbonate) is a promising polymer for these applications because it degrades by surface erosion [47, 139, 141] and unlike the commonly used poly(lactide-co-glycolide)[109], poly(orthoester)s [153], and poly(anhydrides) [55], it does not produce the acidic byproducts [133-135] implicated in protein denaturation [75] and tissue inflammation [117]. However, the degradation of linear PEC degrades too rapidly for these purposes. It is hypothesized that crosslinking this material would slow down the degradation to a more appropriate rate. This work proposes to create biodegradable PEC elastomers, to evaluate biocompatibility and degradation of this new biomaterial, and to conduct preliminary release studies using porous protein-loaded PEC elastomers.

The following objectives outline the scope of this research:

Chapter 3:

1. To prepare PEC elastomers with a range of crosslinking densities, and characterise them using NMR, DSC, ATR-FTIR, tensile testing. The elastomers were prepared by first producing

low molecular weight PEC which was functionalized to possess acrylated end groups, and then UV photocrosslinked. Photo-initiated crosslinking has the advantage of rapid reaction time, and low temperature, and therefore was more suitable for the incorporation of thermally sensitive protein therapeutics than other crosslinking methods.

Chapter 4:

2. Evaluate the *in vivo* biocompatibility of PEC elastomers using a rat model for up to 12 weeks.

3. Measure *in vitro* oxidative degradation of different crosslinking densities to test the hypothesis that oxidative degradation of these elastomers can be tailored based on prepolymer molecular weight.

4. Investigate *in vivo* degradation of PEC elastomer and non-crosslinked PEC in a rat model to test the hypothesis that PEC degradation can be decreased to become more appropriate for its intended applications by crosslinking. Degradation was analyzed by determining mass loss, water uptake, glass transition temperature, and surface morphology over 12 weeks.

Chapter 5:

5. Fabricate PEC elastomers to possess a porous architecture of interconnected pores, using low molecular weight poly(ethylene glycol), PEG, as a porogen. This PEG was selected as a porogen because it is water soluble, non toxic and therefore could be extracted once implanted in the body [30]. This was predicted to provide an extra parameter for release kinetics control.

6. Produce BSA-loaded porous PEC elastomers to be tested by an *in vitro* release study tracking the release of an example protein, BSA. The release of PEG during the course of this release study was also of interest. Several formulations were evaluated with the goal of determining formulation parameters that affect the release kinetics. BSA was used as a

preliminary screening protein as a step towards evaluating the new polymeric system for its potential as an angiogenic growth factor device.

Chapter 3

Preparation and Characterisation of Poly(ethylene carbonate) Elastomers

3.1 Introduction

Polycarbonates are a class of synthetic polymers that are a promising option as a vehicle device for protein delivery since they are one of the only synthetic polymers which do not degrade by hydrolysis to produce acid [133, 134, 138-140]. This acid has been implicated in the denaturation of protein therapeutics, like vascular endothelial growth factor [75], and can even cause tissue inflammation surrounding the implant [117].

While linear poly(trimethylene carbonate) has good biocompatibility and an appropriate *in vivo* degradation rate, it is prone to creep[35, 48, 49, 136, 154]. Since there are many advantages of using biodegradable thermosetting elastomers for flexible protein delivery devices, star-PTMC was crossslinked to form an elastomer but its *in vivo* degradation rate was found to be too slow for many drug delivery and tissue engineering scaffold applications [35]. Linear poly(ethylene carbonate), PEC, which also has shown good biocompatibility, has an *in vivo* degradation rate that is much faster (complete degradation in 2-3 weeks), however it is too rapid for these applications [138-140]. It is anticipated that the degradation rate can be adjusted to a more appropriate level by crosslinking.

Therefore, the main goals of the work presented in this chapter are to prepare PEC-based elastomers of different crosslink densities, characterise prepolymers and elastomers in terms of molecular weight, composition, glass transition temperature, and sol content, and demonstrate that the elastomers prepared from a range of different prepolymers possess different crosslink densities (molecular weights between crosslinks).

3.2 Materials and Methods

Linear poly(ethylene carbonate) (M_w = 60 kDa) was purchased from Empower Materials, Delaware, USA (copolymerization scheme found in Appendix A, Figure 7-1). Ethylene glycol, tin(II)-2-ethyl hexanoate (96%), acryloyl chloride (96%), 4-(dimethylamino)pyridine, triethylamine (99.5%), 2,2-dimethoxy-2-phenyl-acetophenone (99%), dioxane, and magnesium sulphate were purchased from Sigma-Aldrich (Canada). Dichloromethane (DCM), ethanol, methanol, were purchased from Fisher Scientific (Canada). DCM was dried over calcium hydride and distilled under argon. Dimethyl sulfoxide-D6 (DMSO) and deuterated chloroform ($CDCl_3$) for proton nuclear magnetic resonance (^{1}H-NMR) were purchased from Cambridge Isotope Laboratories Inc. (USA).

3.2.1 Depolymerization to Produce Low MW PEC Diol

In order to produce a series of poly(ethylene carbonate) (PEC) elastomers with different crosslink densities, a range of low molecular weight PEC diols was prepared. This was done via depolymerization of 60 kDa linear PEC according to a method outlined by Sant'Angelo *et al*. Ring opening polymerization of ethylene carbonate is not an option due to the positive enthalpy of polymerization [140, 155]. Depolymerization is necessary because the current processes for making PEC (copolymerization of CO_2 and ethylene glycol) cannot produce polymers with

molecular weights lower than 50 kDa [156], while the molecular weight range of interest for this project is 2,000 to 10,000 Daltons. PEC diol above 10,000 Daltons cannot be easily acrylated to a high degree due to more limited end-group mobility and dilution of the functional groups.

The depolymerization mechanism occurs by "unzipping" at polymer chain ends to produce ethylene carbonate and shorter chain PEC. Removal of ethylene carbonate from PEC chain ends is possible due to thermal decomposition of the depolymerization catalyst to form a carboxylate, which is capable of producing alkoxyl-terminated PEC from hydroxyl-terminated PEC.

For each PEC depolymerization batch, 9-10 grams of PEC was cut into pieces of appropriate sizes for fitting into a dry glass ampoule. Tin(II)-2-ethyl hexanoate catalyst (1 mg of catalyst for every gram of polymer), and 5% ethylene glycol (EG) were added to the ampoule. The reaction ampoule was flame sealed under vacuum and placed in an oven for 30 to 200 minutes at a set temperature between 130 ºC (melt flow temp) to 170 ºC (safely below the degradation temp of 240 ºC), depending on the desired final molecular weight of the diol. In order to calibrate this method such that a target molecular weight could be achieved by selecting a certain reaction time and oven temperature, several batches of PEC were prepared for each temperature and reaction time was varied. Once a temperature was selected that was most appropriate for the molecular weight range of interest, the reaction time was altered to produce PEC diols with a range of molecular weights. To purify the low molecular weight PEC diol to remove low molecular weight glycols (including EG), the ampoule contents were dissolved in 75 mL DCM. This solution was added drop-wise into 200 mL of stirred methanol in order to precipitate the polymer. For target molecular weights of less than 3000 Da, methanol was chilled over dry ice prior to precipitation.

An estimate of the number average molecular weight was obtained by proton nuclear magnetic resonance spectroscopy (^{1}H-NMR) (on a 400 MHz Bruker-Avance spectrometer) using end-group analysis. To confirm the location of the terminal hydroxyl peak, whose position can shift depending on pH and temperature [157], ^{1}H-NMR was run in DMSO-d_6 as well as $CDCl_3$. ^{1}H-NMR was conducted before and after the purification to check for a reduction in the level of EG. To confirm this method of using NMR for a relative measure of molecular weights for a series of depolymerized PEC, GPC was also conducted for a random selection of depolymerized samples using a measured value of the differential index of refraction for 60 kDa linear PEC in acetonitrile. The column (Phenogel 5um M3 mixed bed followed by a Phenogel 5um 10^3A, both being 300 x 7.8mm from Phenomenex, in line with a Phenogel 5um 50x7.8mm guard column) was run in acetonitrile (30°C, 1ml/min, 100 μL, double injections).

3.2.2 Acrylation of Low MW PEC to Form Diacryl Prepolymer

Once the low molecular weight PEC was purified and dried to a constant mass to remove residual methanol, terminal hydroxyl groups were acrylated with acryloyl chloride (AC) in order to introduce UV-crosslinkable end-groups. 4-(dimethylamino)pyridine (DMAP) was used as the catalyst, and triethylamine (TEA) as the proton scavenger. Several measures were put into place to ensure that exposure to humidity was minimal. The reaction was conducted in a controlled atmosphere chamber that was purged several times with nitrogen. The DCM used as the reaction solvent and to dilute AC was distilled the day before each reaction. Also, magnesium sulphate was added to the polymer solution and left in overnight to absorb any water that was contained in the polymer. All glassware was oven-dried overnight before use.

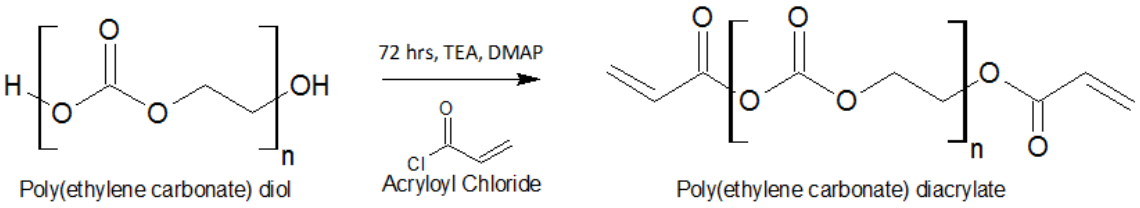

Figure 3-1: Structure of α, ω-diacrylate poly(ethylene carbonate) PEC and the acrylation procedure

The night before each reaction, 100 mL of distilled DCM was added to a 7-9 gram batch of PEC diol, and 0.25 grams or less of magnesium sulphate was added. This suspension was left overnight in the dry box to allow PEC to dissolve in the DCM. Immediately before addition of reactants, the polymer solution was filtered (in the dry box) to remove the magnesium sulphate. DMAP catalyst was added at a molar ratio of 1×10^{-3} mole per mole of PEC terminal hydroxyl group [158]. The amount of AC added was in excess at 1.5-2.0 moles of AC per mole of terminal hydroxyls in the prepolymer in case EG, methanol, or water was present. AC was also diluted 2-5 times with DCM before addition. Due to the presence of a competing side reaction that produces a brown colour (and would reduce the purity of the product and the efficiency of UV crosslinking due to light scatter), the amount of TEA was kept to only 1.5 times the molar amount of terminal hydroxyls. Once filtered and all reactants added, the reaction mixture was left in the dry box to react for 3 days. On the third day, the reaction solution was removed from the dry box, evaporated to 75 mL and added dropwise into 200 mL ethanol to remove unreacted AC and TEA and colour (the TEA-polymer complex). For target molecular weights of less than 3000 Da, the ethanol was chilled over dry ice before the precipitation step.

Proton Nuclear Magnetic Resonance spectroscopy (^{1}H-NMR) in both DMSO and $CDCl_3$was conducted on samples before and after purification to determine purity and the degree of acrylation. The following equation was used to determine the degree of acrylation:

$$Degree\ of\ Acrylation\ (\%) = \frac{I_{acrylate}}{I_{acrylate} + I_{hydroxy}} \times 100 \qquad \textit{Equation 3-1}$$

3.2.3 UV Crosslinking to Produce PEC Elastomers

To produce PEC elastomers, α,ω-diacrylate PEC and the photoinitiator (2,2-dimethoxy-2-phenyl-acetophenone, (DMPA)) were dissolved in dioxane (3 g PEC diacrylate/mL). DMPA is commonly used to initiate the radical polymerization of acrylated biomaterials and is a potent initiator [159, 160] (Appendix A, Figure 7-2). After being mixed and kneaded thoroughly, the sticky solid pre-elastomer was spread into a mold and exposed to UV light (320-480 nm) for several minutes per side to produce a 1 mm thick film of PEC elastomer (Appendix A, Figure 7-3). The mold was covered with a glass slide to shield the surface from oxygen, which may quench free radicals.

It was anticipated that many factors would affect the efficiency of the photo-crosslinking step, which was reflected in the soluble (sol) content measured. The three factors investigated were polymer concentration, initiator amount, and time of exposure to UV light. Therefore, a 2^3 factorial experiment was designed to help decide which conditions of UV photo-crosslinking should be used for preparation of future elastomers in order to minimize the sol content.

It was expected that a higher UV light intensity would produce elastomers with lower sol content, however, since the ultimate application of these elastomers is for protein delivery, crosslinking at or below 30 mW/cm^2 was used since it has been shown that this intensity does not affect vascular endothelial growth factor bioactivity significantly [161]. For all elastomer experiments, only PEC batches with an acrylation of over 80% were used.

Table 3-1 outlines the runs used in this 2^3 factorial experiment to determine the minimum sol content that can be obtained within the ranges of each factor tested. Linear regression was conducted on JMP statistical software to determine parameter estimates and their significance/confidence interval.

Sol content was removed from crosslinked PEC elastomers by immersing them in DCM overnight then replacing the DCM and repeating at least three times. Then elastomers were placed in a vacuum oven until constant mass was achieved. The sol content was calculated by comparing the mass of elastomers immediately after crosslinking to the mass after sol removal according to Equation 3-2.

Table 3-1: 2^3 full factorial experiment for determining the best UV crosslinking conditions

Run #	PEC Concentration in Dioxane (g/ml) X_1	Time (min) X_2	Initiator (w/w) % X_3
1	1.8 g/mL	2 min	1.5 %
2a	3.0 g/mL	2 min	1.5 %
2b	3.0 g/mL	2 min	1.5 %
2c	3.0 g/mL	2 min	1.5 %
3	1.8 g/mL	5 min	1.5 %
4	3.0 g/mL	5 min	1.5 %
5	1.8 g/mL	2 min	3.0 %
6	3.0 g/mL	2 min	3.0 %
7	1.8 g/mL	5 min	3.0 %
8	3.0 g/mL	5 min	3.0 %

$$Sol\ Content\ (\%) = 1 - \left(\frac{m_{dry}}{(m_{total} - m_{dioxane})}\right) \qquad \textit{Equation 3-2}$$

Where m_{dry} is the elastomer's mass after DCM washing and drying step

m_{total} is the total mass of the elastomer immediately after crosslinking

$m_{dioxane}$ is the mass of dioxane during crosslinking

As additional confirmation of successful crosslinking, surface chemistry was evaluated using attenuated total reflection Fourier-transform infrared (ATR-FTIR) spectroscopy (Nicolet 6700 spectrometer equipped with a diamond crystal).

3.2.4 Mechanical Testing of PEC Elastomers

Uniaxial tensile measurements of the elastomers were obtained to ascertain the elastomer mechanical properties. A range of five different prepolymer molecular weights, spanning the range of interest for all other experiments of this project (2,000 to ~15,000 MW) were selected for Young's modulus measurements. These elastomers were prepared into films using a 1 mm mold spacer as described above. A micro-dogbone punch was used to produce dogbone films (each a total length of 8.8 mm, ends were 4.1 mm wide tapering to 1.2 mm in the middle of the sample). This punch was manufactured with dimensions scaled down from Type V ASTM D638-02 punch dimensions (Standard Test Method for Tensile Properties of Plastics, since the punch was designed for testing both linear PEG and elastomers PEC). An Instron uniaxial tensile tester model 4443 was used for measuring mechanical properties, with a crosshead speed of 500 mm/min, as outlined in ASTM D412 (Standard Test Methods for Vulcanized Rubber and Thermoplastic Elastomers – Tension). Merlin 4.11 Series IX software package was used for data analysis as well as the calculations outlined in ASTM D638-02 for determining Young's

Modulus. Uniaxial tensile measurements were conducted in triplicate for each molecular weight and for elastomers before and after sol removal. Sol was removed as described above. Stress and strain at break were also recorded for a select number of elastomers and linear PEC to gauge the extensibility. Differential Scanning Calorimetry (DSC) was also used to characterise the thermal properties of PEC elastomers (Mettler Toledo, DSC1). Glass transition temperature, T_g, was also of interest to anticipate the flexibility *in vivo* (ie. at body temperature, 37°C). A heating ramp from -80°C to 130°C, repeated twice, was utilized to determine the T_g for 6000 MW PEC diol, diacrylate, and elastomer. In case the sample contained residual water or solvent, the T_g was obtained from the second heating cycle.

3.3 Results and Discussion

3.3.1 Depolymerization to Produce Low MW PEC Diol

A range of low molecular weight polymers was accomplished by depolymerization of 60 kDa linear poly(ethylene carbonate) (PEC) with a tin catalyst and ethylene glycol (EG) at temperatures from 130°C to 170°C. To estimate the number average molecular weight ($\overline{M_n}$) of the depolymerization products, ^{1}H-NMR end-group analysis was used according to Equation 3-3. ^{1}H-NMR conducted in $CDCl_3$ confirmed the location of the hydroxyl peak (see Appendix A, Figure 7-4).

$$\overline{M_n}\,(estimate) = \#\ Repeating\ EC\ Units\ \times MW_{ECU} = \left(\frac{\frac{I_{ECU}}{4}}{\frac{I_{OH}}{2}}\right) \times MW_{ECU} \qquad \textit{Equation 3-3}$$

Where I_{ECU} is the integration of the backbone ethylene carbonate unit proton peak,

I_{OH} is the integration of the terminal hydroxyl proton peak,

MW_{ECU} is the molecular weight of one repeating unit of ethylene carbonate.

Equation 3-3 assumes that the structure of PEC was ideal (that is, composed only of ethylene carbonate linkages). However, it has been reported [140] and confirmed herein using the ^{1}H-NMR spectra that the copolymerization of ethylene oxide and carbon dioxide used to produce the starting material PEC results in a polymer composed of ethylene carbonate and ethylene oxide regions. The ^{1}H-NMR spectra show signals at 4.35 ppm, which correspond to ethylene carbonate units (ECU), at 4.25 ppm and 3.65 ppm, which correspond to incorporated ether functions (IEF), and at 3.55 ppm for ether functions (EF) as indicated in Figure 3-2. A representative ^{1}H-NMR spectrum is found in Figure 3-3.

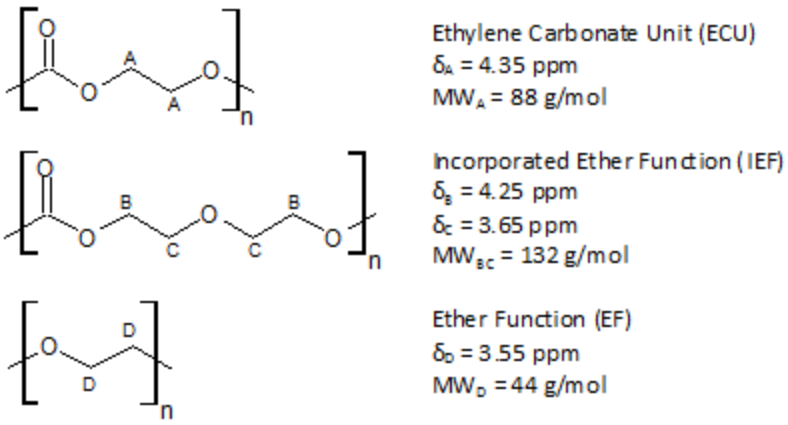

Figure 3-2: Constitutional units in poly(ethylene carbonate).

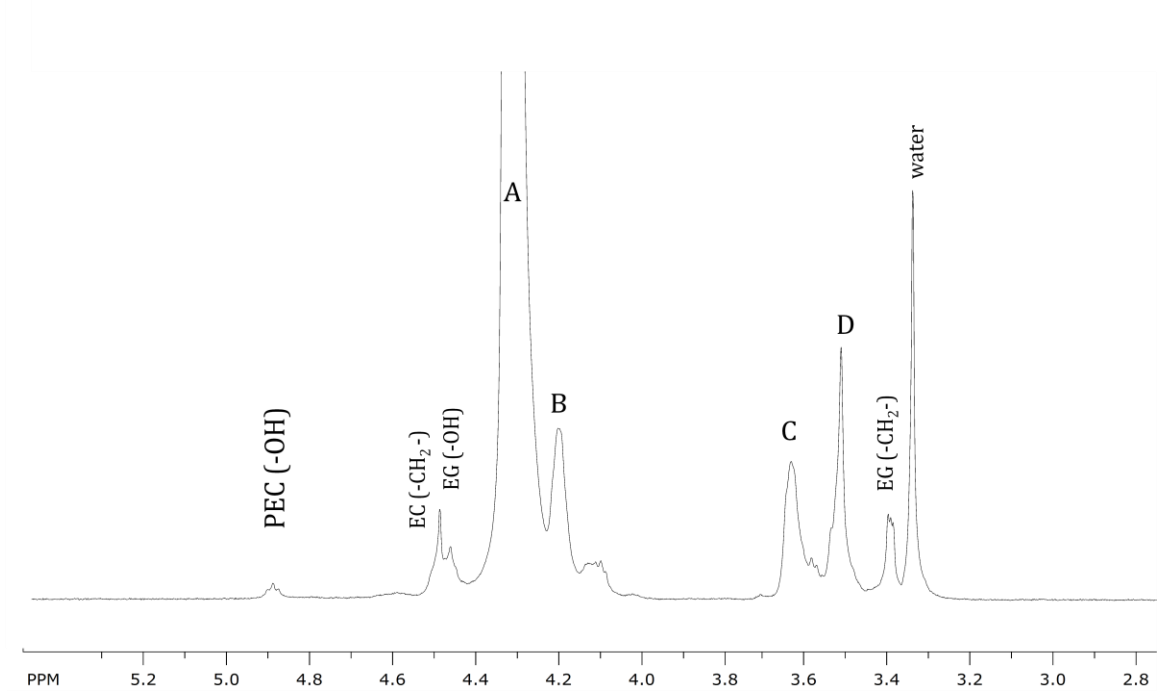

Figure 3-3: NMR spectroscopy of PEC diol after depolymerization and purification, in DMSO. Peaks indicate presence of ethylene carbonate functions, incorporated ether functions, and ethylene oxide functions. "EC" = ethylene carbonate, "EG" = ethylene glycol.

Therefore, the following equations can be used to more accurately calculate the molecular weight from ^{1}H-NMR spectra:

$$\overline{M_n} = \#\ Repeating\ Units \times MW_{RU} \qquad \textit{Equation 3-4}$$

$$\#\ Repeating\ Units = \frac{Backbone\ protons}{Terminal\ protons} = \frac{\left(\frac{I_A}{4} + \left(\frac{I_B}{4}\ OR\ \frac{I_C}{4}\right) + \frac{I_D}{4}\right)}{\frac{I_{OH}}{2}} \qquad \textit{Equation 3-5}$$

$$MW_{RU} = Weighted\ average\ of\ 3\ possible\ constitutional\ units \qquad \textit{Equation 3-6}$$

$$= \left(\left(\frac{I_A}{4}\right) * MW_A\right) + \left(\left(\left(\frac{I_B}{4}\right) * MW_{BC}\right) OR \left(\left(\frac{I_C}{4}\right) * MW_{BC}\right)\right) + \left(\left(\frac{I_D}{4}\right) * MW_D\right) \qquad \textit{Equation 3-7}$$

The estimate of number average molecular weight (Equation 3-3) was used when setting up the calibration of the depolymerization, where a relative measure of $\overline{M_n}$ was of interest to compare the extents of depolymerization of different batches. However, for characterising the low molecular weight PEC diols to be used in subsequent experiments, the $\overline{M_n}$ in Equation 3-4 was used.

A range of temperatures between 130°C to 170°C was investigated when calibrating this method. Depolymerization at low temperatures close to the melt flow temperature (130°C) was initially of interest since a less steep depolymerization profile over time would be expected and therefore better control over the resulting molecular weight would be obtained. However, the products from depolymerization at 130°C and 150°C possessed molecular weights that were too high for this project (above ~10,000 Da). It should be noted that for values much higher than 10,000 Da, ^{1}H-NMR end-group analysis does not yield an accurate measure of molecular weight. Therefore, only molecular weights determined to be below 10,000 Da were reported with the exception of one at approximately 15,000 Da, which was confirmed using GPC.

Depolymerization at 130°C and 150°C tested here, (at least up to 130 minutes) are well above this limit and so future depolymerization batches were made at higher temperatures. On the other hand, depolymerization at 160°C from 60 to 200 minutes produced PEC diol in the range of interest, as can be seen in Figure 3-4. At 170°C, the depolymerization products were 1,000 Da and 1,800 Da for 60 and 110 minutes, respectively, which are too low for the purposes of this project. Therefore 160°C was chosen as the oven temperature to be used for obtaining PEC diol in the range of 3000 to 8000 Da.

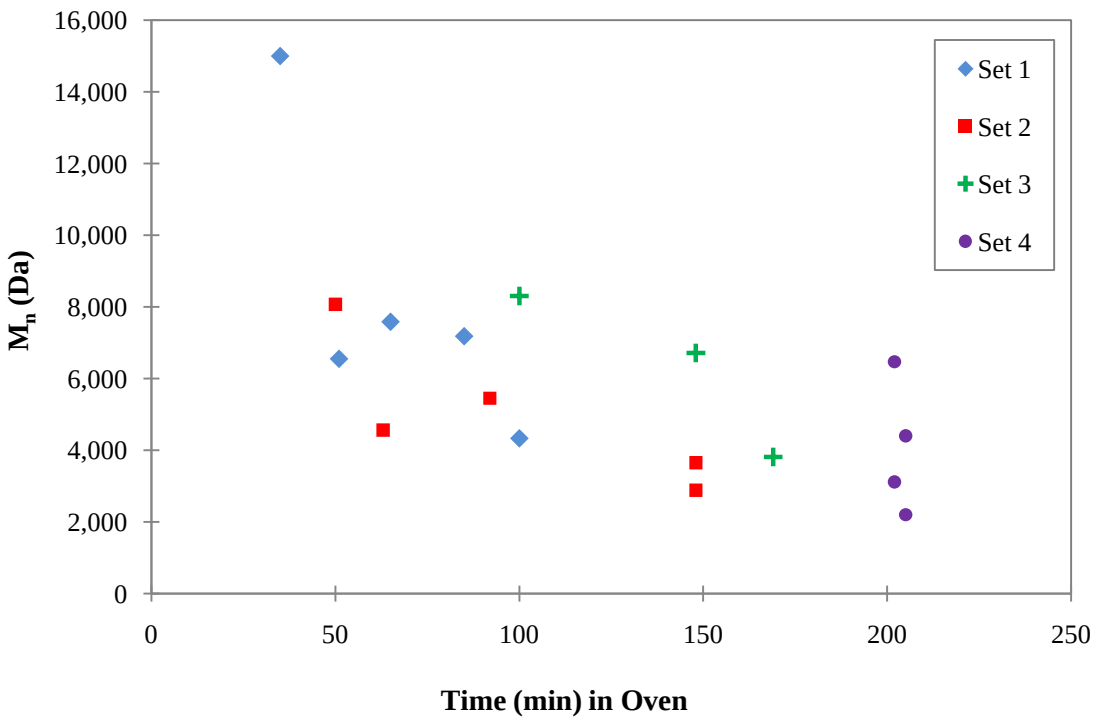

Figure 3-4: Depolymerization of linear poly(ethylene carbonate) at 160°C from 30 to 200 minutes.

The goal of these depolymerization experiments was to obtain a calibration curve which could be used to produce a target molecular weight polymer. However, Figure 3-4 provides only a guideline for the time required to produce a certain molecular weight since there is considerable variability in possible molecular weights at one time point. Each batch set was prepared together and depolymerized on the same day, but Sets 1 to 4 were conducted on four different days. Since there seems to be tighter control when one looks at a single day's data alone, the variability in Figure 3-4 may be due to variations in day-to-day factors such as precise oven temperature, the size of polymer pieces loaded into ampoules, thermal cycling as the oven attempts to maintain the setpoint temperature, and precise location in the oven. Table 3-2 describes the distinct visual changes in cooled ampoule contents that PEC undergoes at 2000-3000 Da and at 6000 Da. It is recommended that after Figure 3-4 is used as a guideline, Table 3-2 is used to make sure that the desired molecular weight is being approached and if not, to adjust the time in the oven.

Table 3-2: Visual observations to aid in PEC depolymerization to a target prepolymer molecular weight.

Target Prepolymer M_n	Visual Observation Once Cooled	Suggested Oven Temp/Time
< 2000 Da	Transparent, flows at room temperature	170 ºC for > 50 minutes
3000-6000 Da	Translucent, tacky solid	160 ºC for 125 to 250 minutes
> 6000 Da	Opaque, solid	160 ºC for < 125 minutes

^{1}H-NMR was used to confirm that the purification method for the low molecular weight diol is effective in reducing the level of ethylene carbonate (EC) and ethylene glycol (EG), which are by-products of the degradation process. Analysis of the ^{1}H-NMR also showed that there was significant reduction in the levels of EG and EC after purification to 2-5 % wt. In the future it is recommended that the step of purifying the depolymerized polymer by precipitation be repeated several times so as to more fully remove EG and EC.

For the batches of low molecular weight PEC which were used in subsequent experiments, the number average molecular weight was calculated using both Equation 3-3 and Equation 3-4. The ratio of ethylene carbonate units (ECU) was calculated to confirm that it is high for all batches of PEC used for subsequent experiments. The content of ether functions (EF) and incorporated ether functions (IEF) often given in the literature. This data is summarized in Table 3-3.

$$ECU\ (\%) = 100 \times \left(\frac{I_A}{(I_A + I_B + I_C + I_D)}\right) \qquad \textit{Equation 3-8}$$

$$EF\ (\%) = 100 \times \frac{(I_A + I_B)}{(I_A + I_B + I_C + I_D)} \qquad \textit{Equation 3-9}$$

$$IEF\ (\%) = \ 100\ \times \frac{I_C}{(I_A + I_C)} \qquad \textit{Equation 3-10}$$

It is noted that the rounded number average molecular weight obtained by simply using the ratio of ethylene carbonate backbone protons to terminal hydroxyl protons and the molecular weight of the repeating unit of PEC is a very good estimate of the true number average molecular weight, which considers ECU, EF, and IEF. For the remainder of this report, the rounded estimate will be used to identify batches for simplicity of labeling.

Table 3-3: Characterisation of low MW PEC diol used in subsequent experiments.

Batch ID#	**Mn (Da) estimate**	**Mn (Da) considering ECU, EF and IEF content**	**ECU %**	**EF %**	**IEF %**
1	2,000	2,100	82.4	10.5	7.9
2	3,000	3,100	83.1	11.1	8.2
3	5,500	5,600	88.6	7.8	4.0
4	6,000	6,100	89.1	6.8	4.4
5	6,500	6,700	89.9	6.8	3.4
6	8,000	8,100	89.7	6.8	3.8
7	15,000	15,100	90.7	6.3	3.2

As expected, batches that were depolymerized to a greater extent (have a lower $\overline{M_n}$) possessed a lower ratio of ethylene carbonate units, since it is these regions whereby the molecular weight is reduced, producing EG and CO_2. Despite a higher ethylene oxide content compared to other batches, the batch with the lowest ECU tested is still very high (82.4%) and therefore results from biocompatibility and degradation studies reflected PEC properties.

3.3.2 Acrylation of Low MW PEC to Form α,ω-Diacrylate Prepolymer

Batches of PEC that had been used to make elastomers for all experiments contained in this report are found in Table 3-4, which summarizes the degree of acrylation and colour after acrylation and purification. The degree of acrylation was calculated as outlined in Equation 3-1 based on the appearance of acrylate group peaks at $\delta = 5.95 – 6.33$ ppm and the disappearance of the terminal hydroxyl peak at $\delta = 4.93$ ppm in the ^{1}H-NMR spectra (see Figure 3-5). With the exception of batch 2, a degree of acrylation of above 95% was achieved for all batches listed. Since higher MW diols are more difficult to acrylate (due to reduced chain mobility and end group dilution), the first attempt to acrylate the 15,000 MW diol was relatively unsuccessful (only 65%). However, after purification, this batch was re-acrylated by following the same steps again and the result was 98% acrylation. The acrylation reactions for several batches that were not used in subsequent experiments were considered unsuccessful (40-85%) likely due to variably high humidity (due to weather), and inefficient removal of ethylene glycol or methanol prior to reaction. There were also numerous acrylation reactions that were considered unsuccessful (despite up to 100% acrylation) due to the presence of a strong orange-to-brown colour which could only be partially removed by post-reaction purification (even after three repeated purification cycles). This colour was present to much less significant extents in successful reactions (*i.e.* batches used for experiments) as well and is believed to be a sign of the formation of a complex between TEA and PEC [162].

Table 3-4: Properties of PEC Diacyl Batches used in All Experiments.

Experiment Name	Batch ID#	Mn (Da) estimate	Degree of Acrylation (%)	Colour	Average Sol Content (%)
Minimize Sol Content	5	6,500	100	light yellow	6 (4 to 10)
Mechanical Testing	1	2,000	96	white	< 5
	2	3,000	88	light yellow	>10
	3	5,500	100	light yellow	< 5
	6	8,000	100	yellow	20
	7	15,000	65, 98	yellow	Not Avail.
In vitro Ox Deg	1	2,000	96	white	5
	5	6,500	100	light yellow	5
	6	8000	100	yellow	20
In vivo Degradation & Biocompatibility	4	6,000	99	white	< 5
Porous Fabrication	2	3,000	88	light yellow	Not Applic.
BSA Release Study	1	2,000	96	white	Not Applic.

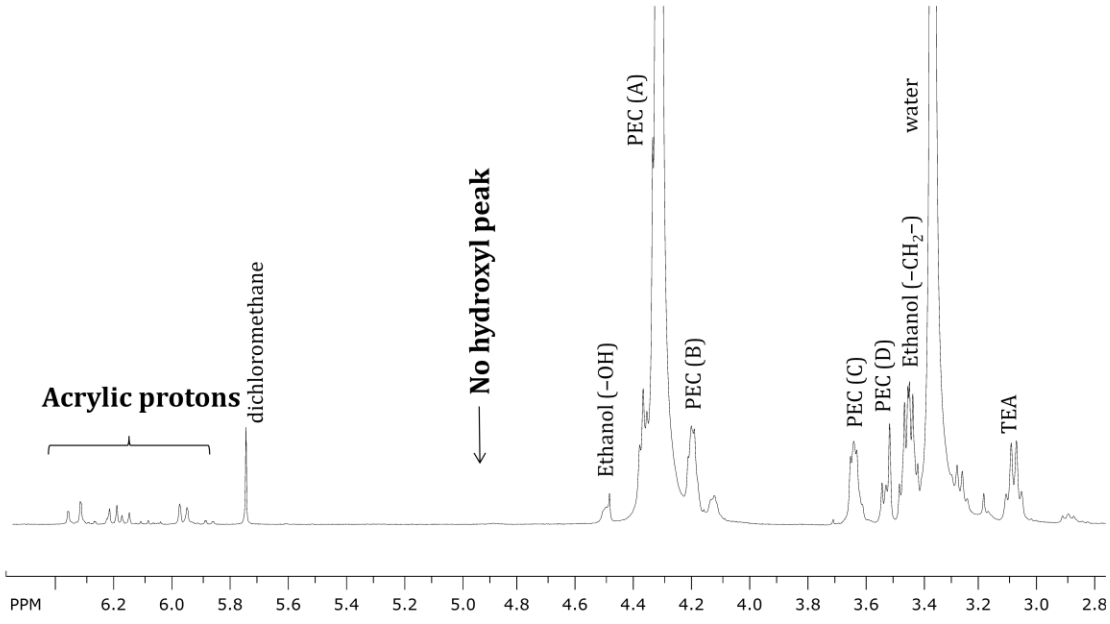

Figure 3-5: NMR spectrum of diacrylated PEC. Note that acrylated group protons present and that there is no peak at 4.9ppm to correspond to the terminal hydroxyl peak, (100% acrylation).

3.3.3 UV Crosslinking to Produce PEC Elastomers

A 2^3 factorial experiment was conducted to determine which conditions of polymer concentration, intitiator amount, and time of exposure to UV light should be used for future UV crosslinking. Before conducting the experiment, the effect that polymer concentration would have on sol content was unknown. A more dilute polymer concentration would dilute free radicals (reducing crosslinking efficiency), but on the other hand a more concentrated polymer concentration would increase the viscosity, impeding the migration (therefore propagation) of the free radicals which are situated at polymer chain ends (reducing crosslinking efficiency). For initiator amount, a higher concentration of initiator provides more opportunity for initiation and results in a higher concentration of free radical end groups during initiation stage. However, the amount of initiator should be kept to a minimum to ensure that there are minimal biocompatibility issues due to initiator. Time was suggested to affect crosslinking completion since more time would allow more decomposition of initiator into free radicals (up to a certain point), however the time exposure to UV light should be kept as short so as to not affect protein stability.

Using the statistical analysis software JMP, linear regression was performed on the Table 3-5 results of UV crosslinking at two levels of each of polymer concentration, time of UV exposure, and amount of initiator. Triplicates were performed for Run #2 (3.0 g PEC per mL dioxane, 2 min UV exposure per side, 1.5wt% of DMPA) to take reproducibility into consideration.

Table 3-5: Results for the UV crosslinking experiment to determine the minimum sol content attainable within the levels tested.

Run #	Sol Content (%), y	PEC Concentration in Dioxane (g/mL), x_1	UV Time (min), x_2	Amount of Initiator (wt %), x_3
1	6.1	1.8	2	1.5
2a	3.7	3.0	2	1.5
3	7.8	1.8	5	1.5
4	5.0	3.0	5	1.5
5	7.4	1.8	2	3.0
6	4.1	3.0	2	3.0
7	9.7	1.8	5	3.0
8	6.1	3.0	5	3.0
2b	6.4	3.0	2	1.5
2c	4.7	3.0	2	1.5

Table 3-6: Results of parameter estimates for the linear regression of UV crosslinking experiment

Term	Estimate	p
X_1	-2.0364	0.0163
X_2	0.4146	0.1433
X_3	0.3958	0.4522

There is no effect of UV time exposure or initiator amount given the ranges tested ($p > 0.05$). However, there may be an effect of polymer concentration in dioxane ($p = 0.0163$). A negative parameter estimate indicates that 3.0 g/mL may have been better than 1.8 g/mL for crosslinking efficiency and therefore, 3.0 g/mL was used for all further crosslinking of PEC. Since the ultimate desired application of this material is for protein delivery, as a precaution to prevent denaturation of protein, 2 minutes per side was chosen for future elastomer batches. Since 1.5% initiator is sufficient, the minimal level was chosen, recognizing that higher photoinitiator amounts may affect biocompatibility.

For each of the PEC elastomers batches used in subsequent experiments, the sol content measured is found in Table 3-4. Sol content is a measure of the efficiency of crosslinking, and with several exceptions, was quite low (usually 5%). It is not surprising that for batch #2 (3000 MW) the sol content is 10% since the degree of acrylation for this batch was only 88%. Sol content for batch #7 was not available due to significant polymer loss against glassware due to sticking during sol removal, which is a sign of high sol content. It is reasonable that batches with a stronger yellow color (batches 6 and 7) have higher sol contents because the UV light during crosslinking could not penetrate through the prepolymer sample depth, but these batches also have a higher molecular weight and therefore the lower sol contents could be also due to higher viscosity during the crosslinking impeding the movement of radical chain ends. Sol content was not measured for batches used in the porous fabrication or BSA release study because the soluble portion was not solely a measure of uncrosslinked material considering the high content of low molecular weight (and therefore soluble) porogen.

As another confirmation of successful crosslinking, the ATR-FTIR results for diacrylated PEC showed a band at 1650 cm^{-1} (corresponding to the acrylate groups) which was not present when ATR-FTIR was conducted on PEC elastomers (see Appendix A, Figure 7-5).

3.3.4 Mechanical Properties of PEC Elastomers

Based on the equation below, which is derived from rubber elasticity theory, Young's Modulus is directly proportional to crosslink density, and inversely proportional to the molecular weight between crosslinks. Thus, low molecular weight PEC diacryl prepolymers, which should result in PEC elastomers with a low molecular weight between crosslinks, will have a high Young's Modulus and will be stiffer.

$$E = 3RT(n) = 3RT(\frac{\rho}{\bar{M}_c}) \qquad \textit{Equation 3-11}$$

Where E = Young's Modulus

R= gas constant

T = temperature

n = crosslink density

ρ = polymer density (1.42 g/cm^3, obtained from Empower Materials)

$\bar{M}_c$ = average molecular weight between crosslinks

The Young's modulus for each of the five PEC elastomers batches before sol removal can be found in Figure 3-6. As expected, PEC prepolymer possessing a lower molecular weight was stiffer, therefore has a higher Young's modulus and, according to Equation 3-11, a higher crosslink density. Furthermore, when fitted with a polynomial curve, Young's modulus is found to be approximately proportional to $\bar{M}_n{}^{-1}$ which is the relationship predicted by the rubber elasticity equation. This also implies that the molecular weight of the prepolymer is approximately equal to the molecular weight between crosslinks.

Sol was removed for all five batches of PEC elastomers, however only three sets produced dogbone shapes that were still intact. For the highest molecular weight (15,000 MW), after the DCM washes during drying, significant polymer had adhered to glassware and was not recoverable. The lowest molecular weight apparently exhibited a low tear resistance since it experienced enough swelling during the sol removal process that crack propagation from small bubbles caused the dogbones to break in half.

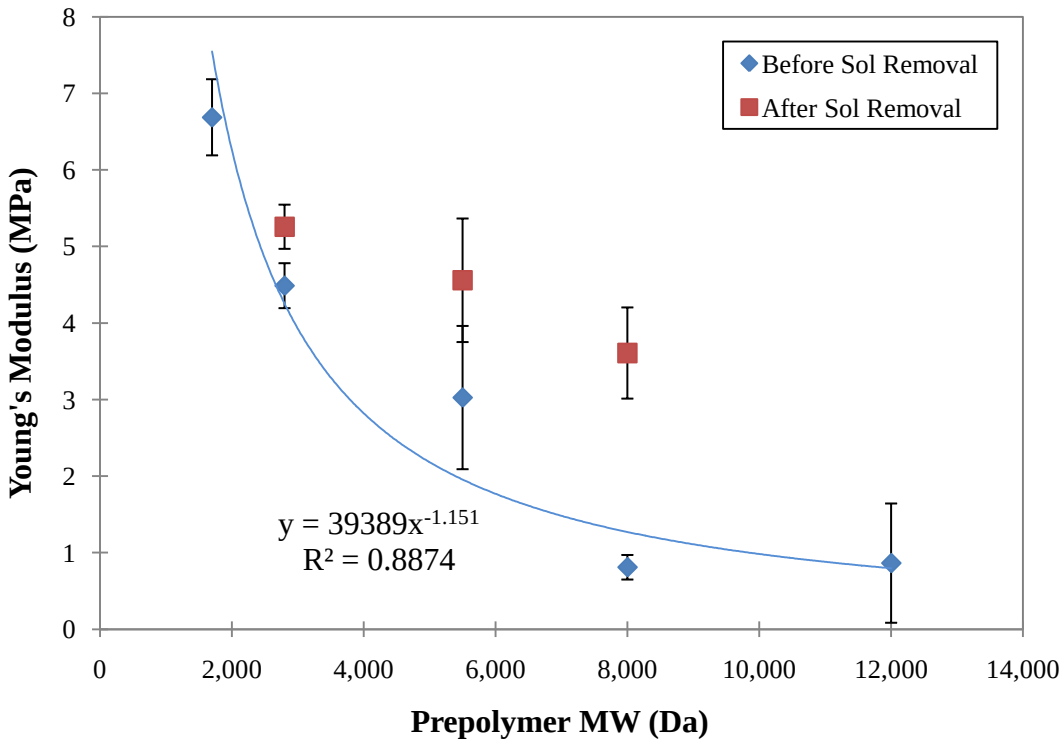

Figure 3-6: Young's modulus for five batches of PEC elastomers before and after sol removal. Data was fit using an power curve for "before sol removal". Insufficient data points were available to curve fit the "after sol" series. Error bars indicate 95% confidence intervals. N = 3.

The overall trend for Young's modulus compared to prepolymer molecular weight for the sol-free elastomers is the same as that for sol-containing elastomers – high molecular weight prepolymers result in more flexible material and vice versa. Due to the plasticizing effect of the soluble content, all values for Young's modulus increased after sol removal. The highest molecular weight (8000 MW) prepolymer had the largest increase in Young's modulus after sol removal, but it also had the highest sol content which may have been due to the stronger yellow color as compared to other batches (preventing UV light from fully transmitting the thickness of the sample), and may be due to the higher viscosity of the 3 g/mL PEC when it is made from a relatively higher MW.

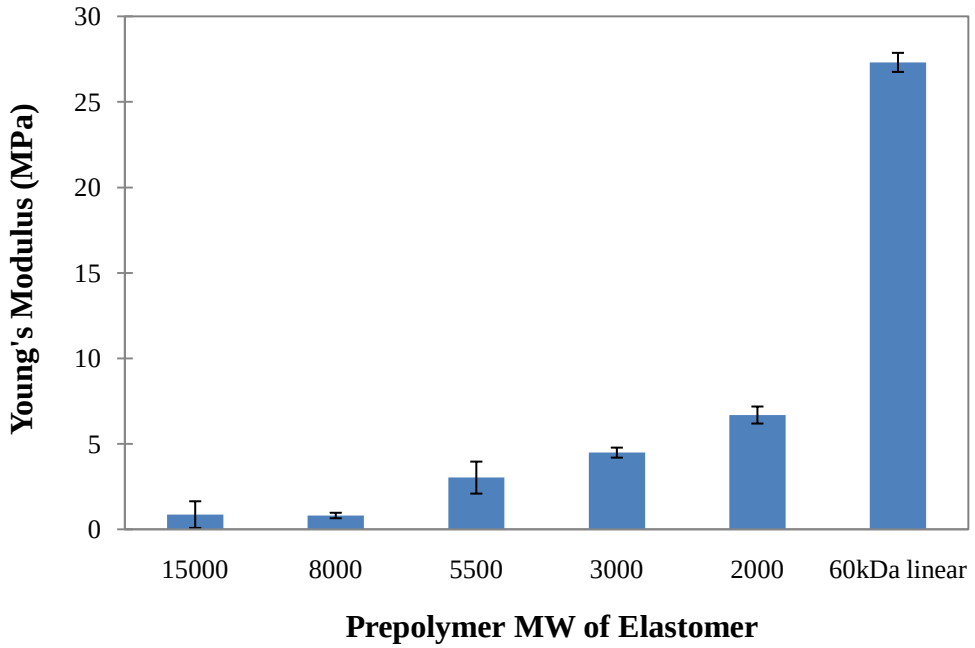

Figure 3-7: Young's modulus of PEC elastomer batches (before sol removal) compared to linear starting material, 60 kDa PEC. Error bars indicate the 95% confidence interval.

It is interesting to note that when the Young's modulus of elastomers is compared to that of the 60 kDa linear PEC starting material, it is apparent that PEC elastomers are not as densely crosslinked as linear PEC. The crosslinks of linear PEC are regions of physical interaction between polymer chains, not covalent bonds, and are therefore not permanent. There are many advantages to using the covalently crosslinked PEC, notably, it allows for a porous structure to be maintained during extraction of porogens. It is expected that strain is more fully recoverable with the elastomers than for linear PEC, which undergoes creep. There is evidence here that crosslink density can be used to tune one measure of the material's mechanical properties, which is relevant for the design of a biomaterial since surrounding tissue will respond differently depending on the mechanical properties of an implant [163]. Furthermore, it is hypothesized that the crosslink density can tailor the cyclic mechanical properties and the *in vivo* degradation rate and this has implications for the use of these elastomers in tissue engineering. The necessity of cyclic

mechanical stimulation in the growth of many elastic soft tissues has well been established[144-148,164, 165].

DSC results are found in Table 3-7. The T_g's for diol and diacrylate PEC (0.0°C and 10.7°C) indicate that they are very soft at room temperature. A possible explanation for the increase in T_g after acrylation is the number of extra purification steps which would have more efficiently removed low molecular weight plasticizing fractions. The T_g for the elastomer is 21.6°C and this increase further confirms successful crosslinking since the molecular weight goes from 6000 Da to essentially infinity. The fact that this temperature is below body temperature indicates that the elastomer will still be flexible when implanted.

Table 3-7: DSC results for 6000 MW diol, diacryl and elastomer.

	Tg (°C)
Diol	0.0
Diacrylate	10.7
Elastomer	21.6

As seen in representative tensile testing diagrams of linear PEC, Elast 5500, and Elast 8000 (in Figure 3-8) the shape of the stress-strain curve is characterised by a long period of linear deformation before rupture at the stress and strain at break points. No strain toughening is observed for elastomers. As expected, Elast 8000 is approximately 1.5 times more extensible than Elast 5500 (see Table 3-8). Linear 60 kDa PEC material is approximately 1.3 times more extensible than Elast 8000.

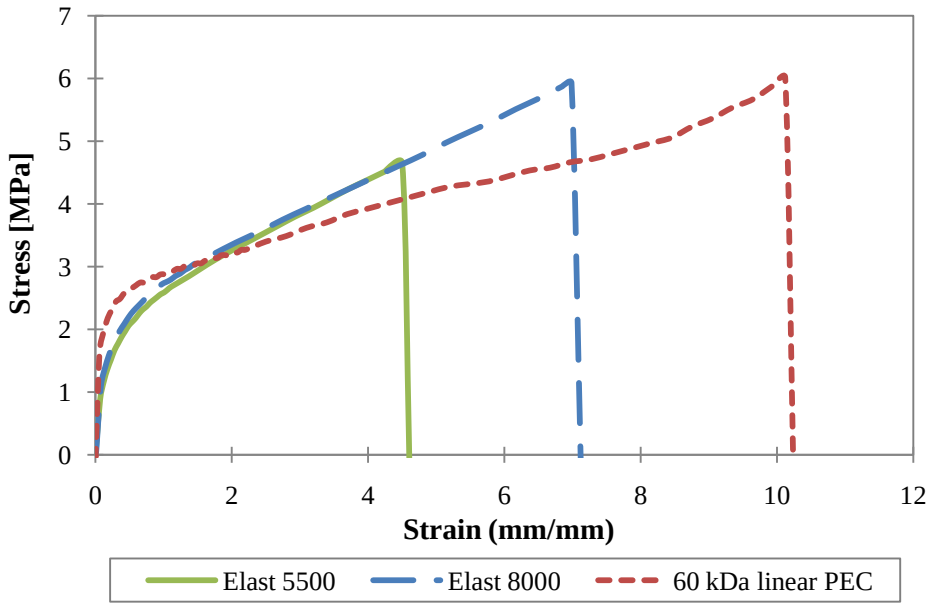

Figure 3-8: Representative stress-strain diagrams of linear non-crosslinked PEC, low crosslink density and medium crosslink density PEC elastomers.

Table 3-8: Stress and strain at break averages for linear PEC and elastomers. Averages reported ± standard deviation. N = 3.

	Strain at Break, ε_b	**Stress at Break, σ_B (MPa)**
60 kDa linear PEC	9.3 ± 1.0	6.2 ± 0.8
Elast 8000	7.1 ± 0.5	5.9 ± 0.7
Elast 5500	4.7 ± 0.9	4.9 ± 0.5

3.4 Conclusions

In conclusion, the depolymerization process was calibrated such that a target molecular weight of low molecular weight PEC (from 2,000 MW to 10,000 MW) can roughly be achieved. It has been confirmed that depolymerization using this method produces PEC with a high ethylene carbonate unit fraction of over 82%. 60 kDa linear PEC was successfully depolymerized, acrylated and crosslinked to produce a range of PEC elastomer crosslink densities for subsequent experiments. UV photoinitiatied crosslinking conditions were determined such

that sol content is low (~5%) and conditions are mild to prevent denaturation of protein drug during delivery experiments. It has been confirmed that PEC elastomers made from different prepolymer molecular weights possess different crosslink densities.

Chapter 4

Degradation and Biocompatibility of PEC Elastomers

4.1 Introduction

The first step in evaluating the potential of PEC as a new biomaterial is to determine its biocompatibility and degradation properties. The literature has shown that linear PEC degrades by a cell-mediated surface erosion mechanism [47]. Polymers that degrade by surface erosion are preferable to bulk eroding material because bulk erosion occurs by hydrolysis which produces acid implicated in protein denaturation [109] and tissue inflammation [117]. Also, surface eroding polymers can possess a more predictable and controlled release profile since bulk erosion can accompany the formation of cracks and crevices that may result in mechanical failure [41].

The degradation rate of linear PEC is too rapid (almost complete degradation in 2-3 weeks for >100 kDa) [138-140] for applications in angiogenic growth factor delivery since they require sustained deliver of the growth factor for 3-4 weeks [75, 79-81]. It was determined by Acemoglu *et al.* that molecular weight and ratio of ethylene carbonate units in the polymer backbone affect the rate of *in vivo* degradation. It is hypothesized that the degradation rate of PEC can be prolonged by crosslinking. Furthermore, it is predicted that the level of crosslink density (controlled by prepolymer molecular weight) and be used to tailor the degradation rate based on the application, as has been done for other crosslinkable biomaterials [166]. The focus of the following chapter is to evaluate the *in vitro* oxidative degradation, and the biocompatibility and degradation properties of the PEC elastomers after subcutaneous implantation into rats.

4.2 Materials and Methods

The materials for the oxidative degradation experiments included potassium superoxide, 18-crown-6-ether, and 6M HCl and were purchased from Sigma Aldrich (Canada). The inhibitor-free tetrahydrofuran (THF) was purchased from Acros Organics. Haematoxylin and eosin stains were purchased from Sigma (Canada) and Masson's trichrome staining kit (Accustain (R) Procedure HT15) was also purchased from Sigma Aldrich. Dichloromethane was purchased from Fisher Scientific.

4.2.1 *In Vitro* Oxidative Degradation

In vivo studies have shown that linear PEC degrades inappropriately fast for applications as a biomaterial for long term growth factor delivery or tissue engineering [138, 140]. To evaluate the hypothesis that the degradation rate of PEC can be prolonged by crosslinking and even tailored by the degree of crosslinking, an experiment was performed that measured *in vitro* oxidative degradation of PEC elastomers (as compared to linear PEC). Due to its structural similarity to poly(trimethylene carbonate)-based elastomers, (PTMC), which degrade predominantly by oxidative degradation [49, 167], oxidative degradation is expected to play a major role in the degradation of PEC elastomers. Stoll *et al.* have also reported that linear PEC was not hydrolysable and was unaffected by the presence of hydrolytic enzymes, however it was degraded by superoxide anion. Others have also found oxidative degradation playing a major role in carbonate containing polymers [168]. It has also been shown (based on infrared spectra) that the superoxide anion is present during the *in vivo* oxidative degradation of linear PEC [141].

Therefore, *in vitro* oxidative degradation of linear and crosslinked PEC was measured by superoxide anion in tetrahydrofuran (THF), a solvent that does not dissolve linear (or elastomeric)

PEC. The procedures from Lee *et al.* and Chapanian *et al.* were adapted, using a mixture of 0.01 M potassium superoxide (KO_2) in anhydrous, inhibitor-free THF. To enhance the solubility of potassium superoxide in THF, 0.002 M 18-crown-6-ether was also part of this oxidative degradation media. These conditions produce a high concentration of the superoxide anion [169] as described in Figure 4-1:

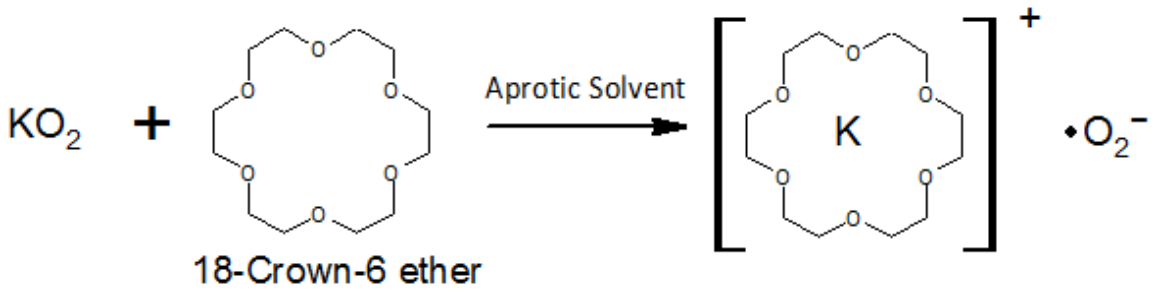

Figure 4-1: Potassium superoxide and 18-crown-6 ether in THF produce a high concentration of the superoxide anion.

All glassware was dried before use, and the balance was purged with nitrogen as KO_2 was being weighed. Every attempt was made to keep conditions dry because potassium superoxide easily absorbs water and reacts quickly to produce potassium hydroxide, accompanied by a change in color from yellow to white.

PEC elastomers were prepared by crosslinking PEC diacrylate batches (2100 MW, 6700 MW and 8100 MW) using the crosslinking conditions established in Section 3.3.3. Coupons for testing were cut using a biopsy punch to produce discs that were approximately 5 mm in diameter and 0.9 mm thick. The sol was extracted and calculated (as previously described) and then all discs to be tested were soaked in THF for 3 nights, changing THF once a day, to ensure that no THF-soluble components remained. The discs were then dried to a constant weight, added to oxidative

degradation media, and stirred on an orbital rocker for 1, 3, and 6 days. The oxidative degradation media was freshly prepared and exchanged (under argon) every two or three days, depending on whether the color of KO_2 was yellow or white.

When sampling after 1, 3, or 6 days, the discs were removed from oxidative media, acidified in approximately 0.5 mL of 6M HCl to terminate the superoxide reaction, washed three times in distilled water and then dried in a vacuum oven until constant weight. For each time point, discs were run in replicates of three or more. Statistical analysis for Day 3 and Day 6 mass loss data sets were conducted using one-way multiple comparisons ANOVA tests on KaleidaGraph statistical software (by Synergy Software, 2008), followed by the Bonferroni post-hoc test. The difference in mean mass loss between groups was considered significant if the p value was found to be less than 0.001 (>99.9% confidence).

4.2.2 *In Vivo* Degradation and Biocompatibility

4.2.2.1 Animal Studies

For *in vivo* degradation and biocompatibility, two groups were tested: (1) 60 kDa linear PEC, and (2) 6000 MW PEC elastomers. Linear PEC was evaluated in this experiment for comparison to PEC elastomers and to confirm previous results from the literature [138, 140, 141]. Linear PEC was prepared by film casting in DCM, and PEC elastomers were prepared, as previously described, using a mould to produce a film approximately 0.9 mm thick. 5 mm discs were cut using a biopsy punch. Linear PEC was dried until a constant weight was obtained, while for the elastomers sol was extracted first using three overnight washes of DCM and then dried in a 40°C vacuum oven until constant weight. All discs were soaked in distilled water for at least 24 hours, air dried, lyophilized, and sterilized using UV light at an intensity of 50 mW/cm^2.

In vivo experiments were performed by subcutaneous implantation into the back of adult male Wistar rats (Charles River Laboratories, P.Q. Canada) weighing on average 350 grams on the date of implantation (see Appendix B, Figure 7-6). All animal care was conducted following the guidelines of the Queen's University Animal Care Committee code of ethics governing animal experimentation (protocol # Amsden 2007-043-R2). The rats were anaesthetized with 0.4mL of tamgesic. After the absence of corneal and tail reflexes, their backs were shaved and disinfected with iodine. The implantation surgery was conducted under aseptic conditions. For each rat, four 2 cm incisions were made to implant four polymer discs subcutaneously (see Appendix B, Figure 7-7). There were two rats per time point, per group. The first time point of interest was 1 week for both linear PEC and PEC elastomers, which was chosen to observe the initial inflammatory response for both groups. Based on mass loss data at each time point, a decision on the following time point was made. This was done to ensure that a range of mass loss was discovered for each group tested, while minimizing the number of animals that were sacrificed. The time points were 1, 2, and 3 weeks for linear PEC, and 1, 6, and 12 weeks for PEC elastomers. Protocols involving the use of rats were approved by the Animal Care Committee of Queen's University in accordance with the guidelines of the Canadian Council on Animal Care.

4.2.2.2 Degradation and Characterisation

At each time point, two rats per group were sacrificed. The tissue surrounding one of the discs (from one of the two posterior positions) from each rat was obtained for histological staining. For the remaining three discs per rat, the explants were removed from surrounding tissue and their wet mass was recorded. These discs were dried in a 50°C vacuum oven until a constant weight was recorded. Discs were not treated with for the removal of adherence cells or thin tissue. The

water uptake was calculated as shown in Equation 4-1, and the mass loss due to *in vivo* degradation was calculated using Equation 4-2.

$$water\ uptake\ (\%) = 100 \times \frac{m_{wet} - m_{dry}}{m_{dry}} \qquad \textit{Equation 4-1}$$

Where m_{wet} is the polymer disc mass immediately after explanation,

m_{dry} is the polymer disc mass after explanted and dried until constant mass.

$$mass\ loss\ (\%) = 100 \times \frac{m_0 - m_{dry}}{m_0} \qquad \textit{Equation 4-2}$$

Where m_0 is the (dry) polymer disc before implantation.

Differential Scanning Calorimetry, DSC (Mettler Toledo, DSC1) was conducted to determine the glass transition temperature, T_g, which is a measure of the flexibility of the polymer disc. Since T_g is a function of bulk disc molecular weight and crosslink density, it provides insight into the degradation mechanism. Scanning Electron Microscopy, SEM (JEOL JSM840 SEM, Peabody) micrograms were obtained for one explant per rat (n=2 per time point), which was first freeze-fractured using liquid Nitrogen, to get qualitative visual information about how the polymer is degrading. Sol content was also measured for PEC elastomers using Equation 4-3:

$$sol\ content\ (\%) = 100 \times \frac{m_{dry} - m_{elast}}{m_{elast}} \qquad \textit{Equation 4-3}$$

Where m_{dry} is the explanted disc mass after drying to a constant mass (before sol extraction)

m_{elast} is the disc mass after sol extraction in DCM and drying.

4.2.2.3 *In Vivo* Biocompatibility

In vivo biocompatibility was assessed by investigating whether the biomaterial elicited a persistent inflammatory response, which was measured by the number and types of cells surrounding the implant and by the presence and size of a fibrous capsule around the implant at each time point during degradation. Hematoxylin and eosin staining (H&E) was used as a simple method of obtaining images of thin sections at low magnification and at high magnification for identifying cell types. Hematoxylin stains cell nuclei blue/black, while the eosin counterstain colours cytoplasm pink. Masson's Trichrome stain was also used to distinguish cells from connective tissue (by staining collagen), therefore allowing the identification and measurement of the fibrous capsule. Using this trichrome staining procedure, cell nuclei appear black, the cytoplasm and muscle are coloured pink, and collagen is blue.

Immediately after explantation, the polymer discs and surrounding tissue were fixed in 4% formalin solution for at least 24 hours at 20°C. After trimming, processing and paraffin embedding the tissue, sections were cut at 5 μm intervals and stained with both H&E and Masson's Trichrome stains. Fibrous capsule thicknesses were measured in ImageJ using microscope pictures of Masson's Trichrome stained discs from at least four different areas of the disc and more than 10 measurements per side of the disc were recorded. The average of these measurements is reported ± one standard deviation.

4.3 Results and Discussion

4.3.1 *In Vitro* Oxidative Degradation

As part of the host reaction to the implantation of a biomaterial, once phagocytes, particularly leukocytes and macrophages, have attached to the surface of the implant they are able to produce

highly reactive oxygen species, such as superoxide ($\bullet O_2^{-}$) and hydrogen peroxide in order to attempt to destroy the foreign material [170, 171170, 171]. These species are highly reactive and participate in the biochemical reaction, referred to as the "respiratory burst", which is characterised by one electron reduction of O_2 into superoxide via NADPH or NADH oxidase [168]. It has been shown by Dadsetan *et al.* that the superoxide anion ($\bullet O_2^{-}$) specifically is present during the *in vivo* degradation of linear PEC [141]. It is clear from the results found in Figure 4-2 that oxidative degradation by superoxide plays a role in the degradation of both linear PEC and PEC elastomers. While the oxidative degradation media simulates the intimate environment between phagocytes and the biomaterial surface (because it produces a high concentration of the superoxide anion), the time frame of degradation in this experiment likely does not reflect *in vivo* degradation rates, but it can be useful for comparison purposes.

To demonstrate the reason for crosslinking, linear PEC degrades under these conditions about twice as fast as the PEC elastomer made from 8000 MW diacrylate (Elast 8000), as can be seen by Figure 4-2. At Day 3, this difference is statistically significant, with a p value of 0.001. The mass loss for linear PEC at Day 3, which is 68 ± 14%, is also statistically higher than that for all other elastomers ($p < 0.0001$). Due to difficulty in handling the delicate linear PEC discs at Day 3 which had lost almost ¾ of its mass, an experiment for Day 6 linear PEC was not practical (especially considering that it was expected to have lost all of its mass by that point). By Day 6, Elast 8000 (low crosslinking density) lost over 84 ± 5% mass, and Elast 6500 lost 24 ± 2% of its mass. This difference between Elast 8000 and Elast 6500 is statistically significant with a p value of less than 0.0001.

Although the experiment for Elast 2000 Day 6 was conducted, it was noticed that the discs were chipped. Considering the brittle nature of this crosslink density (and the damage problems

discovered in Section 3.3.4 while removing sol content of Elast 2000 dogbones), this was not surprising. Subsequently, the data for Day 6 Elast 2000 could not be used for comparison due to disc damage.

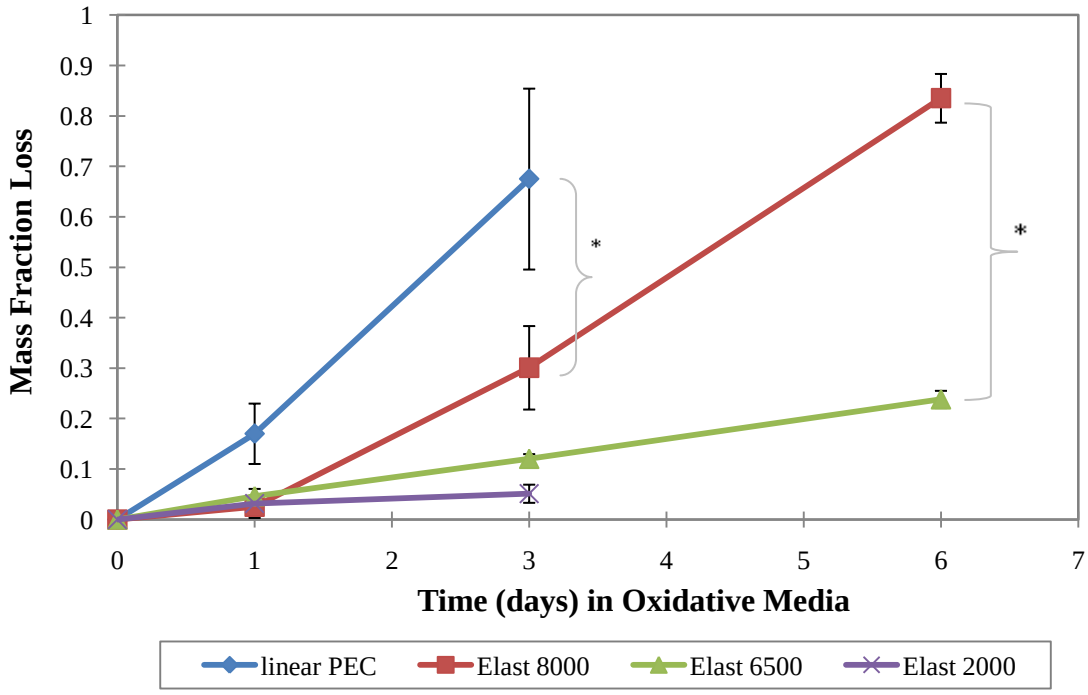

Figure 4-2: *In vitro* oxidative degradation of PEC and PEC elastomers at different crosslinking densities. Each point represents the average of replicates. N = 3 for Day 1 points, and N = 4 for Day 3 and Day 6 points. Error bars represent 95% confidence intervals for the means. Data for 2000 MW elastomer at Day 6 was excluded due to significant disc damage. Series curves were added to aid the reader in series identification only. * indicates that difference is significant (p=0.001 or less).

Based on the different rates of degradation between PEC elastomer groups, this data suggests that the degradation rate can be tailored based on the crosslinking density. An *in vivo* investigation of PEC elastomer degradation with different crosslinking densities would be required to conclude whether or not the degradation rate can be tuned in the body.

4.3.2 *In Vivo* Degradation

Both PEC elastomers and PEC linear discs exhibited a nearly linear mass loss with time, which is indicative of a surface erosion mechanism. Surface erosion has advantages over bulk erosion for a biomaterial since for most bulk erosion processes, cracks and crevices can form throughout the device that may rapidly crumble into pieces [41]. This is especially true for drug delivery applications since cracks and/or failure may cause a bolus/large release of the drug. These fragments may even cause unnecessary tissue irritation depending on the mechanical properties of the material and tissue location of the implant. Bulk eroding materials also possess more limited predictability of erosion and lack of protection of drug molecules to water [42].

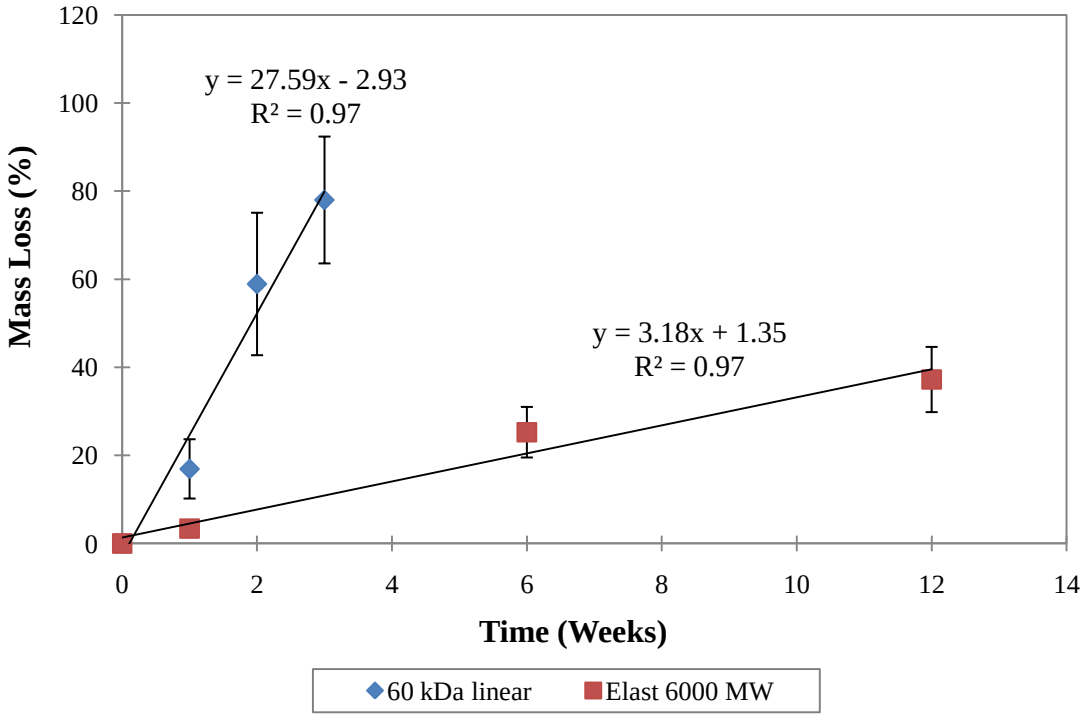

Figure 4-3: *In vivo* mass loss for linear 60 kDa PEC, and PEC elastomer made from 6000 MW PEC diacryl. Each point represents the average of quadruplicate values, where the error bars represent the 95% confidence intervals for the means. Linear trendline fitted to each set, where y = Mass loss (%) and x = Time after implantation in weeks.

The degradation rate of linear PEC is over 9 times greater than that of the PEC elastomer made from 6,000 MW diacrylate (Elast 6000). By Week 3, the linear PEC had lost 78 ± 11% of its mass, while by Week 12 Elast 6000 had only lost 37 ± 4%. This finding demonstrated that, as anticipated from the *in vitro* experiments, crosslinking PEC can be used to slow its *in vivo* degradation rate.

Mass loss during *in vivo* degradation appears to correlate well with the water uptake results seen in Figure 4-4. As degradation occurs, ethylene glycol is produced at the surface which attracts more water. Differential Scanning Calorimetry (DSC) was used to find the glass transition temperatures, (T_g) of the bulk polymers before and after *in vivo* degradation. The midpoint of the T_g found on the second heating cycle was used to measure the T_g since this is a reflection of the material property, not that which reflects the plasticizing effect of water. Therefore this T_g reported would be more useful for elucidating the mechanism of degradation. As seen in the representative thermogram for a PEC elastomer 6 weeks after implantation (Figure 4-5), a large evaporation endoderm is seen at 0°C (8 min) for the first heating cycle only, which is indicative of water retention. This endothermic peak was also seen for linear PEC samples for the first heating cycle only. This water plasticizes the PEC to possess a lower T_g (be more flexible) in the body.

For linear 60 kDa PEC before implantation, the T_g was found to be 15°C. This value is lower than that measured by Unger *et al.* for linear 242 kDa PEC (T_g of 31°C)[142], however this difference is expected due to the difference in molecular weight. Dadsetan *et al.* also reported that the 240-285 kDa linear PEC used in their studies possessed a T_g range from 24-27°C [141]. Unger *et al.* found by wide angle X-ray diffraction that linear PEC is amorphous and so finding a glass transition temperature and not a melting point are to be expected.

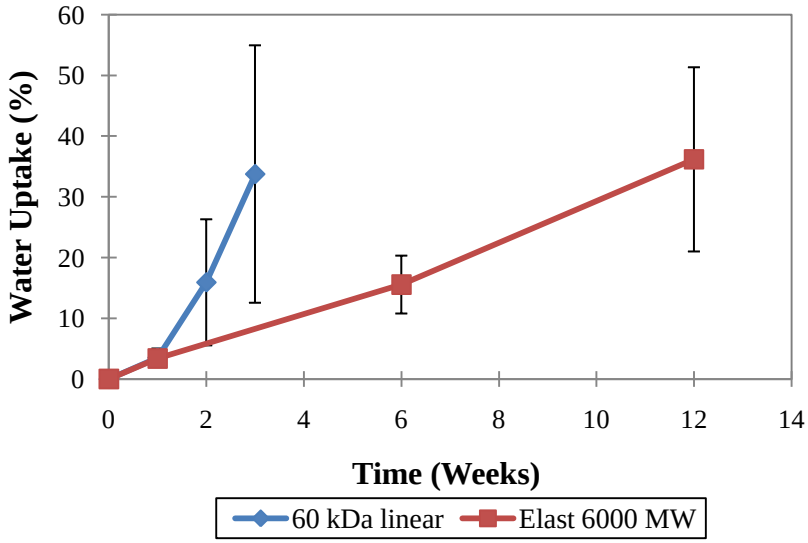

Figure 4-4: Water uptake for PEC *in vivo* degradation study. Each point represents the average of quadruplicate values, where the error bars represent the 95% confidence interval on the mean. Series curves were added to aid the reader in series identification only.

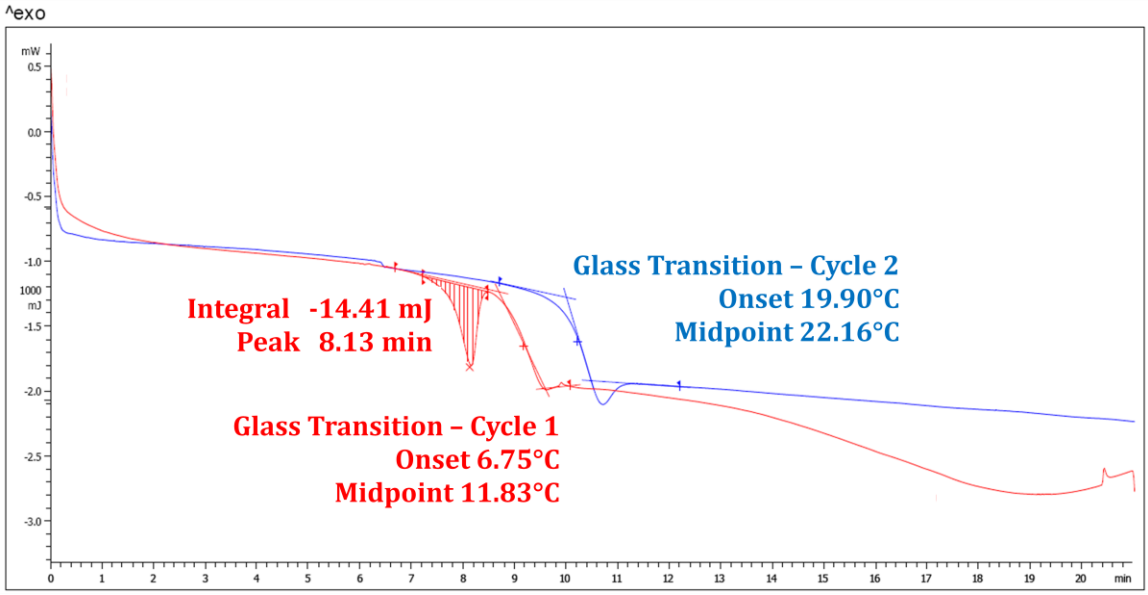

Figure 4-5: Representative thermogram showing two heating cycles for PEC elastomer 6 weeks after implantation. Heating cycle started from -80°C and heated to -130°C at 10°C/min.

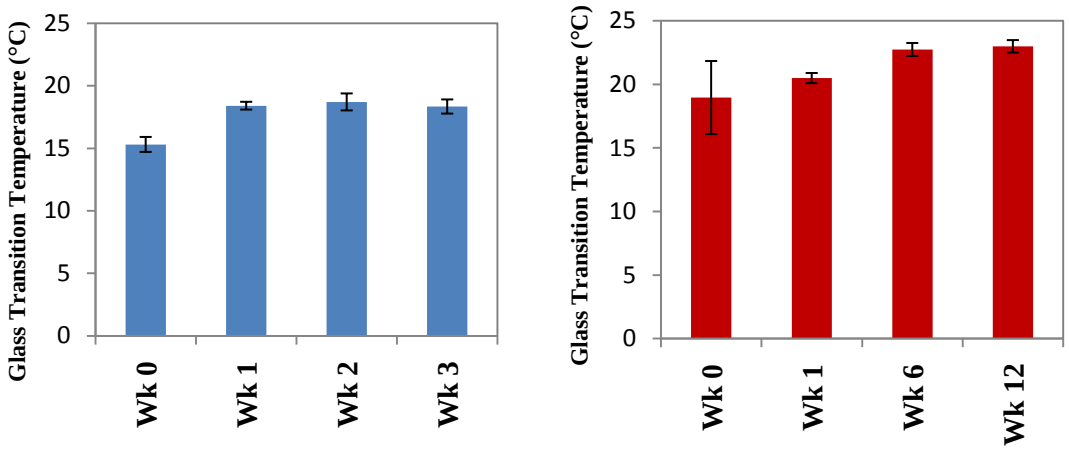

Figure 4-6: Glass transition results for linear PEC (left) and PEC Elastomer (right) during *in vivo* degradation. Error bars represent 95% confidence intervals.

For a surface eroding noncrosslinked material, it is expected that there would be no decrease in molecular weight, and therefore, in glass transition temperature until the polymer has been almost completely degraded, since the glass transition temperature is a bulk property. On the other hand, for bulk eroding materials, the glass transition temperature is expected to decrease as mass loss increases, if not before [172]. No decrease in T_g is seen (Figure 4-6) at any point and therefore the DSC results support a surface erosion mechanism (representative DSC thermograms are found in Appendix B, Figure 7-9). For linear PEC, there is a slight increase in T_g in the first week of *in vivo* degradation from 15°C to 18°C, but from week 1 to week 3, the T_g remains at 18°C. The slight increase in T_g initially may be due to the higher solubility of the lower molecular weight fraction in the *in vivo* extracellular environment, and is extracted from the bulk. This lower molecular weight fraction was plasticizing the bulk in the first week and therefore when it has been extracted, T_g increases.

For the PEC elastomers, T_g increases slightly from 19 to 23 °C in the first two weeks, although it is expected that T_g remains constant throughout elastomer *in vivo* degradation since the molecular

weight does not significantly change for thermosetting elastomers. One possible explanation for this is that either the dangling chain ends at the surface or the lower crosslink density sections are being degraded first, leaving behind regions of higher crosslink density. This is plausible since these are expected to be more accessible to the macrophages. Since dangling chain ends act as a plasticizer, and lower crosslink density sections are more flexible, the residual polymer (if this theory holds true) would be a less flexible material with a higher T_g and so the data supports this possibility.

After one week, the elastomers showed a small measurable sol content of 5 ± 2% and the sol content remains at roughly this value throughout the 12 weeks. This result is indicative of a surface erosion mechanism. Sol content is another bulk property and therefore is not influenced by surface changes. As ethylene glycol is produced during degradation, it is water soluble and is being continuously carried away by surrounding fluid which explains why there is no accumulation of degradation products in the disc which would elevate the sol content throughout degradation. For a surface erosion mechanism, adherent phagocytes release reactive species that have a limited half-life, and therefore their action is limited to the surface [173] where low molecular weight by-products can quickly be extracted.

Table 4-1: Sol content of PEC elastomer explants.

	Average Sol Content (%)	**Standard Deviation**
Week 1	5.26	2.39
Week 6	3.91	1.37
Week 12	5.15	3.12

As can be seen in Figure 4-7 and Figure 4-8, both linear PEC and PEC elastomer degrade by surface erosion. For linear PEC, before implantation there is a relatively smooth surface, with a

few bubbles and surface ripples caused by the film casting process. At Week 1, there are two distinct surface regions: one smooth and relatively unaffected, and a rough pitted region that had been degraded by inflammatory cells. This rough region covered more than half of the face of the disc. By Week 2 these rough surface features had covered the entire pitted surface of the disc and the roughness was coarser, as can be seen by the cross section. The Week 3 sample still had a blanket of tissue surrounding it (fibrous capsule), under which degraded pits can be seen.

The degraded surface of PEC elastomers is similar to that of linear PEC, except less pronounced. Before implantation, a few surface imperfections can be seen, and by Week 1 only a slight roughness was seen on the cross section. By Week 6 (at ~25% mass loss), the surface looked the same as linear PEC did at 1 week (17% mass loss) with regions of roughness. At week 12, a blanket of tissue had surrounded the elastomers, under which a deep pit of degradation could be seen.

4.3.3 *In Vivo* Biocompatibility

To investigate the biocompatibility of the PEC elastomers in the rat model, the area of tissue surrounding the implant was observed, and histological staining was performed. There were no gross signs of inflammation around any polymer discs (redness or swelling) at the time of explantation (see Appendix B, Figure 7-8). Hematoxylin & Eosin (H&E) and Masson's Trichrome stains were used since cellular density, the presence of various types of immune cells, and collagen deposition at the disc-tissue interface were of interest.

a) Wk 0 – 60kDa linear PEC

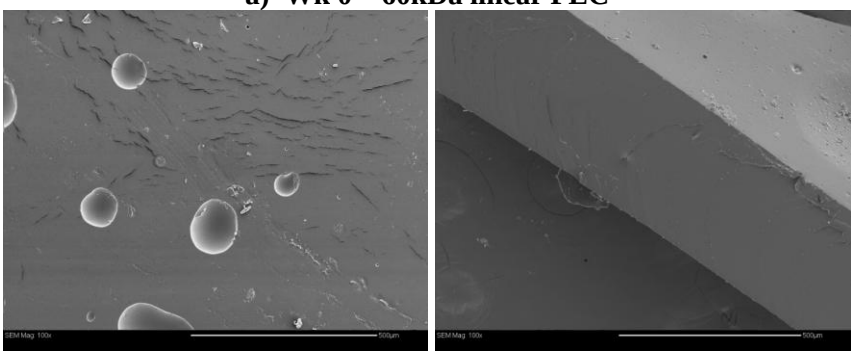

b) Wk 1 – 60kDa linear PEC

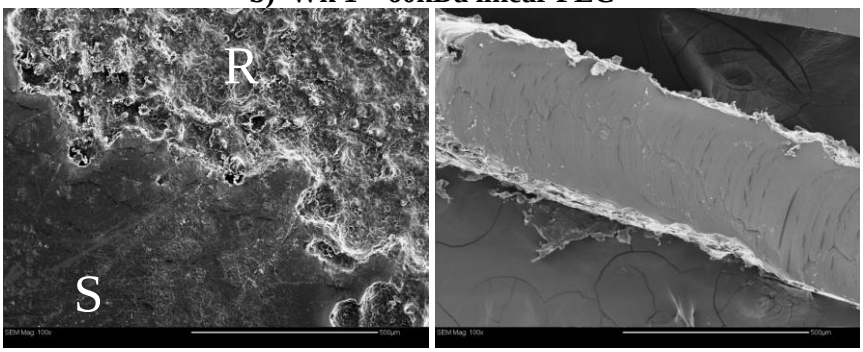

c) Wk 2 – 60kDa linear PEC

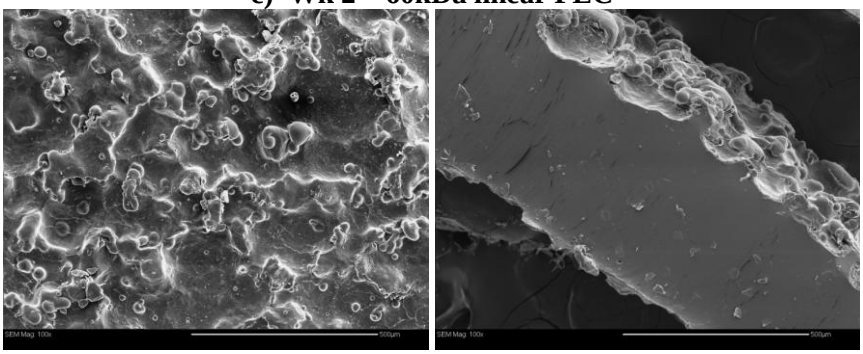

d) Wk 3 – 60kDa linear PEC

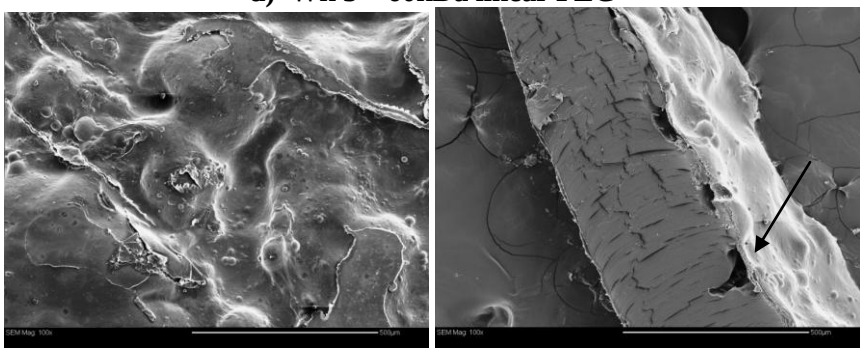

Figure 4-7: SEM micrographs at 100x magnification for 60 kDa linear PEC throughout *in vivo* degradation. (b) R indicates the rough pitted surface area, S indicates the smooth surface area. (d) Arrow highlights the blanket of tissue covering a degraded pit.

a) Wk 0 – PEC Elast 6000

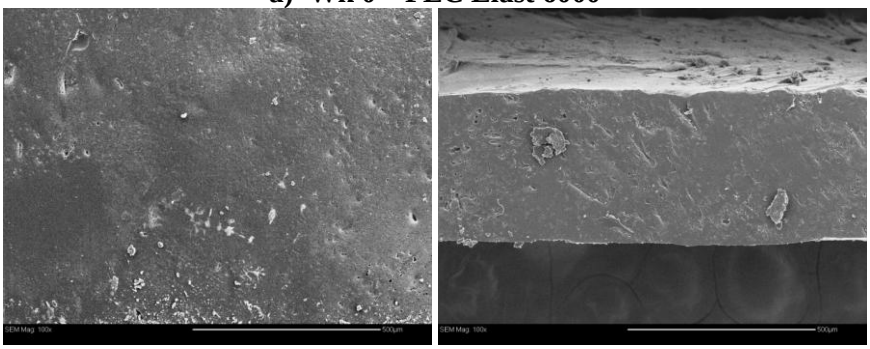

b) Wk 1 – PEC Elast 6000

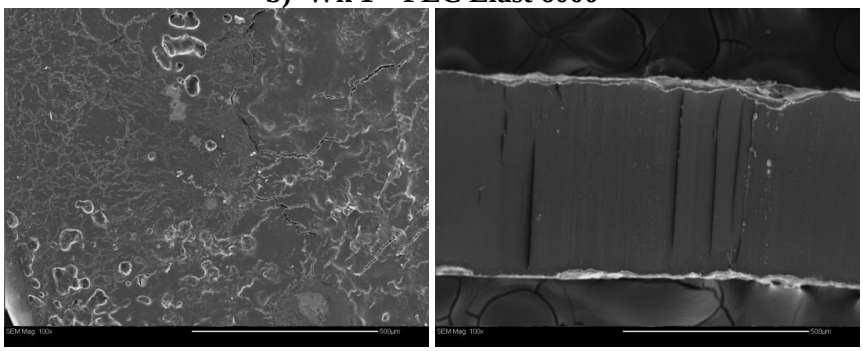

c) Wk 6 – PEC Elast 6000

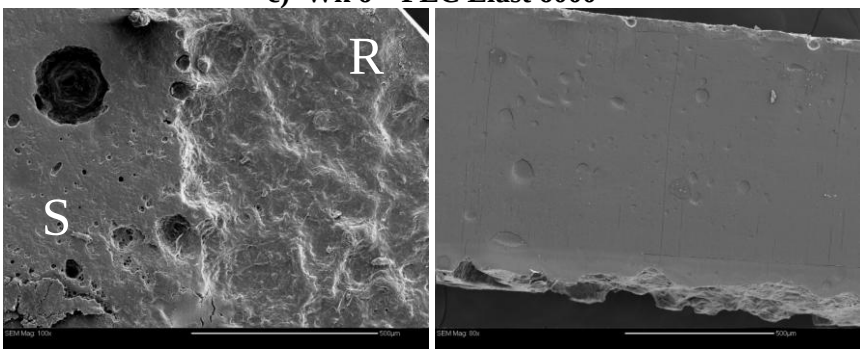

d) Week 12 – PEC Elast 6000

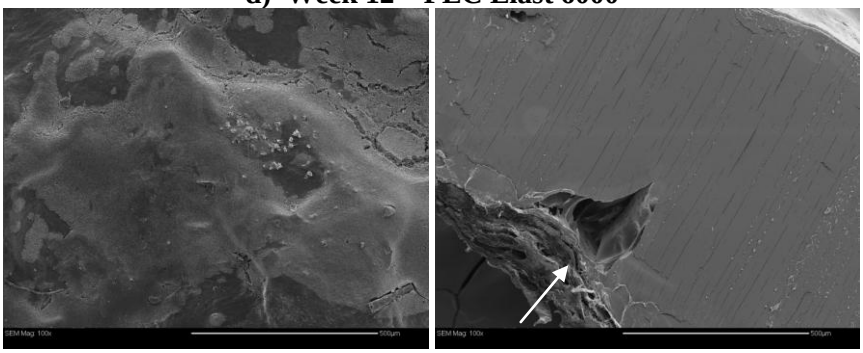

Figure 4-8: SEM micrographs at 100x magnification for PEC elastomer (6000 MW) throughout *in vivo* degradation. (c), R indicates the rough pitted surface area, S indicates the smooth surface area. (d) Arrow highlights the blanket of tissue covering a degraded pit.

For PEC elastomers, an expected inflammatory response was seen at the site of implantation. At Week 1, numerous granulocytes were seen at higher magnification, as identified by multi-lobed nuclei (see Figure 4-9b) as well as cells that appear to be macrophages. The number of granulocytes in the field of view greatly depended on the area from which the picture was taken. The side of the disc that faced the rat's body (rather than skin) had a significantly larger number of granulocytes, which is explained by the shorter distance for leukocyte extravasation from the main bloodstream to the disc. Erythrocytes can also be seen in Figure 4-9b.

At Week 6, cellular density at the interface between the disc and surrounding tissue had decreased and the development of a collagenous layer surrounding the implant was apparent, which measured to be 72 ± 18 μm thick. Vascularization developed around the implant site and could be seen as granulation tissue in Figure 4-9c-d. At Week 12, the fibrous capsule thickness was measured to be 62 ± 11 μm and this layer was avascular. This fibrous capsule was comparable to that seen for poly(trimethylene carbonate)-based elastomers [35].

For linear PEC, although cellular density of what appeared to be macrophages and other inflammatory cells was high surrounding the Week 1 implant, there were very few cells that could be identified as granulocytes on either side of the disc. Perhaps this is due to the fact that there has been significant degradation (almost 20%) by Week 1 and granulocytes are the first inflammatory cells to respond to injury. Linear PEC may degrade so quickly, that in 1 week it is at a more advanced stage of the wound healing process. At Week 3 a collagenous capsule layer was present and its thickness was variable. The fibrous capsule layer was measured to be 78 ± 38 um. As compared to PEC elastomers, the fibrous capsule contained a higher cell density, including large cellular nodules at the disc-tissue interface, which may contain multinucleated giant cells as would be expected.

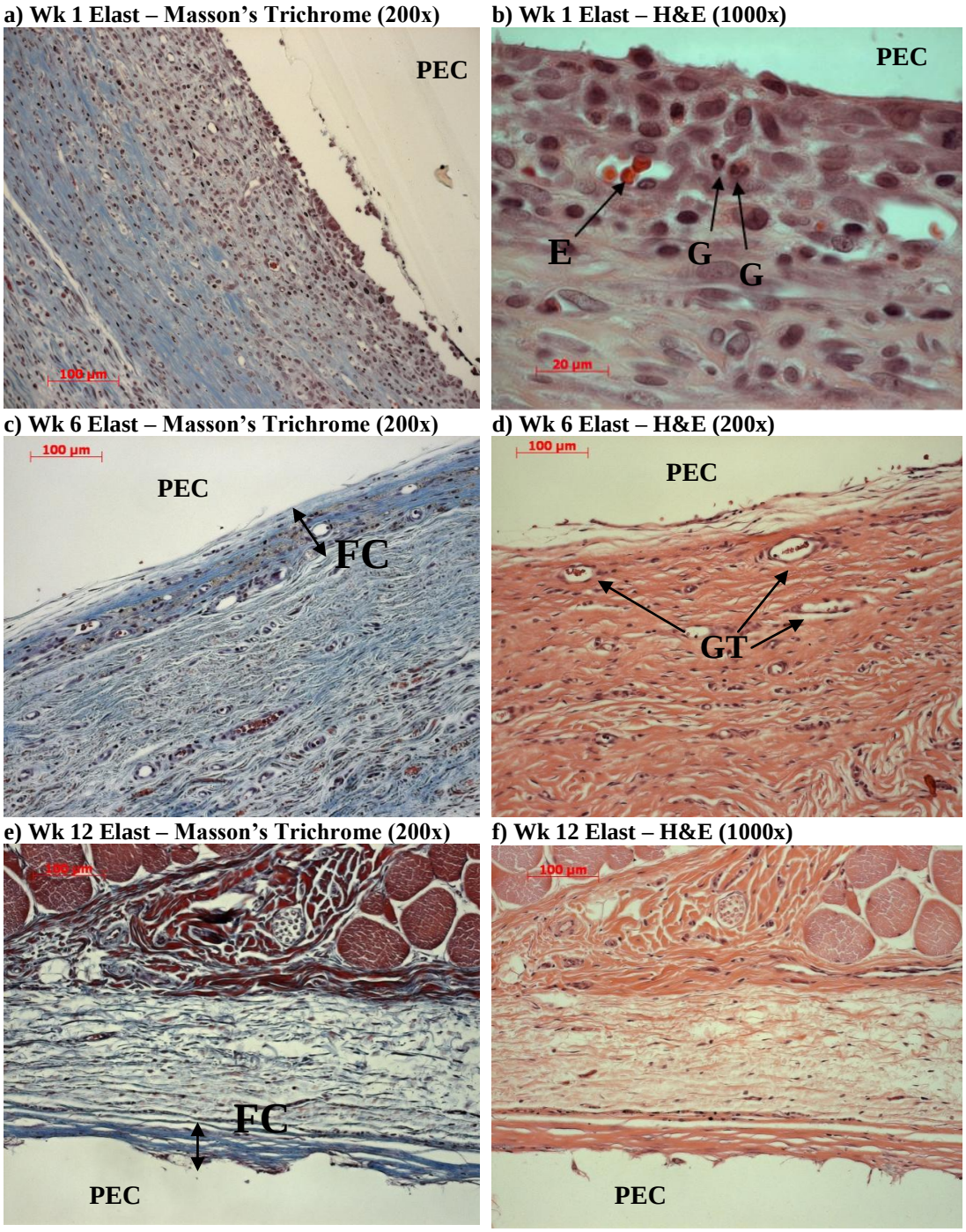

Figure 4-9: Histological sections stained with H&E or Masson's Trichrome for PEC Elast 6000 during *in vivo* degradation. PEC label indicates the implant void, as compared to the surrounding tissue. (b) G= granulocytes (multi-lobed nuclei), E = erythrocytes (c) and (e) FC = fibrous capsule, (d) GT = granulation tissue.

a) Wk 1 linear PEC - Masson's Trichrome (200x)

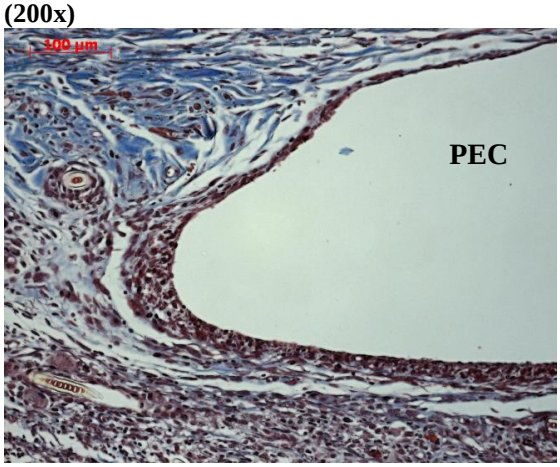

b) Wk 1 linear PEC - H&E (1000x)

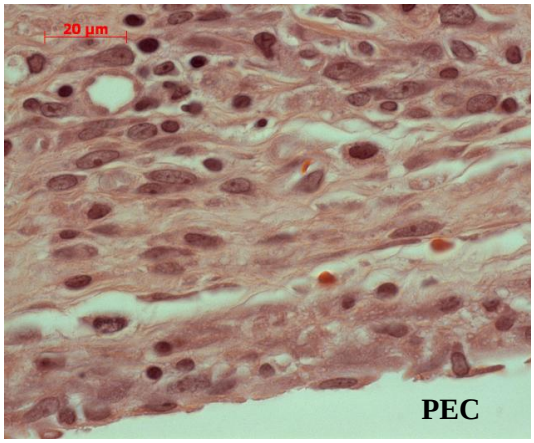

c) Wk 2 linear PEC - Masson's Trichrome (200x)

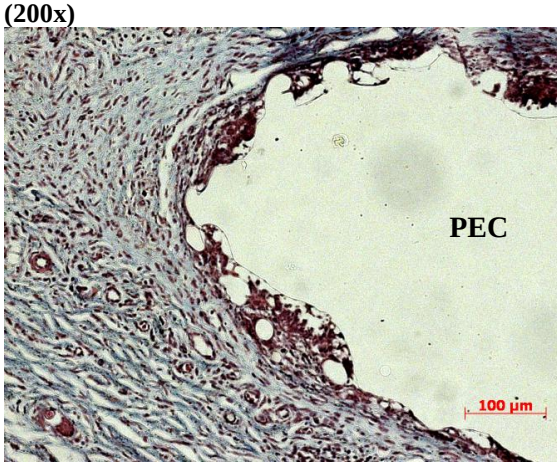

d) Wk 2 linear PEC - H&E (200x)

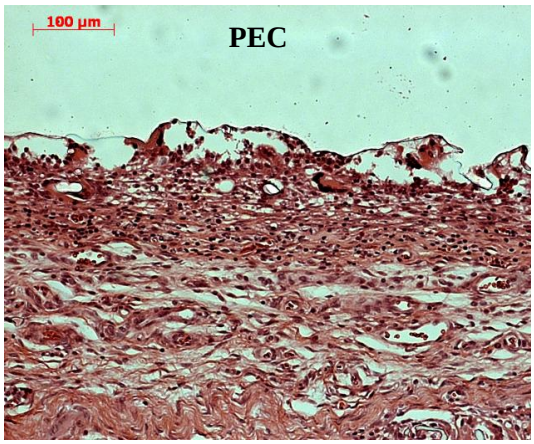

e) Wk 3 linear PEC - Masson's Trichrome (200x)

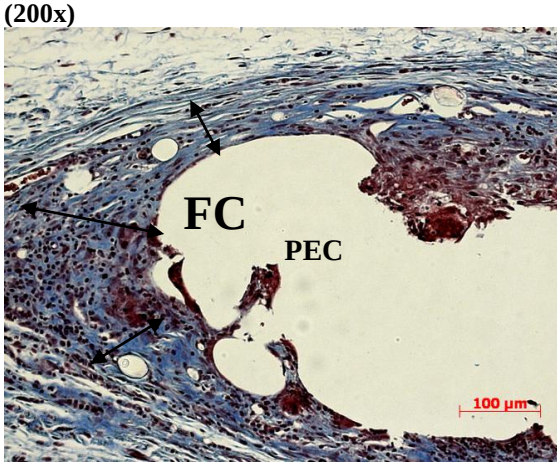

f) Wk 3 linear PEC - H&E (200x)

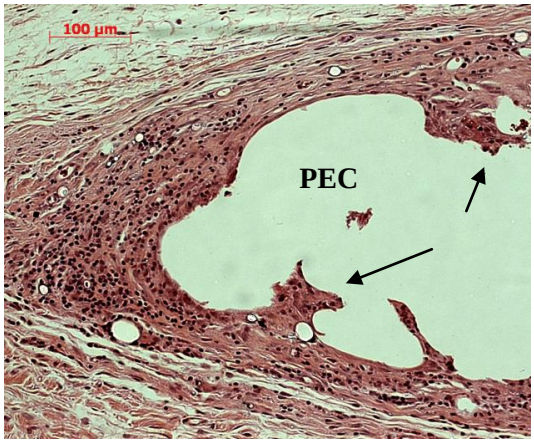

Figure 4-10: Histological sections stained with H&E or Masson's Trichrome for PEC Elast 6000 during *in vivo* degradation. PEC label indicates the implant void, as compared to the surrounding tissue, (e) FC = fibrous capsule, (f) arrows indicate to cell nodules.

The 60 kDa linear PEC investigated in this work degrades *in vivo* at a faster rate than the 72kDa linear PEC in Acemoglu *et al.* when mass loss is normalized to surface area, as seen in Figure 4-11. This is likely due to differences in polymer backbone composition, specifically the ratio of ethylene carbonate to ethylene oxide. Acemoglu *et al.* identify the incorporate ether function ratio (IEF) as a variable that affects the rate of biodegradation. The 60 kDa tested here has an IEF of 3% or less, since the least depolymerised batch has an IEF of 3.2% and the IEF only increases as ethylene carbonate units depolymerise. On the other hand, (while the 72kDa IEF was never explicitly stated) the batch in Acemoglu which is approximately the same molecular weight (66 kDa) has an IEF of 12%. The IEF of the 60 kDa linear PEC could not be measured directly, since NMR is not an appropriate characterisation technique for polymers over 10,000 Da.

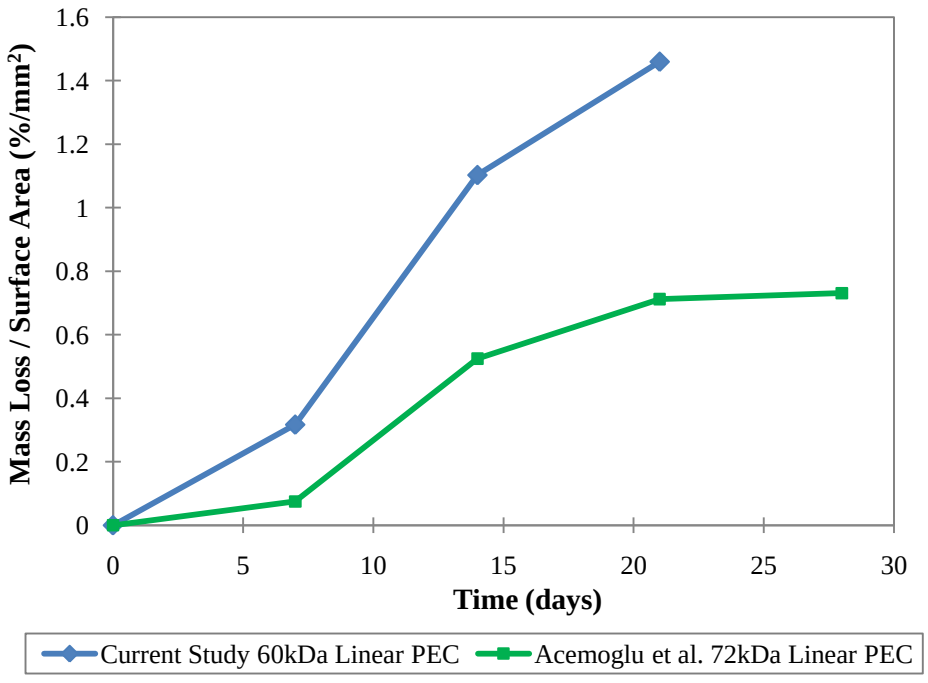

Figure 4-11: Normalized mass loss data comparison for the *in vivo* degradation data found in the present study (60 kDa), as compared to that from Acemoglu *et al*. which was 72 kDa.

The experimental results confirmed that PEC elastomers as well as linear PEC degraded by a surface erosion mechanism and strongly suggest that it is mediated by phagocytic cells. It has also been shown by Stoll *et al.* that linear PEC *in vivo* degradation is a cell-mediated process and is dependent on close contact between PEC and the cells. This was shown by evaluating intraperitoneal *in vivo* degradation using "free" PEC tablets and comparing results to PEC tablets which were enclosed in a Teflon device, separated from the environment by membranes of 10 and 160 micron pore size. After 2 weeks, no degradation was observed for membrane-surrounded tablets but significant mass loss (84%) was seen for "free" PEC [47]. Also, Cha *et al.* observed that degradation on PEC films only occurred where J774.A cells (mouse monocyte-macrophage cell line) had adhered.

The biocompatibility of PEC elastomers is comparable to that of PTMC elastomers in Chapanian *et. al* and they elicit a mild inflammatory response. As compared to that of PEC linear, the fibrous capsule around the PEC elastomer is more defined, however a reduction in inflammatory cells are seen at the interface of the last time point which may indicate a stabilization of the inflammatory response.

4.4 Conclusions

60 kDa Linear PEC degrades much more quickly than PEC Elastomers both *in vitro* and *in vivo*. There is also some evidence to support that the oxidative degradation rate can be tailored by the degree of elastomer crosslinking. Tunable degradability makes PEC elastomers more appropriate for applications in drug delivery and tissue engineering.

Both linear and elastomeric PEC degrade *in vivo* by a cell-mediated surface erosion mechanism as proven by linear mass loss profiles, SEM showing a pitted surface but unaffected bulk cross sections, consistently low sol contents throughout degradation, and glass transition temperatures that do not decrease for the time period investigated.

An inflammatory response accompanies the *in vivo* degradation of PEC. For the PEC elastomer, this is characterised by numerous granulocytes in the first week, followed by granulation tissue, and a thin fibrous capsule. For the linear PEC, many inflammatory cells (that appear to be macrophages) were present at the surface within the first week however, no granulocytes could be identified, likely due to the fact that significant degradation has already occurred by 1 week. Throughout 3 weeks, cell nodules are seen at the interface of the formed fibrous capsule and implant.

Chapter 5

PEC Elastomer as a Porous Protein Delivery Device

5.1 Introduction

The main goal of this section is to investigate the potential of porous PEC elastomers as protein delivery devices, with the ultimate application of therapeutic angiogenesis in mind. This was done by identification and testing of key formulation parameters that were expected to be important in controlling the release profile of bovine serum albumin (BSA) which was used as an example protein. BSA was selected for the purpose of screening the potential of PEC elastomers as delivery devices since it is often used as a diluent/excipient (and a major component) in the final formulation of many growth factor delivery devices and therefore tracking its release is meaningful [86, 174-176]. Albumin is also commonly used as a model/example protein in preliminary drug release testing and therefore literature results can be compared [86, 177-179]. It has also been shown in Chapanian *et al.* that for a trimethylene carbonate based elastomer system, the *in vitro* release rate of rat serum albumin for about 2 weeks was very close to that of VEGF, and therefore preliminary release data based on albumin may provide guidance in choosing the growth factor loading [86].

One requirement of this protein delivery device is that the scaffold is porous. This is expected to reduce the formation of the fibrous capsule since there is greater surface area for host cell infiltration meaning better integration into the tissue [149, 180]. The fibrous capsule can also be a barrier to the diffusion of the drug. Low molecular weight poly(ethylene glycol), PEG, was evaluated as a pore-forming agent for this purpose. PEG was selected because it is water soluble,

nontoxic and biocompatible [30] which means that it can potentially be used as a porogen that is slowly extracted from the device in the body. This was hypothesized to minimize the initial burst release, which is often seen in the first 24 hours [90], and provide another parameter for adjustment of the release kinetics [181]. Molecular weights lower than the renal threshold (10,000 Da) were selected so that PEG could be safely excreted [182]. PEG is widely used in many biomedical applications.

5.2 Materials and Methods

Poly(ethylene glycol)s of 400 Da (PEG 400) and 8000 Da (PEG8000) were purchased from Sigma Aldrich (Canada). Terminally acrylated glycerol-initiated star-poly(trimethylene carbonate) (PTMC) (see Appendix C, Figure 7-10) (used to set up the porogen fabrication process) was prepared as described in Chapanian *et al.* [35]. Bovine serum albumin (BSA) and albumin–fluorescein isothiocyanate conjugate (FITC-BSA) were purchased from Sigma Aldrich (Canada). Isopropanol was purchased from Fisher Scientific. Paraffin wax used to make paraffin beads was "Parowax" (made by CONROS Corporation, North York, ON).

5.2.1 Fabrication of Porous Scaffolds

Two acrylated polycarbonates were used in this section in developing porous polymer elastomers: 3000 Da poly(ethylene carbonate) diacrylate, and 3000 Da star-poly(trimethylene carbonate) triacrylate. PTMC triacrylate was used instead of PEC diacrylate for determining porogen loading/composition due to availability. Once the parameters were established, PEC diacrylate was used to confirm that the desired porous architecture could be achieved for PEC elastomers. Since its chemical structure and physical properties at 3000 Da are similar to that of PEC, PTMC was expected to be an appropriate material for this purpose.

PEG and 2,2-dimethylacetophenone (photoinitiator) were added to the solvent-free acrylated polycarbonate and then thoroughly mixed before spreading onto a glass mould for UV crosslinking using the parameters determined in Section 3.3.3. Unlike the previously described elastomers, the acrylated polycarbonate was not dissolved in dioxane prior to mixing/crosslinking in order to avoid dissolving the PEG. PTMC elastomers were prepared with 0 to 60% (wt/wt) PEG 8000 and/or 0 to 60% (wt/wt) PEG 400. PEC elastomers were prepared using different levels of both PEG 8000 and PEG 400 after the discovery that a combination of the two porogens was required for ease of mixing, ease of handling and to produce elastomers with appropriate mechanical properties and porous structures.

It was hypothesized that after the incorporation of PEG 8000 (a solid crystalline material) into PEC diacrylate, it could be extracted (after crosslinking) to form a defined pore structure within the elastomer. Different ratios of PEG 400, which is a viscous clear liquid at room temperature, were additionally incorporated because it was hypothesized that it could produce microchannels to connect the pores formed by the solid PEG8000 particles. In assessing the resultant porous architectures formed and the role of each PEG 8000 and PEG 400, each elastomer scaffold was carefully removed from the mould, and placed in distilled water to extract PEG. The elastomers were immersed in water for several days changing the water each day, until the dimensions of the elastomer stabilized (indicating full water penetration, dissolving all PEG). The samples were then dried overnight in a 50°C oven.

Porosity was assessed in three ways. The first method was based on a measured density according to Equation 5-1 and Equation 5-2. Three samples were cut from each porous elastomer batch for calculation of ε_1.

$$\varepsilon_1(\%) = 1 - \frac{\rho_{porous}}{\rho_{elast}} \qquad \textit{Equation 5-1}$$

$$\rho_{porous} = \frac{m_{porous}}{\pi\left(\frac{d}{2}\right)^2 \times t} \qquad \textit{Equation 5-2}$$

Where ε_1 (%) = porosity of elastomer based on the disc mass and dimensions.

ρ_{porous} [g/cm^2] = calculated density based on measured disc diameter, d, and measure disc thickness, t, after PEG removal by distilled water.

ρ_{elast} [g/cm^2] = polycarbonate density (1.42 g/cm^2 for PEC, 1.3 g/cm^2 for PTMC).

m_{porous} = mass of elastomer disc after PEG extraction and drying.

The error for ε_1 was determined by estimating the precision of the mass balance and caliper used to measure m_{porous}, d, and t and propagating the error (see Appendix C, Equation 7-1).

The second method for calculating porosity is based on a modified Archimedes Principle technique. Three samples were cut from each porous elastomer batch. Each dry piece was immersed in 2-propanol, sonicated for 60 seconds and placed in a vacuum dessicator (20 in Hg) for 1 hr. During this time, propanol fills all the interconnected void space. Excess propanol was removed carefully, and the disc was weighed immediately. Porosity was calculated using the following equations:

$$V_{voidspace} = \frac{m_{wet} - m_{dry}}{\rho_{isoprop}} \qquad \textit{Equation 5-3}$$

$$V_{elast} = \frac{m_{dry}}{\rho_{elast}}$$ *Equation 5-4*

$$\varepsilon_2(\%) = \frac{V_{voidspace}}{V_{voidspace} + V_{elast}}$$ *Equation 5-5*

Where $V_{voidspace}$ = volume of the pores [cm^3]

V_{elast} = volume of elastomer [cm^3]

m_{dry} = mass before isopropanol immersion [g]

m_{wet} = mass after isopropanol immersion [g]

$\rho_{isoprop}$ = density of isopropanol (0.786 g/cm^2)

ρ_{elast} [g/cm^2] = polycarbonate density (1.42 g/cm^2 for PEC, 1.3 g/cm^2 for PTMC)

Thirdly, scanning electron microscopy, SEM, (JEOL JSM840 SEM, Peabody) was conducted to observe the porous architecture formed. Dry samples were freeze-fractured and pulse gold sputter coated before SEM.

To help assess the distribution and contribution of each of PEG 8000 and PEG 400 in the final porous architecture, Differential Scanning Calorimetry, (DSC) was also conducted on a sample of 40% PEG 8000 + 20% PEG 400 + PEC ("40/20 PEG") before porogen extraction, as well as on PEG 8000 and PEG 400 alone.

5.2.2 BSA Release from Porous PEC Elastomers

For crosslinking porous BSA-loaded elastomers, 1.5% photoinitiator and PEG 400 were mixed well into PEC diacrylate, followed by evenly mixing in PEG 8000. Then, a suspension of protein particles was added, mixed, and the resulting thick polymer solution was transferred into a glass mould. The UV crosslinking conditions used were those determined in Section 3.3.3.

To produce the protein particle suspension, the method in Guan *et al.* [175] was followed with a modified concentration of BSA in DMSO of 275 mg/mL before vortexing at a high speed for 2 minutes. The BSA which was added to the DMSO was composed of 10% FITC-conjugated BSA (FITC-BSA) and 90% BSA and was first dissolved in phosphate buffered saline (PBS pH 7.4), lyophilized, and then sieved through a 45 μm mesh prior to adding to DMSO. The protein concentration in DMSO used here is significantly higher than that used in Guan *et al.* because minimal DMSO is desired to prevent the PEG porogens from dissolving or misshaping. The BSA particles of Guan *et al.* produced particles of 0.3 ± 0.2 μm in diameter as measured by SEM image analysis and since a higher concentration was used here (providing a high shear force to break up particles) the particles within the elastomer should also be on the order of micrometers. Fluorescently-labelled BSA was chosen in order to visualize the protein particles distribution and size before and after the release study.

The formulation parameters of interest were: molecular weight of the PEC diacrylate, BSA loading, protein particle size, and porogen composition. The formulation parameters were evaluated by first attempting to prepare the elastomers described in Table 5-1 with both 2000 MW PEC diacrylate, and 5500 MW PEC diacrylate.

Table 5-1: Elastomers prepared for BSA delivery release experiment. Φ is the volumetric fraction loading of BSA in PEC.

Elast ID	PEG 8000 (%)	PEG 400 (%)	BSA (%)	PEC (%)	Φ	Notes:
A	40	20	0	40	0%	no BSA added (CONTROL)
B	40	20	12	28	30%	BSA added after sieved (no DMSO/vortex)
C	40	20	12	28	30%	BSA added in DMSO (suspension)
D	40	20	5	35	13%	BSA added in DMSO (suspension)
E	60% paraffin		12	28	30%	BSA added in DMSO (suspension), paraffin extracted (THF)
F	50	30	12	8	60%	BSA added in DMSO (suspension)

BSA-loaded porous PEC elastomer formulations are listed in Table 5-1. As a control, Elastomer A contained no protein, but contained 40/20 PEG. To see whether the method used from Guan *et al.* for producing small diameter protein particles was effective and beneficial for this delivery system, Elastomer B was prepared with 12% weight fraction "dry" BSA, which was sieved and then mixed into PEC diacrylate without any DMSO or solvent. Elastomer C was prepared with 40/20 PEG and 12% BSA and was used as a base case for comparison to other formulations. Elastomer D was prepared to evaluate the effect of BSA loading, and contained a lower loading of 5% BSA. To assess the performance of PEG as a porogen, Elastomer E was prepared from paraffin beads for comparison purposes. The paraffin microbeads were fabricated by dropwise addition of melted paraffin wax into a 0.003% PVA solution vigorously stirred and heated to 65°C. Paraffin droplets were solidified by quenching in stirred, ice-cold water. The beads were then sieved to produce 100-250 micron beads. Elastomer F was prepared to evaluate the effect of a higher overall porosity by preparing with 50% PEG 8000 and 30% PEG 400.

Table 5-2 describes the intended comparisons to be made between groups in assessing the effect of the formulation parameters on release characteristics.

Table 5-2: The comparisons made between BSA-loaded elastomer conditions.

Comparison	Reason
A to B	Identify BSA on SEM (and its effect on porous structure if applicable)
B to C	Effect of DMSO on release kinetics and porous structure
C to D	Effect of BSA loading on release profile
C to E	Compare choice of porogen
C to F	Effect of overall porosity on release profile

Half of the Elastomer C batch was also washed in THF overnight for seven nights in an attempt to extract PEG. Differential scanning calorimetry (DSC) was used to measure the PEG remaining. The intention was to perform a release study on Elastomer C both with or without PEG so that it could be determined whether PEG minimizes the burst release, as hypothesized. However, it was not possible to fully remove PEG even after 1 week of THF washing, and therefore only Elastomer C containing PEG (without any THF/PEG extraction) was used in the release studies.

To conduct the BSA release study, batches were lyophilized to remove DMSO until they measured a constant weight, or for 1 week (whichever was longer) and then 5 mm discs were punched out of each elastomer listed in Table 5-1. Four discs were punched for each group (three discs for quantification of BSA and a fourth disc to determine PEG remaining through DSC). Each disc was placed in 1.75 mL of release media, which consisted of PBS (pH 7.4) containing 0.01% sodium azide to prevent bacterial growth and 0.0005% BSA as a sacrificial protein for adsorption to the sample vial. The vials were gently stirred on an orbital shaker at 37°C for a month.

At sampling points, each disc was removed from the vial, dabbed on a KimWipe and transferred to a vial containing fresh PBS. The disc dimensions were recorded before and after the release experiment, and at various sampling points. The release solutions were filtered and assayed using HPLC injecting duplicate 100/200 μL of each sample depending on the concentration (Thermo Scientific HyPURITY C18 column 5um particle size with column dimensions 250mm x 4mm with a 10x4mm drop-in guard column cartridge, mobile phase A: 99.9%v/v water, 0.1% TFA, mobile phase B: 80% v/v acetonitrile, 19% water, 0.1% TFA; UV detection at 214 nm). DSC was also performed at 1 week and 4 week time point discs to measure the amount of PEG remaining. SEM was used after the release experiment to observe the porous structure formed by the expected extraction of PEC and BSA particles. Laser scanning confocal microscopy was also used before and after release to evaluate the particle size and size distribution, which was calculated using the "Analyze Particles" tool of ImageJ, analyzing four confocal images per group taken before the release of each disc.

5.3 Results and Discussion

5.3.1 Fabrication of Porous Scaffolds

Porosity measurements for all porous PTMC scaffolds prepared are found in Table 5-3. Based on Equation 5-1 and Equation 5-3, ε_1 is a measure of all void/non-polymer space, but ε_2 considers only the interconnected void space (space contacted by isopropanol). Therefore, the comparison of these two values provides a measure of interconnectivity of the porous structure.

Table 5-3: Porosity of porous PTMC elastomers prepared. ε_1 values are the mean of triplicates ± 95% confidence intervals. ε_2 values are the mean of triplicates ± 95% confidence intervals.

PTMC 3000			
PEG 400 (wt/wt %)	**PEG 8000 (wt/wt %)**	**ε_1 (%) from measured density**	**ε_2 (%) from 2-propanol**
0	29	33.3 ± 3.2	15.6 +/- 4.2
0	38	40.2 ± 3.4	24.6 +/- 6.0
0	60	64.4 ± 2.0	66.4 +/- 0.4
38	0	5.2 ± 5.3	6.3 +/- 3.7
60	0	47.8 ± 2.9	32.2 +/- 13.0
25	12	17.4 ± 4.6	11.5 +/- 2.7
21	39	55.0 ± 2.5	49.9 +/- 4.2
20	40	55.0 ± 2.5	55.2 +/- 4.8

SEM micrographs were also examined to characterise the porous structures formed, as seen in Figure 5-1. When a low loading of PEG 8000 is the only porogen is used (29% or 38%), the pores were not fully interconnected, as seen by a discrepancy in measured porosity values. SEM showed a well-defined closed pore structure with pores from 50 to 250 μm in diameter. In addition, elastomers made with only PEG 8000 (especially 60% PEG 8000) were very difficult to evenly mix, and once crossslinked were fragile. PEG 400 incorporated on its own was not a very effective porogen, as seen by low porosities measured and based on SEM cross sections, with only a few small pores/bubbles. However, when both PEG 8000 and PEG 400 were incorporated pores were formed that were more interconnected. These pores were not as circular and well defined as the pores in Figure 5-1 a) and b), but they were also approximately 50 to 250 μm in diameter.

As expected PEG 8000 was the major pore-former, and PEG 400 helped to connect the void space by plasticizing the PTMC during mixing before UV crosslinking. DSC results for PEG 8000 and PEG 400 as compared to that for Elast 40/20 PEG provide additional confirmation that

PEG 8000 is the pore-former and PEG 400 is more dispersed throughout the elastomer matrix (see Appendix C, Figure 7-11). The PEG 400 incorporation is also very important in order to produce elastomers that can be handled with ease.

It was decided that a total porogen weight fraction of about 60% was an appropriate starting point to produce the desired porous structure. This was selected based on the ease of mixing the formulations in the previous section. It was expected that if enough PEG was added then the fraction of acrylated PEC would be too little to effectively crosslink. To confirm which combination of PEG 8000 and PEG 400 was the best choice for creating PEC elastomers, four different PEC elastomers were prepared as outlined in Table 5-4:

Table 5-4: Porosity of porous PEC elastomers prepared. Values for ε_1 porosity are the mean of triplicates, including 95% confidence intervals based on error propagation and estimated precision of mass balance and calliper (see Appendix C, Equation 7-1). Values for ε_2 porosity listed are the mean of triplicates, with 95% confidence intervals.

PEC 3000			
PEG 400 (%)	**PEG 8000 (%)**	**ε_1 (%) from measured density**	**ε_2 (%) from 2-propanol**
20	40	58.9 ± 2.5	56.4 +/- 2.9
10	50	61.3 ± 2.4	59.6 +/- 1.2
30	30	57.6 ± 2.6	49.6 +/- 5.0
15	37	52.0 ± 2.9	48.7 +/- 4.2

a) 60% PEG 8000 + PTMC (20x)

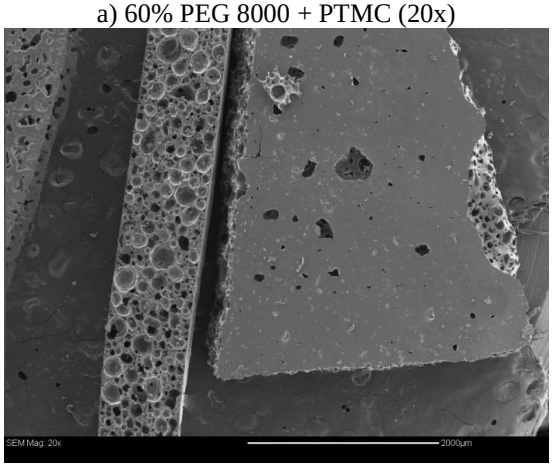

b) 60% PEG 8000 + PTMC (100x)

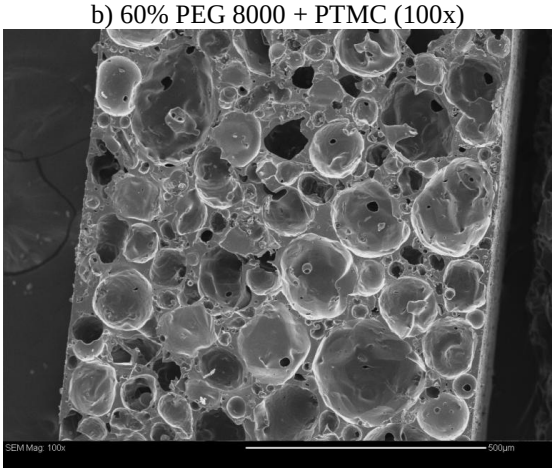

c) 60% PEG 400 + PTMC (30x)

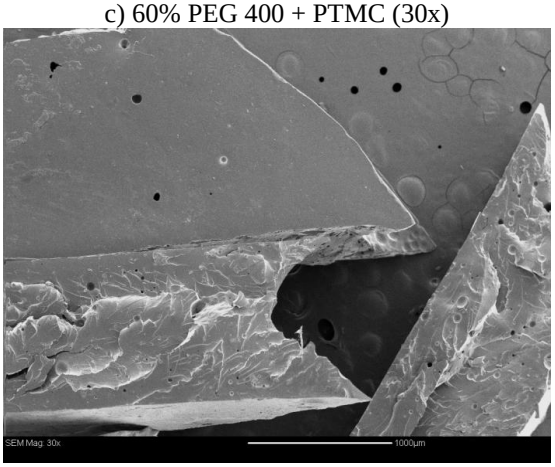

d) 60% PEG 400 + PTMC (100x)

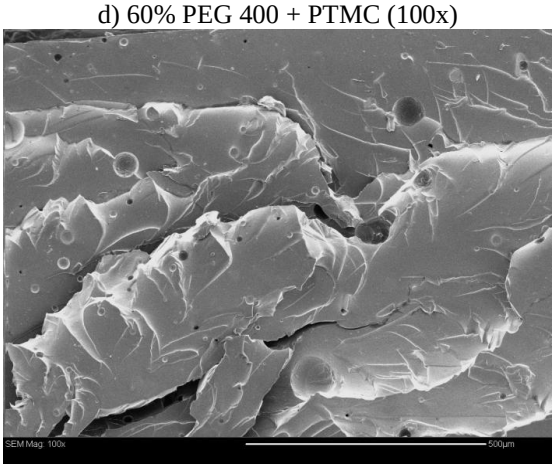

e) 40% PEG8000 + 20% PEG400 + PTMC (20x)

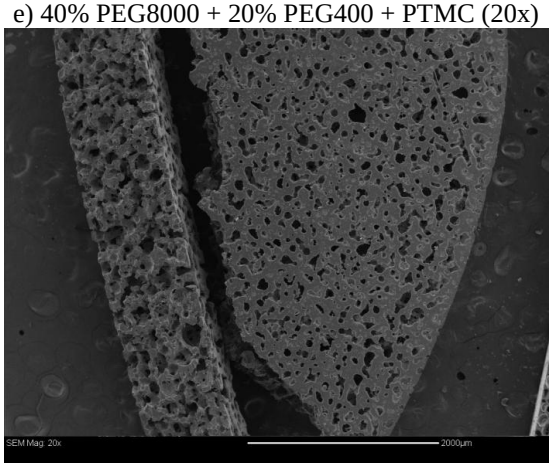

f) 40% PEG 8000 + 20% PEG 400 + PTMC (100x)

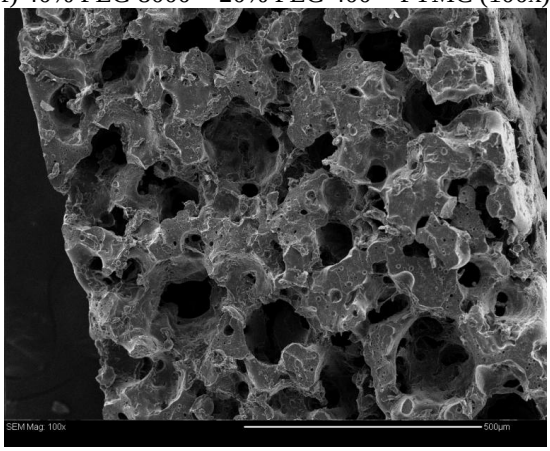

Figure 5-1: SEM micrographs of PTMC porous elastomers at low (20x or 30x) and high (100x) magnification.

Since porosity measurements are close, and based on the SEM micrographs the porous structures formed once again are highly porous and interconnected. The best elastomer in terms of a balance of properties when handling and the measured porosities was 40% PEG 8000 + 20% PEG 400 ("40/20 PEG") and so this porogen level was selected for use in subsequent experiments.

As compared to the 40/20 PEG of PTMC, the pores are less defined and less circular for PEC. This may have been a result of more thorough mixing, but mixing is difficult to standardize for small scale processes. It is unknown how exactly this difference in pore morphology (between two samples with approximately equal porosity and interconnectivity but different pore shape) would affect cell response. It is also unknown how the cells would respond to PEG initially contained in the pores and slowly releasing out. Therefore, these would be interesting questions to answer in future work. Keeping this in mind, and especially that the mixing process is not standardized, SEM images must be examined for each batch.

40% PEG8000 + 20% PEG400 + PEC (20x)

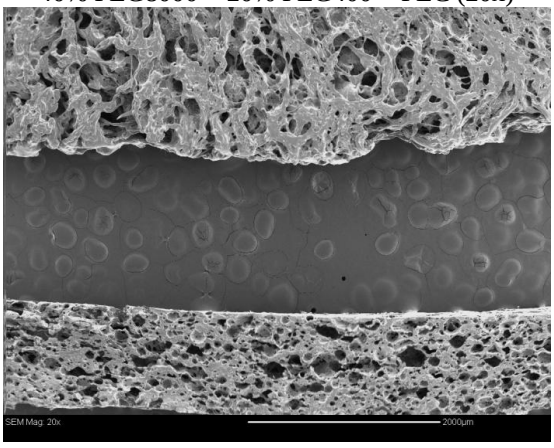

40% PEG8000 + 20% PEG400 + PEC (100x)

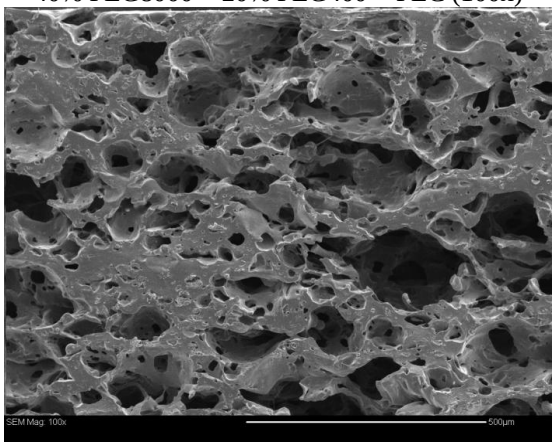

Figure 5-2: SEM of PEC porous elastomers at low (20x) and high (100x) magnification.

5.3.2 BSA Release from Porous PEC Elastomers

In order to investigate the potential of PEC elastomers as protein delivery devices, bovine serum albumin (BSA) was used as an example protein. BSA has been used often for preliminary

screening of protein delivery devices, and is commonly used as an excipient in final formulations. BSA is a hydrophilic globular protein with a molecular weight of 66 kDa [183] so its release would provide insight into the potential of the approach for delivering a growth factor (e.g. Human recombinant VEGF is 38.2 kDa and also hydrophilic [184]).

Elastomers from Table 5-1 were prepared and crossslinked successfully with 2000 MW PEC diacrylate, with the exception of Elastomer F. For Elastomer F, the fraction of PEC was very low (8%) and therefore acrylate content was not high enough to effectively crosslink (as indicated by a liquid suspension in the mould after crosslinking, rather than an elastomeric solid film).

It was anticipated that the molecular weight of the PEC diacrylate would affect the fabrication process by changing the difficulty of mixing in components, potentially resulting in a different porous structure. However, it was discovered that even a molecular weight of 5500 Da was too high to evenly mix in all components. Since it was not possible for the 5500 Da PEC, only 2000 MW PEC elastomers listed in Table 5-1 were used for the release study.

HPLC was used to measure the concentration of total BSA in the release media at every time point. Using this data and calibration information (see Appendix C, Figure 7-12), the cumulative mass fraction released was calculated and compared for all groups (see Figure 5-3). As expected, for Elastomer A there was no peak corresponding to BSA released at any sampling time point. When 12% weight fraction of BSA was incorporated into the elastomer without the DMSO and vortexing steps (Elastomer B), the release of protein was extremely fast, and reached its plateau of 72% total release in only 2 days. The release of BSA from Elastomer D, which possessed 5% BSA that was prepared with DMSO and vortexed before loading, was slightly slower, but reached a plateau of 60% after 5 days.

The volumetric fraction loading (φ) for Elastomer B is above the typical percolation threshold of ~30% for polymer matrices [185, 186] and therefore (assuming the BSA filled pores are randomly distributed within the polymer matrix) this quick release is reasonable, but undesirable for controlled drug delivery applications. According to percolation theory, at a high loading, the pores are connected and therefore there are many paths that BSA can use to escape into release media[187]. At a low loading, most of the BSA pores are isolated and only a few are connected and able to transport the BSA outside the disc. On this basis, the high efficiency of release of Elastomer B is not surprising. However, percolation theory cannot explain the difference in release profile between Elastomer C (φ =30%) and Elastomer D (φ=13). Although Elastomer C possessed a higher initial loading of BSA of 12% weight fraction (φ above the typically observed critical value), the release of BSA was more prolonged but incomplete (maximum of only 25%, reaching this value by 19-24 days). Interestingly, the release of Elastomer E, which is also 12% BSA (φ=30%), had the lowest efficiency of release (maximum of 10% released) but more quickly reached its plateau by 4 days. Therefore, the release profiles cannot be explained simply by percolation theory.

These results showed that the use of BSA without DMSO/vortex or using paraffin wax as a porogen does not result in favourable release characteristics and demonstrated the most common problems faced in protein delivery (very rapid release, or very low incomplete release). It was originally thought that Elastomer B would possess larger particles than that of the other groups since the DMSO/vortexing step was omitted. However, based on confocal image analysis in ImageJ, the average particle size for Elastomer B and Elastomer C are approximately the same (13.0 ± 1.1 μm for Elastomer B, 14.4 ± 1.4 μm for Elastomer C). In fact, this analysis revealed that the average particle size across all elastomer groups was about 9-14 μm and that over 75% of

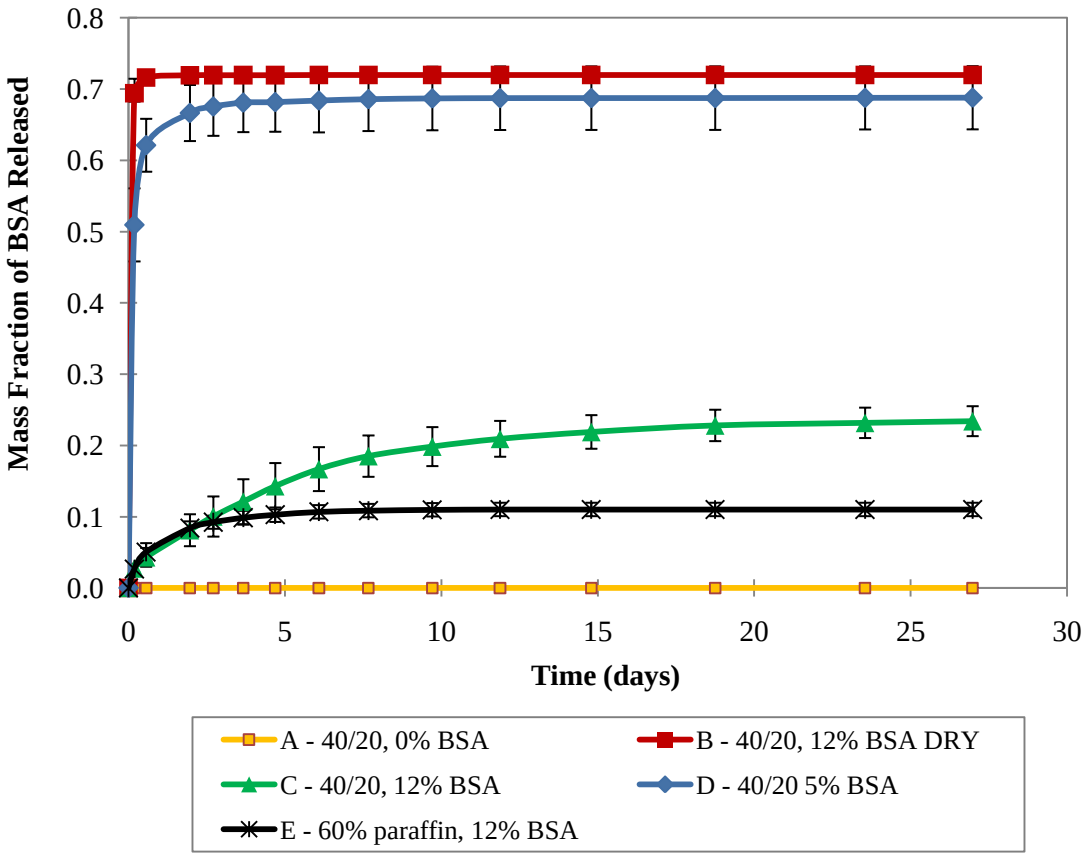

Figure 5-3: BSA release results for PEC elastomers. Error bars represent standard deviation.

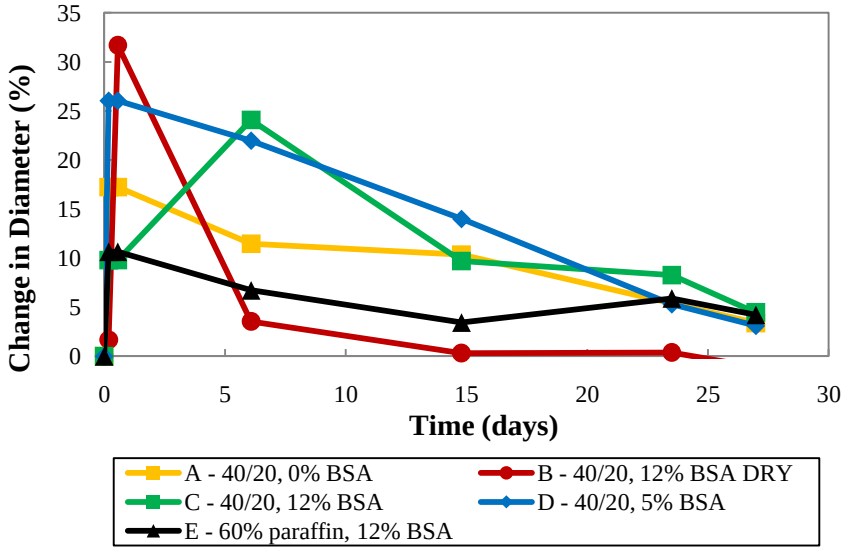

Figure 5-4: Change in PEC elastomer disc size during BSA release study, expressed as percent increase from the initial value.

all particles analyzed were between 3 and 11 μm. Therefore, the differences in release profiles seen in Figure 5-3 were related to factors other than particle size differences. Confocal microscope images also confirmed that there was an even distribution of BSA initially (around the PEG-filled pores) for all elastomer groups and the conclusion of incomplete release in Elastomers C and E (Figure 5-5).

In order to evaluate how long PEG stays within the pores of each elastomer, disc size and DSC analysis were used. Figure 5-4 indicates the change in disc size throughout release as PEG (a highly water soluble substance) draws in water from the release media. There may also be some water drawn in due to the BSA present which is also very hydrophilic, as seen for Elastomer E which contains no PEG and swells to 10%. As PEG and BSA are released, the water content and size of the disc decreases. Results for disc size correlate well with the DSC results in Table 5-5, showing higher integrations of endothermic PEG melting peaks when disc swelling is higher.

Table 5-5: DSC results showing the integration of endothermic melting peaks for PEC elastomers throughout BSA release experiment. Melt temperature value reported is the average of the temperatures at 0, 1, and 4 weeks ± standard deviation. Midpoint of the temperature is reported. No melting points were found for Elastomer E before release.

	PEG Enthalpy of melting Before Release (J/g)	PEG Enthalpy of melting 1 Week (J/g)	PEG Enthalpy of melting 4 Weeks (J/g)	Melt Temperature (°C)
A	-78.70	-4.08	-4.98	59.0 ± 1.7
B	-77.68	-0.53	-1.27	60.3 ± 0.6
C	-72.56	-21.24	-6.64	62.0 ± 1.7
D	-81.17	-3.10	-1.86	60.0 ± 1.0

Not surprisingly, Elastomer B swelled immediately to over 30% as PEG (and as a result BSA) was being released from the disc. By 5 days, almost all of the PEG (and BSA) had been

extracted, as indicated by shrinking of the elastomer to almost its original size and by DSC at 1 week. Elastomer D results were very similar: the rapid increase in disc size to over 25% (PEG extraction) accompanied the rapid release of BSA, corresponding with a very low PEG content remaining, as measured by DSC. Elastomer A provides the control for comparison. In the presence of 40/20 PEG only, water was quickly drawn in to a maximum disc size increase of over 15% by half a day. In contrast to all other elastomers tested, Elastomer C takes 6 days to reach its maximum of almost 25% increase. This slower PEG extraction matched with a slower BSA release, which is expected to be due to decreased interconnectivity. This hypothesis was confirmed clearly by observing the SEM micrographs of Elastomer C compared to all other groups (see Figure 5-6 and Figure 5-7). Elastomer C possessed many small pores, with an average diameter of 10 μm (measured in ImageJ) and only very few large pores (diameter 50μm). The cross section showed very little visible interconnectivity between void spaces. DSC results confirm that unlike any other elastomers tested, there is significant PEG still remaining at 1 and 4 weeks.

This difference for Elastomer C of slower PEG extraction, slower disc size increase, slower and incomplete BSA release can be attributed to more DMSO added before crosslinking which reduced the interconnectivity of the overall porous network. In order to maintain the same vortexing conditions (and therefore the same shear force on the particles which presumably determines particle size), the concentration of BSA in DMSO remained the same between Elastomer C and D. As a result, in order to achieve twice the BSA loading, Elastomer C contained twice as much DMSO as Elastomer D and this may have caused the PEG to molecularly distribute to an undesirable extent, leaving behind porosity that was not interconnected.

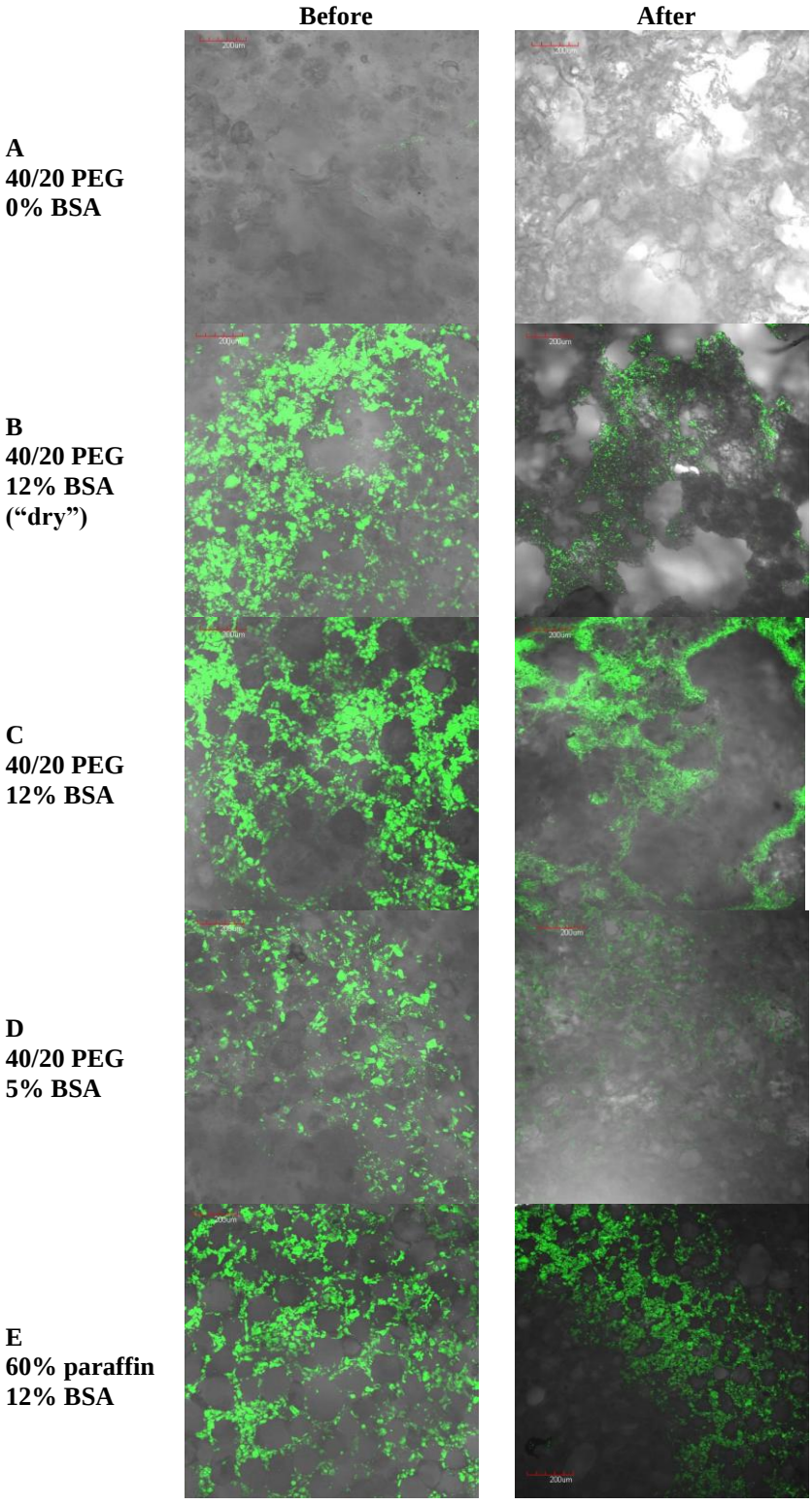

Figure 5-5: Confocal microscope images of BSA-loaded PEC Elastomers before and after release. 100X magnification. Red scale bars represent 200 µm.

Porosity data again confirms this hypothesis, that Elastomer C was less interconnected, as shown by a difference in ε_1 (44%) and ε_2 (12%) (see Table 5-6). The porosities for other elastomer groups were expected based on the results in the previous section.

For the control disc, Elastomer A, the SEM micrograph is similar to that previously fabricated (in the previous section). The result of this fabrication process is a highly porous, highly interconnected architecture with average pore size of about 100 μm and micropores within the walls of the larger pores of 10-15 μm as determined by ImageJ.

Table 5-6: Porosity measurements of PEC elastomers after completed BSA release study.

	Porosity, ε_1 (%)	**Porosity, ε_2 (%)**
A	61	59
B	66	60
C	44	12
D	52	46
E	58	54

The release of BSA from Elastomer E was rapid but incomplete. It is possible that this result is due to complete entrapment of most of the remaining BSA particles.

No release profile presented in Figure 5-3 represents the ideal profile for the delivery of protein drugs for controlled release. However, the results from Elastomers B, C and D demonstrate that the level of DMSO added affects the release rate: the more DMSO that is added, the narrower the interconnected channels and the slower and less complete the release of BSA is. A more promising release profile might be obtained by investigating the release of BSA from an intermediate loading fraction of BSA (7% BSA for example).

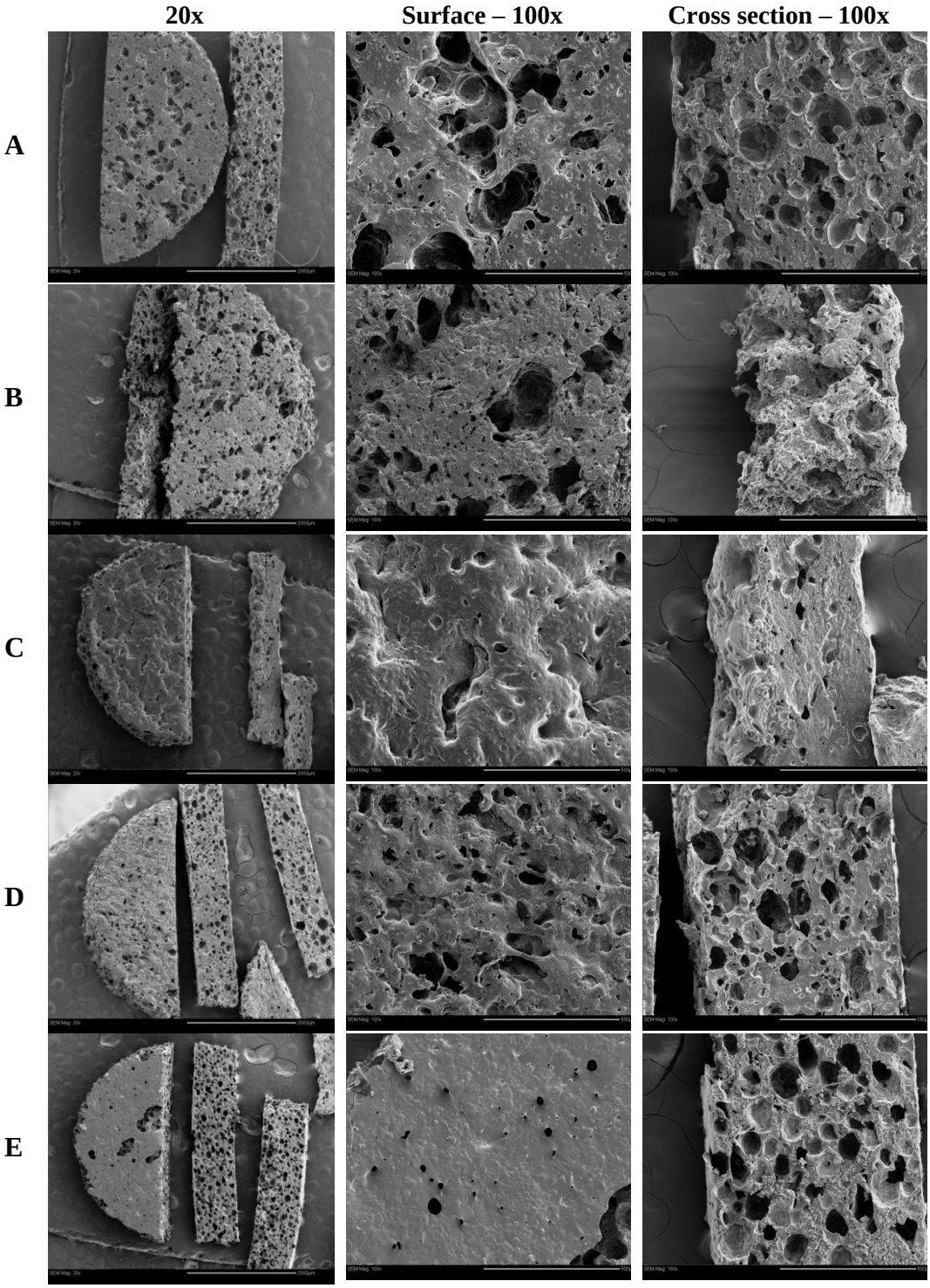

Figure 5-6: SEM micrographs of PEC elastomers after BSA release.

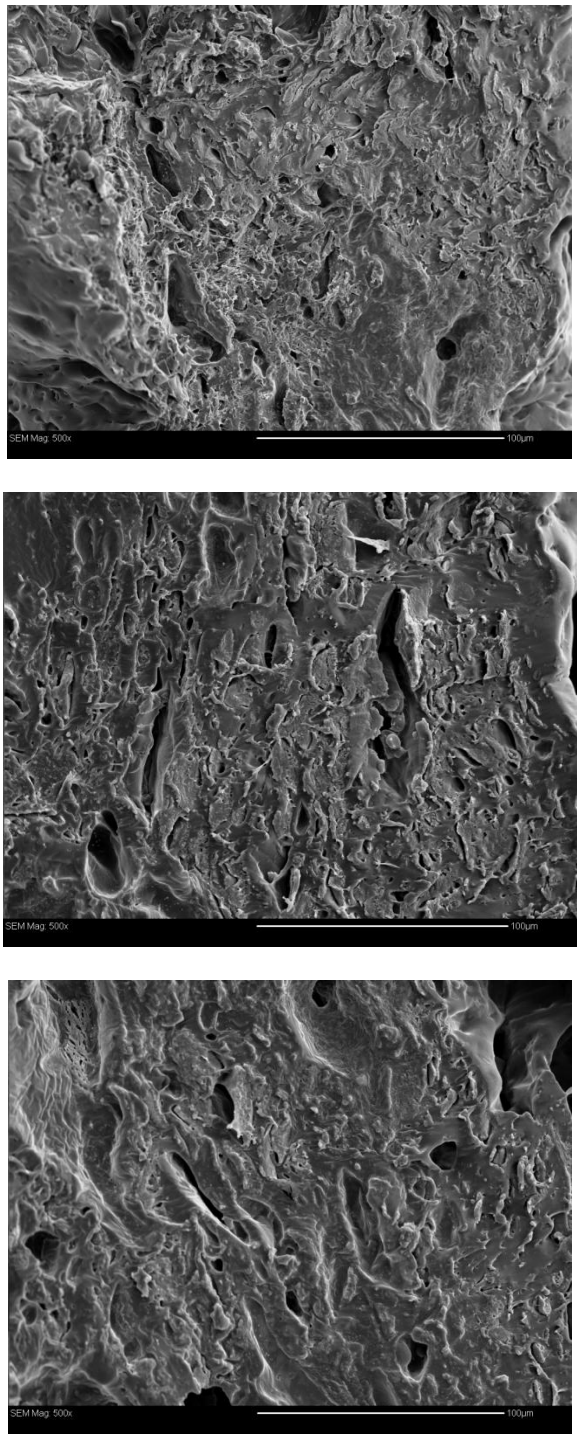

Figure 5-7: High magnification (500x) SEM micrographs of Elastomer C.

5.4 Conclusions

PEG can be incorporated into PEC or PTMC before UV crosslinking to create a highly porous structure (almost 60%) which is interconnected. PEG performs better as a porogen for BSA delivery than paraffin beads which result in a quick release for about 4 days, and a low plateau of released drug. Preliminary release results in PBS (pH 7.4) at 37°C can be explained by hypothesizing that added DMSO allows the PEG to be well dispersed within the elastomer disc, creating pores which are not interconnected. Due to this, PEG extraction and BSA release are slower and incomplete at 4 weeks.

Chapter 6

Conclusions and Recommendations

Therapeutic angiogenesis is one of the many promising applications of local protein delivery. Linear poly(ethylene carbonate), PEC, has many advantages as a protein delivery device since it degrades without producing acidic byproducts (like many other commonly used synthetics), and possesses good cytocompatibility and immunocompatibility. However, high molecular weight linear PEC degrades almost completely in 2-3 weeks, which is inappropriately fast for the application of therapeutic angiogenesis since it has been shown that the delivery of angiogenic growth factors must be sustained for 3-4 weeks to producing functional, stable new blood vessels. It was hypothesized that the *in vivo* degradation rate could be decreased to a more appropriate rate if PEC was crossslinked. Therefore, the goal of this work was to create biodegradable crossslinked PEC elastomers, to evaluate them as a new biomaterial in terms of biocompatibility and degradation properties, and to conduct preliminary release studies using porous protein-loaded PEC elastomers.

Solid PEC elastomers of a range of crosslink densities were successfully prepared using a photo-initiated free radical crosslinking reaction of highly acrylated PEC from 2000 Da to 12, 000 Da for characterisation by NMR, DSC, ATR-FTIR, sol content, and uniaxial tensile testing. These elastomers possessed a high ethylene carbonate unit fraction of over 82%, and the UV crosslinking conditions were selected such that the sol content was high (~5%) and conditions were mild to prevent denaturation of protein therapeutics.

Data presented here and in the literature indicated that the degradation mechanism of PEC elastomers is the same as that for linear PEC observed. This *in vivo* degradation mechanism is a cell-mediated surface erosion mechanism that is initiated by the superoxide anions secreted by adherent inflammatory cells. This is evidenced from the surface morphology which shows surface pitting, linear mass loss profiles for up to 12 weeks after subcutaneous implantation in rats, and *in vitro* oxidative degradation which confirm that the superoxide anion causes significant degradation of PEC elastomers. The *in vivo* degradation rate of PEC elastomers prepared from 6000 Da acrylated prepolymer was over 9 times slower than that of linear PEC (37 ± 4% in 12 weeks for PEC elastomers compared to linear PEC which had degraded to 78 ± 11% mass loss in only 3 weeks). This finding supports the hypothesis that the degradation rate of linear PEC can be prolonged to become more appropriate for protein delivery applications when crossslinked to form an elastomer. Furthermore, *in vitro* oxidative degradation results for different crosslink densities suggest that the oxidative degradation rate may be adjusted by the prepolymer molecular weight. This has positive implications for applications of PEC as a tissue engineering scaffold for a range of soft tissues since the desired degradation rate of the scaffold is determined by the rate of tissue regeneration.

A mild inflammatory response was observed during *in vivo* degradation studies of PEC. The response after 1 week for the PEC elastomer was characterised by numerous granulocytes at the implant-tissue interface, followed by granulation tissue, a fibrous capsule which was measured to be 72 ± 18 μm at Week 6 and 62 ± 11 μm at Week 12. For linear PEC at 1 week, while many inflammatory cells were observed at the interface, no granulocytes could be identified, likely due to the fact that significant degradation has already occurred by 1 week and therefore the inflammatory response is in a later stage. At Week 3, the fibrous capsule was variable in thickness and was 78 ± 38 μm and the disc-tissue interface contained large cellular nodules which

may have contained multinucleated giant cells as would be expected for a typical foreign body response.

For preliminary protein release screening, release experiments were performed for various formulations of BSA-loaded porous elastomers that were prepared by adding a vortexed DMSO suspension of BSA particles (3-14 μm diameter) into the acrylated polymer before crosslinking. The process for creating these particles was adapted from the literature in Guan *et al.* where it was shown that prepared basic fibroblast growth factor particles prepared in this way were found to be bioactive for 21 days into the *in vitro* release[175]. A process of making these elastomers porous was developed which simply involved the additional incorporation of low and high molecular weight PEG into the acrylated polymer before crosslinking. Porous material that had been prepared with 40% PEG 8000 and 20% PEG 400 in this way possessed highly interconnected pores from 50 to 250 μm in diameter and overall porosity of up to 60%. PEG was selected because it is water soluble, non-toxic and does not elicit a significant immune response and therefore can be extracted within the body as a hypothesized parameter for controlling the release.

BSA release results showed that PEG was a better porogen for this purpose than paraffin beads since elastomers prepared with paraffin beads resulted in a quick release of about 4 days, and a low plateau of released drug of only 10%, which may be due to limited interconnectivity. For comparable conditions, the release results for PEG created porous elastomers showed a prolonged release of about 2 weeks and then reached a final plateau of about 25%. Although this release was the more favourable release profile out of the formulations screened (which displayed extremely rapid release), it is still not the ideal protein release profile for this application which would release at a sustained rate for 3-4 weeks reaching nearly 100% release. Nevertheless, it

was identified that the amount of DMSO in the protein particle suspension which is mixed into the acrylated polymer mixture before crosslinking is an important formulation parameter that affects the release profile by more evenly distributing the porogen therefore restricting pore interconnectivity. This was demonstrated by release results, disc swelling, PEG extraction profile, and SEM micrographs to come to this conclusion. Without DMSO, the release of BSA from 12% BSA loaded elastomer is complete within a few days. On the other hand, when DMSO has been used in protein particle fabrication, the BSA release from 12% BSA loaded elastomers reaches a plateau of only about 25% in 19-24 days. Although the release profiles shown here are not appropriate for angiogenic growth factor delivery due to high burst release and/or incomplete release as they have been formulated, a formulation parameter was identified that can be used to adjust the release potentially showing a more appropriate release profile.

To further investigate the properties of PEC elastomers for applications as a new biomaterial, the following is a list of recommendations:

1. Optimize the purification process for depolymerized and acrylated polymers when higher purity products are of interest (e.g. for future *in vivo* experiments).
2. Acrylate using 0°C (ice bath) to reduce the formation of TEA-complex coloured product, which may decrease the efficiency of the crosslinking step.
3. Prepare the PEC diol polymer in the range of 3,000 to 8,000 MW for future studies since this is the most promising region (in terms of ease of acrylation, handling and processing).
4. Conduct an *in vivo* study to measure degradation of different PEC crosslink densities testing the suggested result presented here: that the *in vivo* degradation rate can be adjusted by the crosslink density (by the prepolymer molecular weight). Full

characterisation (molecular weight, and ethylene carbonate composition) is required to equally compare PEC *in vivo* degradation results.

5. Conduct immunohistochemistry to confirm the identification and number of macrophages during future biocompatibility studies.

While the present study shows that PEC elastomers may be promising as a new biomaterial for many applications, the protein-loaded porous formulations produce release rates that were not ideal for angiogenic growth factor delivery since they experienced burst release and/or incomplete release. In the future development of PEC elastomers as protein delivery devices, it is recommended that:

1. A formulation should be prepared for BSA release investigation which is intermediate to that of Elastomer C (12% BSA) and Elastomer B (5% BSA) since this is likely to produce a more prolonged release that is more efficient (complete). While the protein suspension concentration in DMSO was held constant between DMSO-containing elastomers within this work in order to maintain the same protein particle size, it was found that this DMSO vortexing step did not significantly decrease the size of the protein particles. The addition of DMSO was beneficial in prolonging the release, however. Therefore, it is also recommended that a different protein particle suspension concentration be investigated.

Chapter 7

References

1. Leader B, Baca QJ, Golan DE. Protein therapeutics: A summary and pharmacological classification. Nature Reviews Drug Discovery 2008 JAN;7(1):21-39.

2. Pennisi E. Bioinformatics - gene counters struggle to get the right answer. Science 2003 AUG 22;301(5636):1040-1.

3. Reichert JM. Trends in development and approval times for new therapeutics in the united states. Nature Reviews Drug Discovery 2003 SEP;2(9):695-702.

4. Tayalia P, Mooney DJ. Controlled growth factor delivery for tissue engineering. Adv Mater 2009 SEP 4;21(32-33):3269-85.

5. Yancopoulos GD, Davis S, Gale NW, Rudge JS, Wiegand SJ, Holash J. Vascular-specific growth factors and blood vessel formation. Nature 2000 SEP 14;407(6801):242-8.

6. Wildemann B, Bamdad P, Holmer C, Haas NP, Raschke M, Schmidmaier G. Local delivery of growth factors from coated titanium plates increases osteotomy healing in rats. Bone 2004 MAY;34(5):862-8.

7. Asahara T, Bauters C, Pastore C, Kearney M, Rossow S, Bunting S, Ferrara N, Symes JF, Isner JM. Local-delivery of vascular endothelial growth-factor accelerates reendothelialization and attenuates intimal hyperplasia in balloon-injured rat carotid-artery. Circulation 1995 JUN 1;91(11):2793-801.

8. Ji QX, Deng J, Xing XM, Yuan CQ, Yu XB, Xu QC, Yue J. Biocompatibility of a chitosan-based injectable thermosensitive hydrogel and its effects on dog periodontal tissue regeneration. Carbohydr Polym 2010 NOV 11;82(4):1153-60.

9. Khanna O, Moya ML, Opara EC, Brey EM. Synthesis of multilayered alginate microcapsules for the sustained release of fibroblast growth factor-1. J Biomed Mater Res Part A 2010 NOV;95A(2):632-40.

10. Choi JS, Yoo HS. Pluronic/chitosan hydrogels containing epidermal growth factor with wound-adhesive and photo-crosslinkable properties. J Biomed Mater Res Part A 2010 NOV;95A(2):564-73.

11. Zisch AH, Lutolf MP, Ehrbar M, Raeber GP, Rizzi SC, Davies N, Schmokel H, Bezuidenhout D, Djonov V, Zilla P, Hubbell JA. Cell-demanded release of VEGF from synthetic, biointeractive cell-ingrowth matrices for vascularized tissue growth. Faseb Journal 2003 OCT;17(13):2260.

12. Azrin M. Angiogenesis, protein and gene delivery. Br Med Bull 2001;59:211-25.

13. Ou M, Kim T, Yockman J, Borden BA, Bull DA, Kim SW. Polymer transfected primary myoblasts mediated efficient gene expression and angiogenic proliferation. Journal of Controlled Release 2010;142:61-69.

14. Cellular & Gene Therapy Products [Internet]: U.S. Department of Health and Human Servies; c2009 [cited 2010 11/01]. Available from: http://www.fda.gov/BiologicsBloodVaccines/CellularGeneTherapyProducts/default.htm.

15. Statistics Canada. CANSIM table 102-0529: Deaths, by cause, chapter IX: Diseases of the circulatory system (I00 to I99), age group and sex, canada, annual (number), 2000 to 2006. ; Released May 4, 2010.

16. Rouwkema J, Rivron NC, van Blitterswijk CA. Vascularization in tissue engineering. Trends in Biotechnology 2008 August, 2008;26(8):434-41.

17. Zisch AH, Lutolf MP, Hubbell JA. Biopolymeric delivery matrices for angiogenic growth factors. Cardiovascular Pathology 2003 November - December, 2003;12(6):295-310.

18. Lee H, Chung HJ, Park TG. Perspectives on: Local and sustained delivery of angiogenic growth factors. J Bioact Compatible Polym 2007 January 1;22(1):89-114.

19. Carmeliet P. Mechanisms of angiogenesis and arteriogenesis. Nat Med 2000 APR;6(4):389-95.

20. Risau W. Mechanisms of angiogenesis. Nature 1997;386(6626):671.

21. Boontheekul T, Mooney DJ. Protein-based signaling systems in tissue engineering. Curr Opin Biotechnol 2003 OCT;14(5):559-65.

22. Edelman ER, Nugent MA, Karnovsky MJ. Perivascular and intravenous administration of basic fibroblast growth-factor - vascular and solid organ deposition. Proc Natl Acad Sci U S A 1993 FEB 15;90(4):1513-7.

23. Jay SM, Saltzman WM. Controlled delivery of VEGF via modulation of alginate microparticle ionic crosslinking. J Controlled Release 2009 FEB 20;134(1):26-34.

24. Lazarous DF, Shou M, Scheinowitz M, Hodge E, Thirumurti V, Kitsiou AN, Stiber JA, Lobo AD, Hunsberger S, Guetta E, Epstein SE, Unger EF. Comparative effects of basic fibroblast growth factor and vascular endothelial growth factor on coronary collateral development and the arterial response to injury. Circulation 1996 SEP 1;94(5):1074-82.

25. Tessmar JK, Goepferich AM. Matrices and scaffolds for protein delivery in tissue engineering. Adv Drug Deliv Rev 2007 MAY 30;59(4-5):274-91.

26. Amsden BG. Biodegradable elastomers in drug delivery. Expert Opin Drug Deliv 2008 Feb;5(2):175-87.

27. Wu F, Jin T. Polymer-based sustained-release dosage forms for protein drugs, challenges, and recent advances. Aaps Pharmscitech 2008 DEC;9(4):1218-29.

28. Frokjaer S, Otzen DE. Protein drug stability: A formulation challenge. Nature Reviews Drug Discovery 2005 APR;4(4):298-306.

29. Brazel CS, Peppas NA. Temperature- and pH-sensitive hydrogels for controlled release of anti-thrombotic agents. Mater Res Soc Symp Proc 1994;331:211-216.

30. Saltzman WM. Drug delivery engineering principles for drug therapy. Oxford University Press; 2001. .

31. Chung HJ, Park TG. Surface engineered and drug releasing pre-fabricated scaffolds for tissue engineering. Adv Drug Deliv Rev 2007 MAY 30;59(4-5):249-62.

32. Uchegbu I, Schatzlein A. Polymers in drug delivery. ; 2006. .

33. Amsden B. Review of osmotic pressure driven release of proteins from monolithic devices. J Pharm Pharm Sci 2007;10(2):129-43.

34. Wei C, Hou C, Gu Q, Jiang L, Zhu B, Sheng A. A thermosensitive chitosan-based hydrogel barrier for post-operative adhesions' prevention. Biomaterials 2009 OCT;30(29):5534-40.

35. Chapanian R.
DEVELOPMENT AND CHARACTERIZATION OF BIODEGRADABLE ELASTOMERS FOR LOCALIZED ANGIOGENIC GROWTH FACTOR DELIVERY. Queen's University, Kingston, Ontario; 2009.

36. Malin M, HiljanenVainio M, Karjalainen T, Seppala J. Biodegradable lactone copolymers .2. hydrolytic study of epsilon-caprolactone and lactide copolymers. J Appl Polym Sci 1996 FEB 22;59(8):1289-98.

37. Karjalainen T, HiljanenVainio M, Malin M, Seppala J. Biodegradable lactone copolymers .3. mechanical properties of epsilon-caprolactone and lactide copolymers after hydrolysis in vitro. J Appl Polym Sci 1996 FEB 22;59(8):1299-304.

38. den Dunnen WFA, Meek MF, Grijpma DW, Robinson PF, Schakenraad JM. In vivo and in vitro degradation of poly[(50)/(50) ((85)/(L)(15)/(D))LA/epsilon-CL], and the implications for the use in nerve reconstruction. J Biomed Mater Res 2000 SEP 15;51(4):575-85.

39. Reed AM, Gilding DK. Biodegradable polymers for use in surgery - poly(glycolic)-poly(lactic acid) homo and co-polymers .2. invitro degradation. Polymer 1981;22(4):494-8.

40. Storey RF, Hickey TP. Degradable polyurethane networks based on D,l-lactide, glycolide, epsilon-caprolactone, and trimethylene carbonate homopolyester and copolyester triols. Polymer 1994;35(4):830-8.

41. Ratner BD, Hoffman AS, Schoen FJ, Lemons JE, editors. Biomaterials science: An introduction to materials in medicine. Second Edition ed. San Diego, California: Elsevier Academic Press; 2004. .

42. Uhrich KE, Cannizzaro SM, Langer RS, Shakesheff KM. Polymeric systems for controlled drug release. Chemical Reviews 1999;99(11):3181-3198.

43. Hurrell S, Cameron RE. Polyglycolide: Degradation and drug release. part I: Changes in morphology during degradation. J Mater Sci -Mater Med 2001 SEP;12(9):811-6.

44. Weir NA, Buchanan FJ, Orr JF, Dickson GR. Degradation of poly-L-lactide: Part 1: In vitro and in vivo physiological temperature degradation. Proceedings of the Institution of Mechanical Engineers Part H-Journal of Engineering in Medicine 2004 SEP;218(H5):307-19.

45. Leenslag JW, Pennings AJ, Bos RRM, Rozema FR, Boering G. Resorbable materials of poly(l-lactide) .7. invivo and invitro degradation. Biomaterials 1987 JUL;8(4):311-4.

46. Pitt CG, Gratzl MM, Kimmel GL, Surles J, Schindler A. Aliphatic polyesters .2. the degradation of poly(dl-lactide), poly(epsilon-caprolactone), and their copolymers invivo. Biomaterials 1981;2(4):215-20.

47. Stoll GH, Nimmerfall F, Acemoglu M, Bodmer D, Bantle S, Muller I, Mahl A, Kolopp M, Tullberg K. Poly(ethylene carbonate)s, part II: Degradation mechanisms and parenteral delivery of bioactive agents. J Control Release 2001 Oct 19;76(3):209-25.

48. Zhang Z, Kuijer R, Bulstra SK, Grijpma DW, Feijen J. The in vivo and in vitro degradation behavior of poly(trimethylene carbonate). Biomaterials 2006 Mar;27(9):1741-8.

49. Chapanian R, Tse MY, Pang SC, Amsden BG. The role of oxidation and enzymatic hydrolysis on the in vivo degradation of trimethylene carbonate based photocrosslinkable elastomers. Biomaterials 2009 January, 2009;30(3):295-306.

50. Wang YD, Kim YM, Langer R. In vivo degradation characteristics of poly(glycerol sebacate). Journal of Biomedical Materials Research Part a 2003 JUL 1;66A(1):192-7.

51. Acemoglu M. Chemistry of polymer biodegradation and implications on parenteral drug delivery. Int J Pharm 2004 Jun 11;277(1-2):133-9.

52. Christenson EM, Patel S, Anderson JM, Hiltner A. Enzymatic degradation of poly(ether urethane) and poly(carbonate urethane) by cholesterol esterase. Biomaterials 2006 JUL;27(21):3920-6.

53. Schwach-Abdellaoui K, Heller J, Gurny R. Hydrolysis and erosion studies of autocatalyzed poly(ortho esters) containing lactoyl-lactyl acid dimers. Macromolecules 1999 JAN 26;32(2):301-7.

54. Kumar N, Langer RS, Domb AJ. Polyanhydrides: An overview. Advanced Drug Delivery Reviews 2002 October 16, 2002;54(7):889-910.

55. Tabata Y, Gutta S, Langer R. Controlled delivery systems for proteins using polyanhydride microspheres. Pharm Res 1993 APR;10(4):487-96.

56. Tang Y, Singh J. Controlled delivery of aspirin: Effect of aspirin on polymer degradation and in vitro release from PLGA based phase sensitive systems. Int J Pharm 2008 JUN 5;357(1-2):119-25.

57. Quaglia F, Ostacolo L, Nese G, De Rosa G, La Rotonda MI, Palumbo R, Maglio G. Microspheres made of poly (epsilon-caprolactone)-based amphiphilic copolymers: Potential in sustained delivery of proteins. Macromolecular Bioscience 2005 OCT 20;5(10):945-54.

58. Nishino S, Kishida A, Yoshizawa H. Morphology control of polylactide microspheres enclosing irinotecan hydrochloride with polylactide based polymer surfactant for reduction of initial burst. Int J Pharm 2007 FEB 7;330(1-2):32-6.

59. Patil SD, Papadmitrakopoulos F, Burgess DJ. Concurrent delivery of dexamethasone and VEGF for localized inflammation control and angiogenesis. J Controlled Release 2007 JAN 22;117(1):68-79.

60. Meyenburg S, Lilie H, Panzner S, Rudolph R. Fibrin encapsulated liposomes as protein delivery system - studies on the in vitro release behavior. J Controlled Release 2000 OCT 3;69(1):159-68.

61. Hobo K, Shimizu T, Sekine H, Shin'oka T, Okano T, Kurosawa H. Therapeutic angiogenesis using tissue engineered human smooth muscle cell sheets. Arteriosclerosis Thrombosis and Vascular Biology 2008 APR;28(4):637-43.

62. Kim JY, Khang D, Lee JE, Webster TJ. Decreased macrophage density on carbon nanotube patterns on polycarbonate urethane. J Biomed Mater Res Part A 2009 FEB;88A(2):419-26.

63. Aschkenasy C, Kost J. On-demand release by ultrasound from osmotically swollen hydrophobic matrices. J Controlled Release 2005 DEC 10;110(1):58-66.

64. Dill KA. Dominant forces in protein folding. Biochemistry (N Y) 1990 AUG 7;29(31):7133-55.

65. Volkin DB, Klibanov AM. Minimizing protein inactivation. In: Protein function A practical approach. ; 1989. .

66. Kavanagh CA, Gorelova TA, Selezneva II, Rochev YA, Dawson KA, Gallagher WM, Gorelov AV, Keenan AK. Poly(N-isopropy acrylamide) copolymer films as vehicles for the sustained delivery of proteins to vascular endothelial cells. J Biomed Mater Res Part A 2005 JAN 1;72A(1):25-35.

67. Gu F, Amsden B, Neufeld R. Sustained delivery of vascular endothelial growth factor with alginate beads. J Controlled Release 2004 MAY 18;96(3):463-72.

68. Ferrara N. Vascular endothelial growth factor: Basic science and clinical progress. Endocr Rev 2004 AUG;25(4):581-611.

69. VEGF improves myocardial blood flow but produces EDRF-mediated hypotension in porcine hearts. Journal of surgical research; JUN; ; 1996. .

70. Horowitz JR, Rivard A, vanderZee R, Hariawala M, Sheriff DD, Esakof DD, Chaudhry GM, Symes JF, Isner JM. Vascular endothelial growth factor vascular permeability factor produces nitric oxide-dependent hypotension - evidence for a maintenance role in quiescent adult endothelium. Arteriosclerosis Thrombosis and Vascular Biology 1997 NOV;17(11):2793-800.

71. Lee RJ, Springer ML, Blanco-Bose WE, Shaw R, Ursell PC, Blau HM. VEGF gene delivery to myocardium - deleterious effects of unregulated expression. Circulation 2000 AUG 22;102(8):898-901.

72. Kim TK, Burgess DJ. Pharmacokinetic characterization C-14-vascular endothelial growth factor controlled release microspheres using a rat model. J Pharm Pharmacol 2002 JUL;54(7):897-905.

73. Kim TK, Burgess DJ. Pharmacokinetic characterization C-14-vascular endothelial growth factor controlled release microspheres using a rat model. J Pharm Pharmacol 2002 JUL;54(7):897-905.

74. Goolcharran C, Cleland JL, Keck R, Jones AJS, Borchardt RT. Comparison of the rates of deamidation, diketopiperazine formation, and oxidation in recombinant human vascular endothelial growth factor and model peptides. Aaps Pharmsci 2000;2(1):5.

75. Development of poly-(D,L-lactide-coglycolide) microsphere formulations containing recombinant human vascular endothelial growth factor to promote local angiogenesis. Journal of controlled release; MAY 14; ; 2001. .

76. Post MJ, Laham R, Sellke FW, Simons M. Therapeutic angiogenesis in cardiology using protein formulations. Cardiovasc Res 2001 FEB 16;49(3):522-31.

77. Epstein SE, Fuchs S, Zhou YF, Baffour R, Kornowski R. Therapeutic interventions for enhancing collateral development by administration of growth factors: Basic principles, early results and potential hazards. Cardiovasc Res 2001 FEB 16;49(3):532-42.

78. Yla-Herttuala S, Alitalo K. Gene transfer as a tool to induce therapeutic vascular growth. Nat Med 2003 JUN;9(6):694-701.

79. Annex BH, Simons M. Growth factor-induced therapeutic angiogenesis in the heart: Protein therapy. Cardiovasc Res 2005 FEB 15;65(3):649-55.

80. Dor Y, Djonov V, Abramovitch R, Itin A, Fishman GI, Carmeliet P, Goelman G, Keshet E. Conditional switching of VEGF provides new insights into adult neovascularization and pro-angiogenic therapy. EMBO J 2002 APR 15;21(8):1939-47.

81. von Degenfeld G, Banfi A, Springer ML, Wagner RA, Jacobi J, Ozawa CR, Merchant MJ, Cooke JP, Blau HM. Microenvironmental VEGF distribution is critical for stable and functional vessel growth in ischemia. Faseb Journal 2006 DEC;20(14):2657,+.

82. Davies N, Dobner S, Bezuidenhout D, Schmidt C, Beck M, Zisch AH, Zilla P. The dosage dependence of VEGF stimulation on scaffold neovascularisation. Biomaterials 2008 September, 2008;29(26):3531-8.

83. Richardson TP, Peters MC, Ennett AB, Mooney DJ. Polymeric system for dual growth factor delivery. Nature Biotechnology 2001;19(11):1029.

84. Hao X, Silva EA, Mansson-Broberg A, Grinnemo K, Siddiqui AJ, Dellgren G, Wardell E, Brodin LA, Mooney DJ, Sylven C. Angiogenic effects of sequential release of VEGF-A(165) and PDGF-BB with alginate hydrogels after myocardial infarction. Cardiovasc Res 2007 JUL 1;75(1):178-85.

85. Xin XH, Yang SY, Ingle G, Zlot C, Rangell L, Kowalski J, Schwall R, Ferrara N, Gerritsen ME. Hepatocyte growth factor enhances vascular endothelial growth factor-induced angiogenesis in vitro and in vivo. Am J Pathol 2001 MAR;158(3):1111-20.

86. Chapanian R, Amsden BG. Combined and sequential delivery of bioactive VEGF(165) and HGF from poly (trimethylene carbonate) based photo-cross-linked elastomers. J Controlled Release 2010 APR 2;143(1):53-63.

87. Papavasiliou G, Cheng M, Brey EM. Strategies for vascularization of polymer scaffolds. J Invest Med 2010 OCT;58(7):838-44.

88. Freeman I, Cohen S. The influence of the sequential delivery of angiogenic factors from affinity-binding alginate scaffolds on vascularization. Biomaterials 2009 4;30(11):2122-31.

89. Sokolsky-Papkov M, Agashi K, Olaye A, Shakesheff K, Domb AJ. Polymer carriers for drug delivery in tissue engineering. Adv Drug Deliv Rev 2007 May 30;59(4-5):187-206.

90. Ziegler J, Mayr-Wohlfart U, Kessler S, Breitig D, Gunther KP. Adsorption and release properties of growth factors from biodegradable implants. J Biomed Mater Res 2002 MAR 5;59(3):422-8.

91. Wei G, Jin Q, Giannobile WV, Ma PX. The enhancement of osteogenesis by nano-fibrous scaffolds incorporating rhBMP-7 nanospheres. Biomaterials 2007 APR;28(12):2087-96.

92. Sohier J, Vlugt TJH, Cabrol N, Van Blitterswijk C, de Groot K, Bezemer JM. Dual release of proteins from porous polymeric scaffolds. Journal of Controlled Release 2006 March 10, 2006;111(1-2):95-106.

93. Cleland JL, Johnson OL, Putney S, Jones AJS. Recombinant human growth hormone poly(lactic-co-glycolic acid) microsphere formulation development. Adv Drug Deliv Rev 1997 OCT 13;28(1):71-84.

94. Kim HK, Park TG. Microencapsulation of human growth hormone within biodegradable polyester microspheres: Protein aggregation stability and incomplete release mechanism. Biotechnol Bioeng 1999 DEC 20;65(6):659-67.

95. Wang W. Protein aggregation and its inhibition in biopharmaceutics. Int J Pharm 2005 JAN 31;289(1-2):1-30.

96. Tillmann HC, Kuhn B, Kranzlin B, Sadick M, Gross J, Gretz N, Pill J. Efficacy and immunogenicity of novel erythropoietic agents and conventional rhEPO in rats with renal insufficiency. Kidney Int 2006 JAN;69(1):60-7.

97. Shi Y, Li LS. Current advances in sustained release systems for parenteral drug delivery. Expert Opinion on Drug Delivery 2005;6:1039.

98. Biondi M, Ungaro F, Quaglia F, Netti PA. Controlled drug delivery in tissue engineering. Adv Drug Deliv Rev 2008;60(2):229-42.

99. Ko HCH, Milthorpe BK, McFarland CD. Engineering thick tissues - the vascularisation problem. Eur Cells Mater 2007 JUL-DEC;14:1-18.

100. Lutolf MP, Hubbell JA. Synthetic biomaterials as instructive extracellular microenvironments for morphogenesis in tissue engineering. Nat Biotechnol 2005 JAN;23(1):47-55.

101. Vaquette C, Fawzi-Grancher S, Lavalle P, Frochot C, Viriot ML, Muller S, Wang X. In vitro biocompatibility of different polyester membranes. Biomed Mater Eng 2006;16(4):S131-6.

102. Montjovent MO, Mathieu L, Hinz B, Applegate LL, Bourban PE, Zambelli PY, Manson JA, Pioletti DP. Biocompatibility of bioresorbable poly(L-lactic acid) composite scaffolds obtained by supercritical gas foaming with human fetal bone cells. Tissue Eng 2005 NOV;11(11-12):1640-9.

103. Yue H, Zhang L, Wang Y, Liang F, Guan L, Li S, Yan F, Nan X, Bai C, Lin F, Yan Y, Pei X. Proliferation and differentiation into endothelial cells of human bone marrow mesenchymal stem cells (MSCs) on poly DL-lactic-co-glycolic acid (PLGA) films. Chin Sci Bull 2006 JUN;51(11):1328-33.

104. Li CM, Vepari C, Jin HJ, Kim HJ, Kaplan DL. Electrospun silk-BMP-2 scaffolds for bone tissue engineering. Biomaterials 2006 JUN;27(16):3115-24.

105. van de Weert M, Hennink WE, Jiskoot W. Protein instability in poly(lactic-co-glycolic acid) microparticles. Pharm Res 2000 OCT;17(10):1159-67.

106. Middleton JC, Tipton AJ. Synthetic biodegradable polymers as orthopedic devices. Biomaterials 2000 DEC;21(23):2335-46.

107. Tamada J, Langer R. The development of polyanhydrides for drug delivery applications. Journal of Biomaterials Science-Polymer Edition 1992;3(4):315-53.

108. Ambrosio AMA, Allcock HR, Katti DS, Laurencin CT. Degradable polyphosphazene/poly(alpha-hydroxyester) blends: Degradation studies. Biomaterials 2002 APR;23(7):1667-72.

109. Chen L, Apte RN, Cohen S. Characterization of PLGA microspheres for the controlled delivery of IL-1 alpha for tumor immunotherapy. J Controlled Release 1997 JAN 18;43(2-3):261-72.

110. Yang J, Cleland JL. Factors affecting the in vitro release of recombinant human interferon-gamma (rhIFN-gamma) from PLGA microspheres. J Pharm Sci 1997 AUG;86(8):908-14.

111. Hora MS, Rana RK, Nunberg JH, Tice TR, Gilley RM, Hudson ME. Controlled release of interleukin-2 from biodegradable microspheres. Bio-Technology 1990 AUG;8(8):755-8.

112. Park TG, Lu WQ, Crotts G. Importance of in-vitro experimental conditions on protein release kinetics, stability and polymer degradation in protein encapsulated poly(d,l-lactic acid-co-glycolic acid) microspheres. J Controlled Release 1995 FEB;33(2):211-22.

113. Johnson RE, Lanaski LA, Gupta V, Griffin MJ, Gaud HT, Needham TE, Zia H. Stability of atriopeptin-iii in poly(d,l-lactide-co-glycolide) microspheres. J Controlled Release 1991 SEP;17(1):61-7.

114. Takahata H, Lavelle EC, Coombes AGA, Davis SS. The distribution of protein associated with poly(DL-lactide co-glycolide) microparticles and its degradation in simulated body fluids. J Controlled Release 1998 JAN 2;50(1-3):237-46.

115. Zambaux MF, Bonneaux F, Gref R, Dellacherie E, Vigneron C. Preparation and characterization of protein C-loaded PLA nanoparticles. J Controlled Release 1999 AUG 5;60(2-3):179-88.

116. Aubert-Pouessel A, Bibby DC, Venier-Julienne MC, Hindre F, Benoit JP. A novel in vitro delivery system for assessing the biological integrity of protein upon release from PLGA microspheres. Pharm Res 2002 JUL;19(7):1046-51.

117. Ekholm M, Hietanen J, Lindqvist C, Rautavuori J, Santavirta S, Suuronen R. Histological study of tissue reactions to epsilon-caprolactone-lactide copolymer in paste form. Biomaterials 1999 JUL;20(14):1257-62.

118. McCarthy SJ, Meijs GF, Mitchell N, Gunatillake PA, Heath G, Brandwood A, Schindhelm K. In-vivo degradation of polyurethanes: Transmission-FTIR microscopic characterization of polyurethanes sectioned by cryomicrotomy. Biomaterials 1997 NOV;18(21):1387-409.

119. Schubert MA, Wiggins MJ, Schaefer MP, Hiltner A, Anderson JM. Oxidative biodegradation mechanisms of biaxially strained poly(etherurethane urea) elastomers. J Biomed Mater Res 1995 MAR;29(3):337-47.

120. Lee H, Park TG. Photo-crosslinkable, biomimetic, and thermo-sensitive pluronic grafted hyaluronic acid copolymers for injectable delivery of chondrocytes. J Biomed Mater Res A 2008 Mar 31.

121. Bioadsorbable polymer scaffolds for tissue engineering capable of sustained growth factor delivery. Journal of controlled release; FEB 14; AMSTERDAM; PO BOX 211, 1000 AE AMSTERDAM, NETHERLANDS: ELSEVIER SCIENCE BV; 2000. NR: 36; TC: 176; J9: J CONTROL RELEASE; PG: 12; GA: 285FK.

122. Zhu GZ, Mallery SR, Schwendeman SP. Stabilization of proteins encapsulated in injectable poly (lactide-co-glycolide). Nat Biotechnol 2000 JAN;18(1):52-7.

123. Ding AG, Schwendeman SP. Acidic microclimate pH distribution in PLGA microspheres monitored by confocal laser scanning microscopy. Pharm Res 2008 SEP;25(9):2041-52.

124. Lee KY, Yuk SH. Polymeric protein delivery systems. Prog Polym Sci 2007 JUL;32(7):669-97.

125. Bryant SJ, Anseth KS. The effects of scaffold thickness on tissue engineered cartilage in photocrosslinked poly(ethylene oxide) hydrogels. Biomaterials 2001 MAR;22(6):619-26.

126. Metters AT, Anseth KS, Bowman CN. Fundamental studies of a novel, biodegradable PEG-b-PLA hydrogel. Polymer 2000 MAY;41(11):3993-4004.

127. Mann BK, Gobin AS, Tsai AT, Schmedlen RH, West JL. Smooth muscle cell growth in photopolymerized hydrogels with cell adhesive and proteolytically degradable domains: Synthetic ECM analogs for tissue engineering. Biomaterials 2001 NOV;22(22):3045-51.

128. Manipulation of hydrogel assembly and growth factor delivery via the use of peptide-polysaccharide interactions. Journal of controlled release; AUG 28; ; 2006. SI: Sp. Iss. SI.

129. Extensive in vivo angiogenesis following controlled release of human vascular endothelial cell growth factor: Implications for tissue engineering and wound healing. Artificial organs; JUL; 2001.

130. Harada K, Grossman W, Friedman M, Edelman ER, Prasad PV, Keighley CS, Manning WJ, Sellke FW, Simons M. Basic fibroblast growth-factor improves myocardial-function in chronically ischemic porcine hearts. J Clin Invest 1994 AUG;94(2):623-30.

131. Laham RJ, Sellke FW, Edelman ER, Pearlman JD, Ware JA, Brown DL, Gold JP, Simons M. Local perivascular delivery of basic fibroblast growth factor in patients undergoing coronary bypass surgery - results of a phase I randomized, double-blind, placebo-controlled trial. Circulation 1999 NOV 2;100(18):1865-71.

132. Boontheekul T, Kong H-, Mooney DJ. Controlling alginate gel degradation utilizing partial oxidation and bimodal molecular weight distribution. Biomaterials 2005 May, 2005;26(15):2455-65.

133. Albertsson AC, Eklund M. Influence of molecular-structure on the degradation mechanism of degradable polymers - in-vitro degradation of poly(trimethylene carbonate), poly(trimethylene carbonate-co-caprolactone), and poly(adipic anhydride). J Appl Polym Sci 1995 JUL 5;57(1):87-103.

134. Pego AP, Poot AA, Grijpma DW, Feijen J. In vitro degradation of trimethylene carbonate based (co)polymers. Macromolecular Bioscience 2002 DEC 30;2(9):411-9.

135. Sharifpoor S, Amsden B. In vitro release of a water-soluble agent from low viscosity biodegradable, injectable oligomers. Eur J Pharm Biopharm 2007 Mar;65(3):336-45.

136. Pego AP, Van Luyn MJA, Brouwer LA, van Wachem PB, Poot AA, Grijpma DW, Feijen J. In vivo behavior of poly(1,3-trimethylene carbonate) and copolymers of 1,3-trimethylene carbonate with D,L-lactide or epsilon-caprolactone: Degradation and tissue response. J Biomed Mater Res Part A 2003 DEC 1;67A(3):1044-54.

137. Chapanian R, Amsden BG. Osmotically driven protein release from photo-cross-linked elastomers of poly(trimethylene carbonate) and poly(trimethylene carbonate-CO-D,L-lactide). European Journal of Pharmaceutics and Biopharmaceutics 2010 FEB;74(2):172-83.

138. Kawaguchi T, Nakano M, Juni K, Inoue S, Yoshida Y. Examination of biodegradability of poly(ethylene carbonate) and poly(propylene carbonate) in the peritoneal cavity in rats. Chem Phar Bull 1983;31(4):1400.

139. Cha Y, Reardon P, Mah S, Whitcomb L. In vitro enzymatic surface erosion of polyethylene carbonate in the presence of macrophages. Proceed Intern Symp Control Rel Bioact Mater 1994;21.

140. Acemoglu M, Nimmerfall F, Bantle S, Stoll G. Poly(ethylene carbonate)s, part I: Syntheses and structural effects on biodegradation. Journal of Controlled Release 1997 December 15, 1997;49(2-3):263-76.

141. Dadsetan M, Christenson EM, Unger F, Ausborn M, Kissel T, Hiltner A, Anderson JM. In vivo biocompatibility and biodegradation of poly(ethylene carbonate). J Control Release 2003 Dec 12;93(3):259-70.

142. Unger F, Westedt U, Hanefeld P, Wombacher R, Zimmermann S, Greiner A, Ausborn M, Kissel T. Poly(ethylene carbonate): A thermoelastic and biodegradable biomaterial for drug eluting stent coatings? Journal of Controlled Release 2007 February 26, 2007;117(3):312-21.

143. Gu F, Neufeld R, Amsden B. Sustained release of bioactive therapeutic proteins from a biodegradable elastomeric device. J Control Release 2007 Jan 22;117(1):80-9.

144. Niklason LE, Gao J, Abbott WM, Hirschi KK, Houser S, Marini R, Langer R. Functional arteries grown in vitro. Science 1999 Apr 16;284(5413):489-93.

145. Scaffolds for engineering smooth muscle under cyclic mechanical strain conditions. Journal of biomechanical engineering-transactions of the asme; JUN; ; 2000. .

146. Waldman SD, Spiteri CG, Grynpas MD, Pilliar RM, Kandel RA. Long-term intermittent compressive stimulation improves the composition and mechanical properties of tissue-engineered cartilage. Tissue Eng 2004 Sep-Oct;10(9-10):1323-31.

147. S. Sideman, R. Beyar, A. Landesberg, editors. Extracellular stimulation in tissue engineering. Communicative cardiac cell; ANNALS OF THE NEW YORK ACADEMY OF SCIENCES; 2005. .

148. Stegemann JP, Nerem RM. Phenotype modulation in vascular tissue engineering using biochemical and mechanical stimulation. Ann Biomed Eng 2003 Apr;31(4):391-402.

149. Anderson JM. Biological responses to materials. Annu Rev Mater Res 2001;31(81):110.

150. Mikos AG, Thorsen AJ, Czerwonka LA, Bao Y, Langer R, Winslow DN, Vacanti JP. Preparation and characterization of poly(l-lactic acid) foams. Polymer 1994;35(5):1068-77.

151. Whang K, Thomas CH, Healy KE, Nuber G. A novel method to fabricate bioabsorbable scaffolds. Polymer 1995 FEB;36(4):837-42.

152. Nam YS, Yoon JJ, Park TG. A novel fabrication method of macroporous biodegradable polymer scaffolds using gas foaming salt as a porogen additive. J Biomed Mater Res 2000 FEB;53(1):1-7.

153. Heller J. Use of poly(ortho esters) and polyanhydrides in the development of peptide and protein delivery systems. Formulation and Delivery of Proteins and Peptides 1994;567:292-305.

154. Pego AP, Grijpma DW, Feijen J. Enhanced mechanical properties of 1,3-trimethylene carbonate polymers and networks. Polymer 2003 OCT;44(21):6495-504.

155. Inoue S, Koinuma H, Tsuruta T. Copolymerisation of carbon dioxide and epoxide. J Polymer Sci B 1969;7:287.

156. Sant'Angelo JG, Chen X, inventors. Process for obtaining lower molecular weight poly(alkylene carbonate) from higher molecular weight poly(alkylene carbonate). WO/2000/039172. 2000.

157. Pavia DL, Lampman GM, Kriz GS. Nuclear magnetic resonance spectroscopy part one: Basic concepts, acidic and exchangeable protons: Hydrogen bonding. In: Introduction to spectroscopy. 2nd ed. Saunders College Publishing; 1996. .

158. Amsden BG, Misra G, Gu F, Younes HM. Synthesis and characterization of a photo-cross-linked biodegradable elastomer. Biomacromolecules 2004 NOV-DEC;5(6):2479-86.

159. Fisher JP, Dean D, Engel PS, Mikos AG. Photoinitiated polymerization of biomaterials. Ann Rev Mater Res 2001;31:171-81.

160. Kurdikar DL, Peppas NA. Method of determination of initiator efficiency - application to uv polymerizations using 2,2-dimethoxy-2-phenylacetophenone. Macromolecules 1994 JAN 31;27(3):733-8.

161. Gu F, Neufeld R, Amsden B. Maintenance of vascular endothelial growth factor and potentially other therapeutic proteins bioactivity during a photo-initiated free radical cross-linking reaction forming biodegradable elastomers. Eur J Pharm Biopharm 2007 Apr;66(1):21-7.

162. Lendlein A, Schmidt AM, Schroeter M, Langer R. Shape-memory polymer networks from oligo(epsilon-caprolactone)dimethacrylates. J Polym Sci Pol Chem 2005 APR 1;43(7):1369-81.

163. Eisenbarth E. Biomaterials for tissue engineering. Advanced Engineering Materials 2007 DEC;9(12):1051-60.

164. Butcher JT, Barrett BC, Nerem RM. Equibiaxial strain stimulates fibroblastic phenotype shift in smooth muscle cells in an engineered tissue model of the aortic wall. Biomaterials 2006 Oct;27(30):5252-8.

165. Levental I, Georges PC, Janmey PA. Soft biological materials and their impact on cell function. Soft Matter 2007;3(3):299-306.

166. Chapanian R, Tse MY, Pang SC, Amsden BG. Long term in vivo degradation and tissue response to photo-cross-linked elastomers prepared from star-shaped prepolymers of poly(epsilon-caprolactone-co-D,L-lactide). Journal of Biomedical Materials Research Part a 2010 MAR 1;92A(3):830-42.

167. Bat E, van Kooten TG, Feijen J, Grijpma DW. Macrophage-mediated erosion of gamma irradiated poly(trimethylene carbonate) films. Biomaterials 2009 AUG;30(22):3652-61.

168. Lee KH, Won CY, Chu CC, Gitsov I. Hydrolysis of biodegradable polymers by superoxide ions. Journal of Polymer Science Part A-Polymer Chemistry 1999 SEP 15;37(18):3558-67.

169. Valentine JS, Curtis AB. Convenient preparation of solutions of superoxide anion and reaction of superoxide anion with a copper(ii) complex. J Am Chem Soc 1975;97(1):224-6.

170. Badwey J, Karnovsky ML. Active oxygen species and the functions of phagocytic leukocytes. Ann Rev Biochem 1980;49:695-726.

171. Devereux DF, O'Connell SM, Liesch JB, Weinstein M, Robertson FM. Induction of leukocyte activation by meshes surgically implanted in the peritoneal cavity. The American Journal of Surgery 1991 9;162(3):243-6.

172. Blanco MD, Sastre RL, Teijon C, Olmo R, Teijon JM. Degradation behaviour of microspheres prepared by spray-drying poly(D,L-lactide) and poly(D,L-lactide-co-glycolide) polymers. Int J Pharm 2006 DEC 1;326(1-2):139-47.

173. Jones CF, Grainger DW. In vitro assessments of nanomaterial toxicity. Adv Drug Deliv Rev 2009 JUN 21;61(6):438-56.

174. Gu F, Neufeld R, Amsden B. Osmotic-driven release kinetics of bioactive therapeutic proteins from a biodegradable elastomer are linear, constant, similar, and adjustable. Pharm Res 2006 Apr;23(4):782-9.

175. Guan J, Stankus JJ, Wagner WR. Biodegradable elastomeric scaffolds with basic fibroblast growth factor release. J Controlled Release 2007 JUL 13;120(1-2):70-8.

176. Parajo Y, d'Angelo I, Welle A, Garcia-Fuentes M, Jose Alonso M. Hyaluronic acid/Chitosan nanoparticles as delivery vehicles for VEGF and PDGF-BB. Drug Deliv 2010 NOV;17(8):596-604.

177. Hile DD, Amirpour ML, Akgerman A, Pishko MV. Active growth factor delivery from poly(D,L-lactide-co-glycolide) foams prepared in supercritical CO2. J Controlled Release 2000 MAY 15;66(2-3):177-85.

178. Wernike E, Hofstetter W, Liu Y, Wu G, Sebald H, Wismeijer D, Hunziker EB, Siebenrock K, Klenke FM. Long-term cell-mediated protein release from calcium phosphate ceramics. Journal of Biomedical Materials Research Part a 2010 FEB;92A(2):463-74.

179. Hou Q, Walsh MC, Freeman R, Barry JJA, Howdle SM, Shakesheff KM. Incorporation of proteins within alginate fibre-based scaffolds using a post-fabrication entrapment method. J Pharm Pharmacol 2006 JUL;58(7):895-902.

180. Anderson JM, Rodriguez A, Chang DT. Foreign body reaction to biomaterials. Semin Immunol 2008 4;20(2):86-100.

181. Shivanand P, Sprockel OL. A controlled porosity drug delivery system. Int J Pharm 1998 JUN 1;167(1-2):83-96.

182. Pechar M, Ulbrich K, Subr V, Seymour LW, Schacht EH. Poly(ethylene glycol) multiblock copolymer as a carrier of anti-cancer drug doxorubicin. Bioconjug Chem 2000 MAR-APR;11(2):131-9.

183. Sandor M, Enscore D, Weston P, Mathiowitz E. Effect of protein molecular weight on release from micron-sized PLGA microspheres. J Controlled Release 2001 OCT 19;76(3):297-311.

184. Ferrara N, Henzel WJ. Pituitary follicular cells secrete a novel heparin-binding growth-factor specific for vascular endothelial-cells. Biochem Biophys Res Commun 1989 JUN 15;161(2):851-8.

185. Siegel RA, Kost J, Langer R. Mechanistic studies of macromolecular drug release from macroporous polymers .1. experiments and preliminary theory concerning completeness of drug release. J Controlled Release 1989 MAR;8(3):223-36.

186. Saltzman WM, Langer R. Transport rates of proteins in porous materials with known microgeometry. Biophys J 1989 JAN;55(1):163-71.

187. Wyatt TL, Saltzman WM. Protein delivery: Physical systems (pharmaceutical biotechnology) ; 1997.

Appendix A

Preparation and Characterisation of Poly(ethylene carbonate) Elastomers

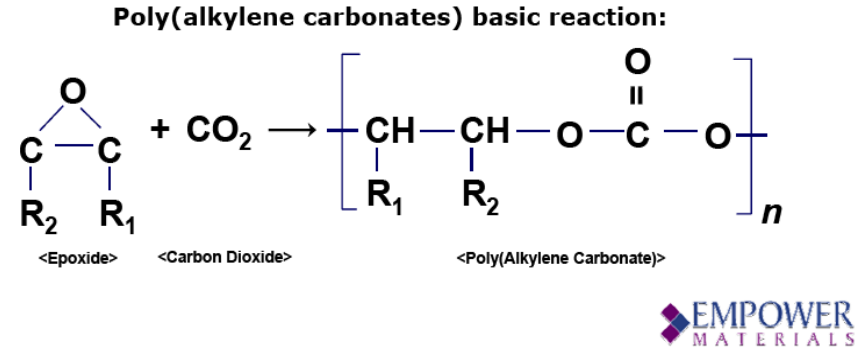

Figure 7-1: Copolymerization of poly(alkylene carbonates) from Empower Materials.

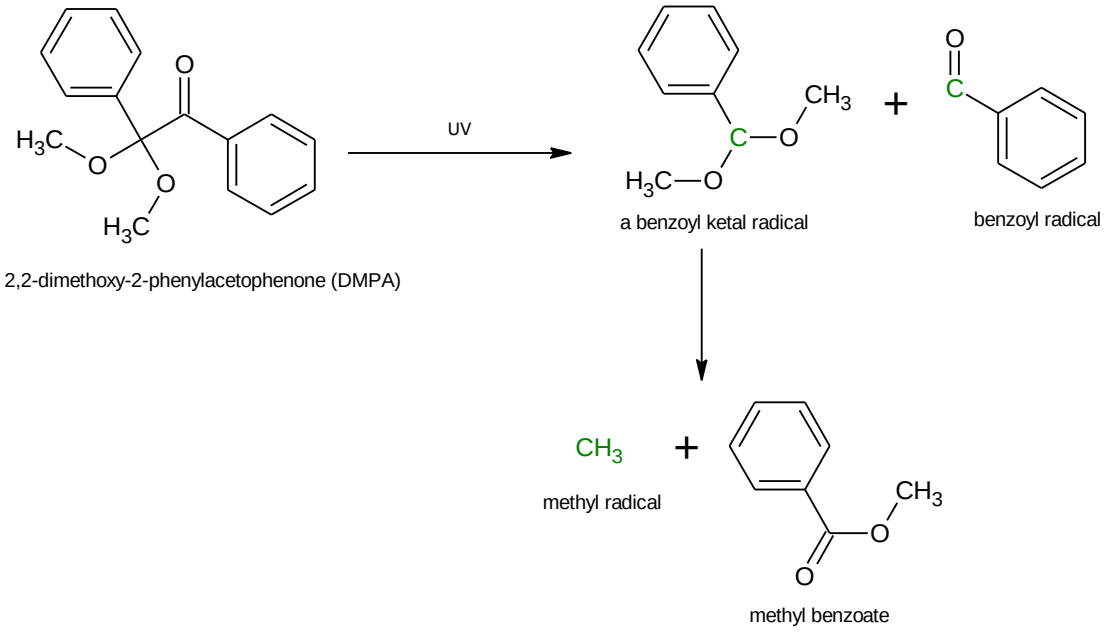

Figure 7-2: During photoinitiator decomposition, 2,2-dimethoxy-2-phenylacetophenone (DMPA) undergoes α-cleavage to form a benzoyl radical and a benzoyl ketal radical, and subsequently the benzoyl ketal undergoes β-cleavage to form a methyl radical and methyl benzoate (Borer, 1978). The benzoyl and methyl radicals are most effective in initiating chains, thus attacking the monomer molecule to form an active monomer molecule which can undergo propagation reactions [160].

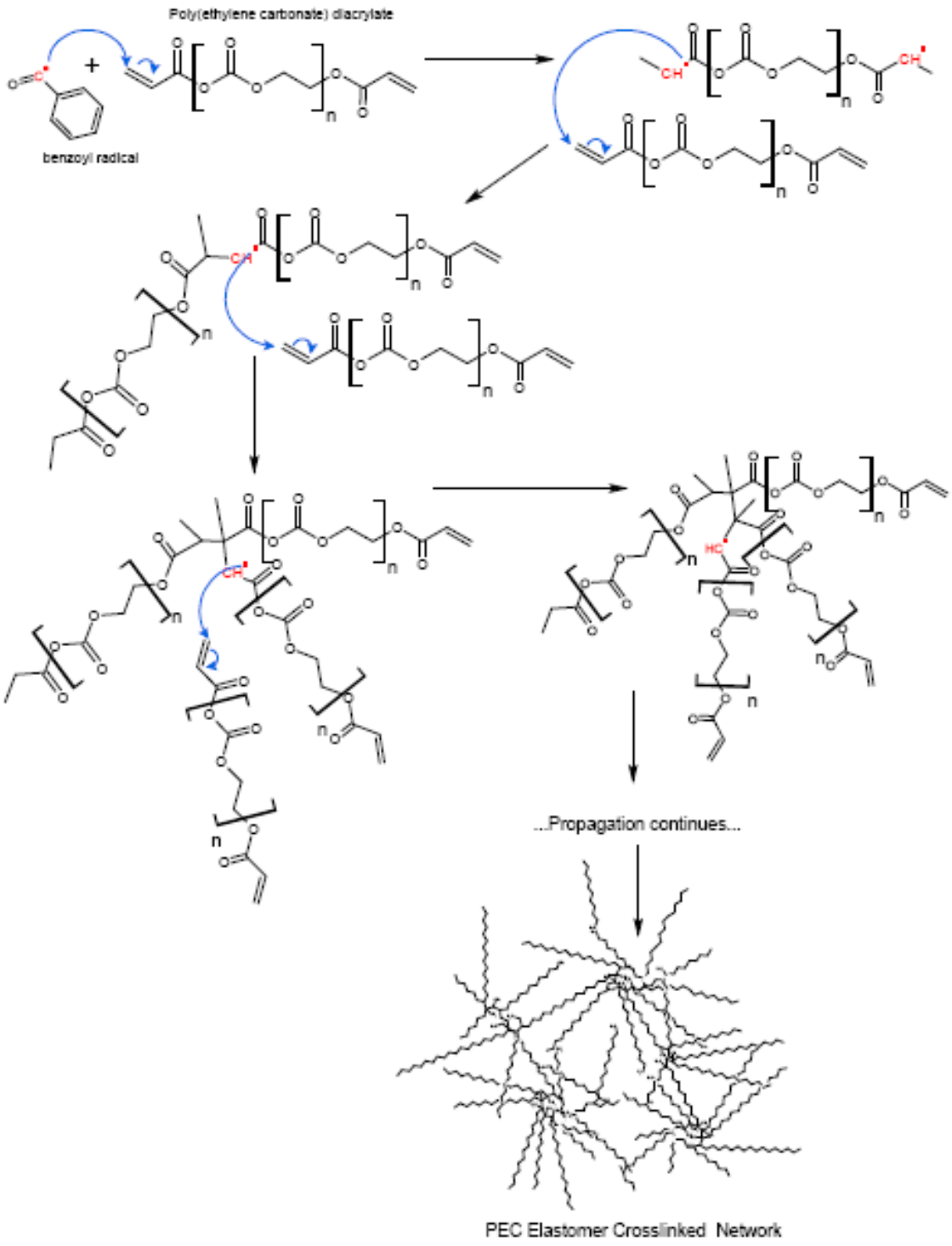

Figure 7-3: Photoinitiated crosslinking of PEC to form an elastomeric polymer network.

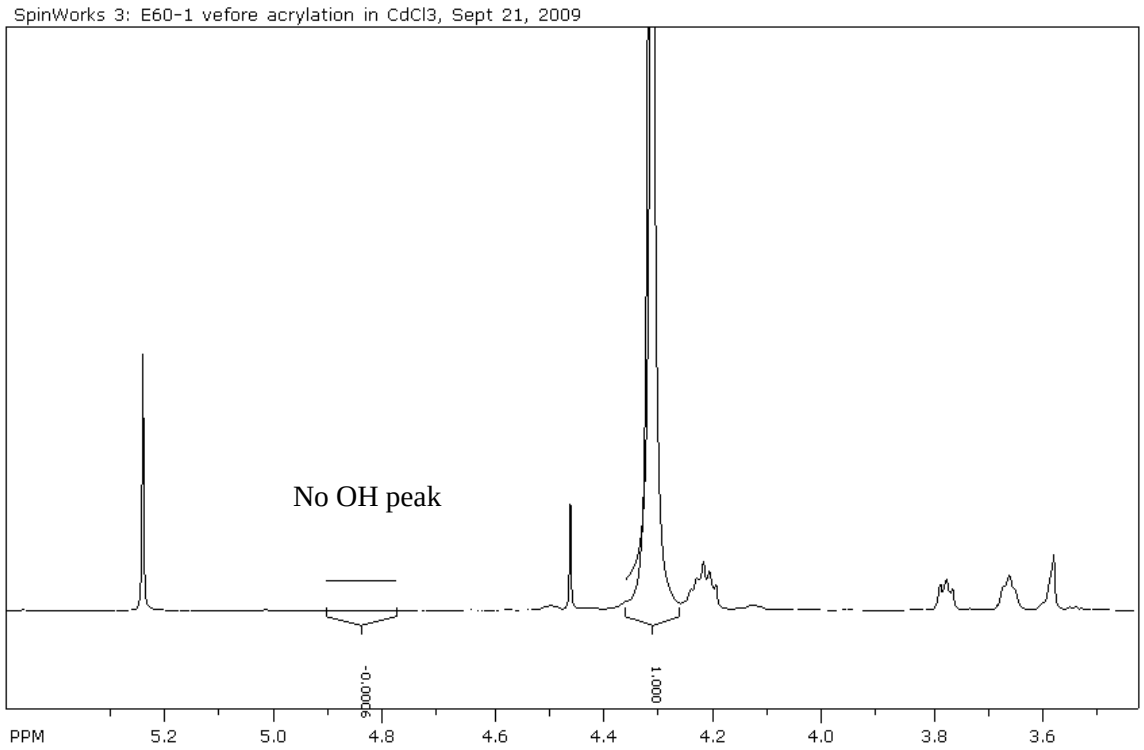

Figure 7-4: Batch #1 diol after purification in $CDCl_3$. Note that the terminal hydroxyl peak disappeared (not exchangeable).

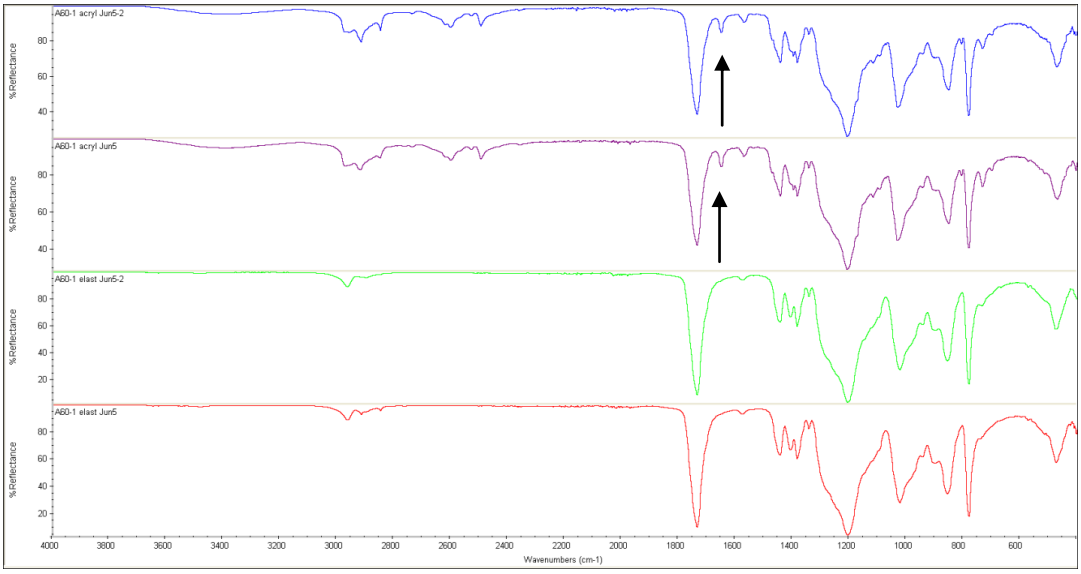

Figure 7-5: ATR-FTIR results for PEC diacrylates (top two spectra), and PEC elastomers (bottom two spectra). The band at 1650cm^{-1} (indicated arrows) corresponds to the acrylated groups which disappear after crosslinking, as expected.

Appendix B

Degradation and Biocompatibility of PEC Elastomers

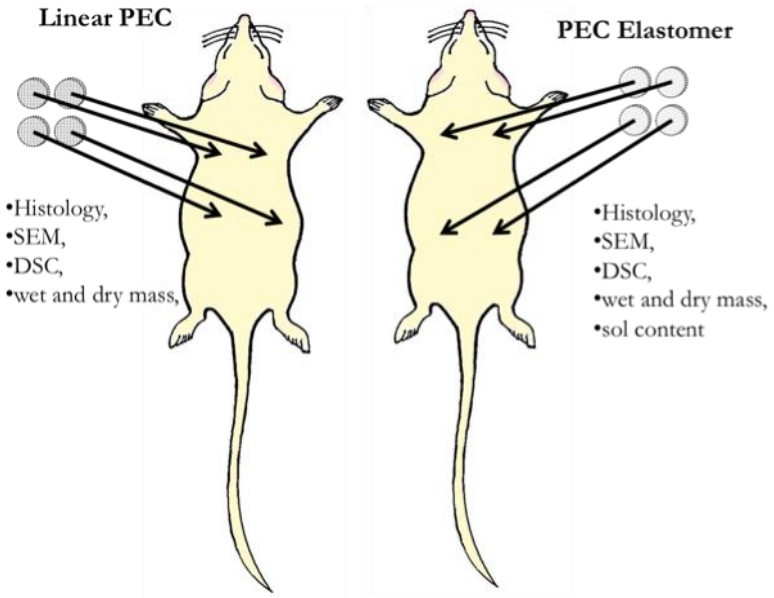

Figure 7-6: Location of subcutaneous PEC disc implantation into Male Wistar rats.

Figure 7-7: Representative photograph of rat sacrificed at Week 1 containing PEC elastomer implants with four sutures intact.

Figure 7-8: Representative photograph of PEC elastomer implanted into subcutaneous pocket at the time of explantation. No signs of inflammation (redness or swelling) can be seen macroscopically. (Week 6 time point)

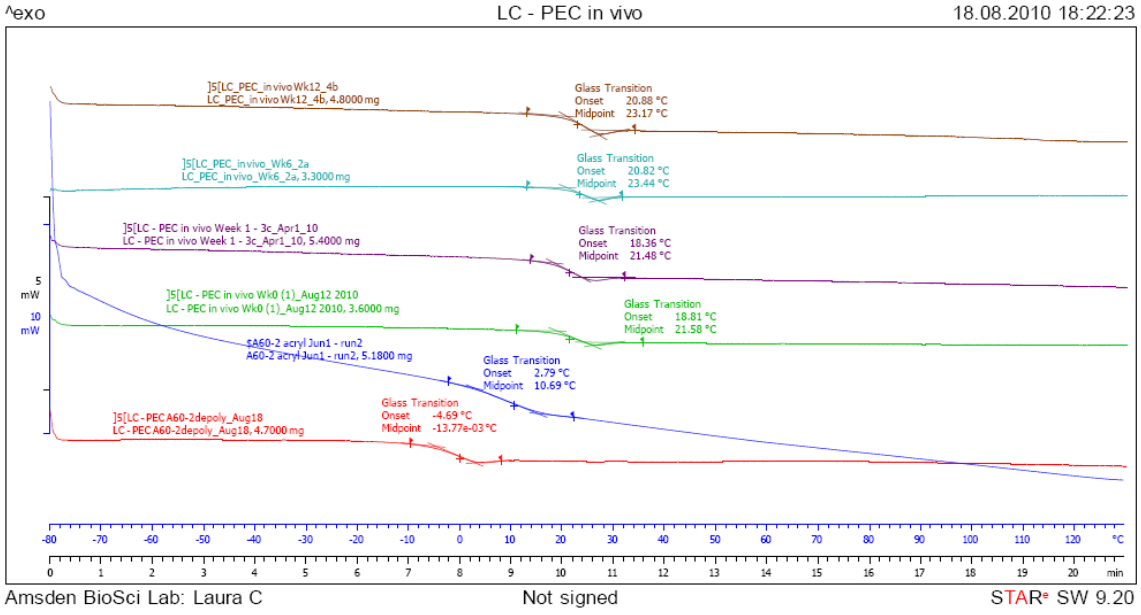

Figure 7-9: Differential Scanning Calorimetry results for PEC depoly (red), PEC diacryl (dark blue), PEC Elast 6000 at Week 0 (green), PEC Elast 6000 at Week 1 (purple), PEC Elast 6000 at Week 6 (light blue), PEC Elast 6000 at Week 12 (brown).

Appendix C

PEC Elastomer as a Porous Protein Delivery Device

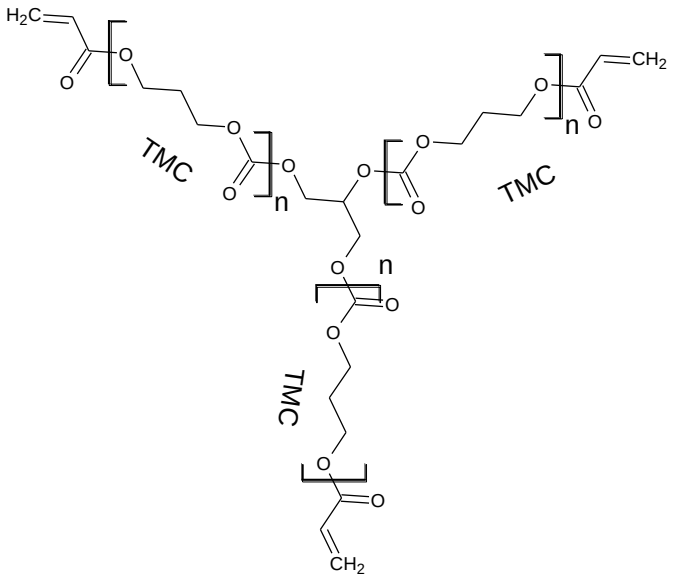

Figure 7-10: Chemical structure of terminally acrylated glycerol-initiated star-poly(trimethylene carbonate) (star-PTMC)

$$\Delta\rho = \rho\left[\frac{\Delta m}{m} + 2\frac{\Delta D}{D} + \frac{\Delta h}{h}\right]. \qquad \textit{Equation 7-1}$$

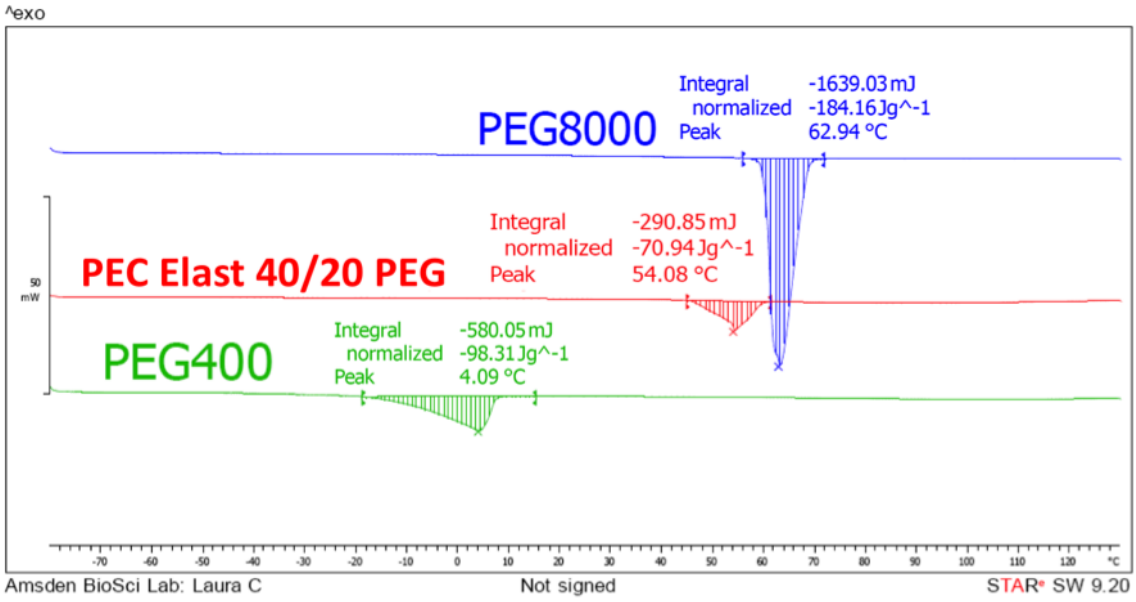

Figure 7-11: DSC for porous PEC elastomer with 40/20 PEG, as compared to that of PEG 8000 alone or PEG 400 alone.

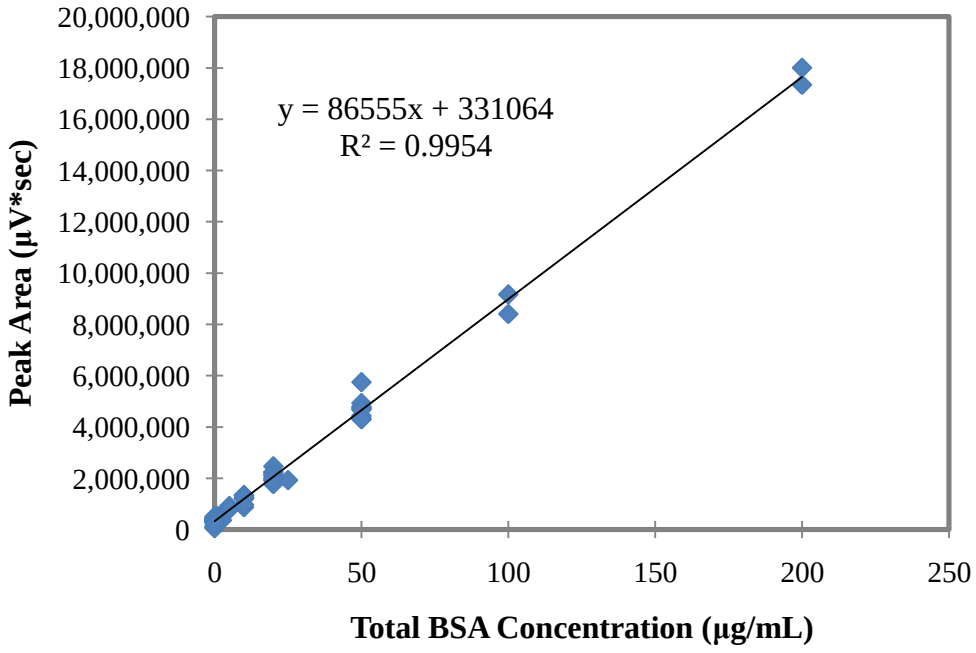

Figure 7-12: Calibration curve for total BSA (10% FITC-BSA, 90% BSA) for HPLC assay.